الجمهورية الجزائرية الديمقراطية الشعبية
People's Democratic Republic of Algeria
وزارة التعليم العالي والبحث العلمي
Ministry of Higher Education and Scientific Research

جامعة زيان عاشور بالجلفة
Ziane Achour University of Djelfa

كلية العلوم و التكنولوجيا
Faculty of Science and Technology

Department: Electrical Engineering

DOCTORAL THESIS

3rd Cycle Doctoral (D-LMD)

Presented by

Ali Nasser Edddine BENDENIDINA

With a view to obtaining the doctoral diploma in 3rd Cycle Doctoral (D-LMD)

Branch: Automatic

Specialty: Automatic

Topic

Contribution to the analysis and control of underactuated systems

Supported, on 25 /05 / 2026, before the jury composed of:

Mr Lakhdar BESSISSA	Professor	Université of Djelfa	President
Mr Kamel GUESMI	Professor	Université of Djelfa	Supervisor
Mr Aissa REBAI	Associate Prof	University of Ghardaia	Co-Supervisor
Mr Mohammed BELKHEIRI	Professor	University of Laghouat	Examiner
Ms Khansa BDIRINA	Associate Prof	University of Djelfa	Examiner

Djelfa University, FST - 2026

Acknowledgements

All praise is due to Almighty God, who granted me the faith, perseverance, and strength necessary to complete this work.

I would like to express my sincere and profound gratitude to my supervisor, Professor Kamel GUESMI of Djelfa University, for the trust he placed in me throughout this research. His constant guidance, availability, insightful advice, and constructive feedback played a crucial role in the successful completion of this thesis.

I am also deeply thankful to Dr. Aissa Rebai from Ghardaia University for co-supervising this work. His valuable guidance, patience, encouragement, and continuous support were instrumental during the different stages of this research.

My sincere appreciation is extended to all those who contributed, directly or indirectly, to the improvement of this manuscript through their comments, suggestions, and constructive remarks.

I would like to express my heartfelt gratitude to my parents, brothers, and entire family for their unwavering support, encouragement, and prayers, which provided me with the motivation and confidence to accomplish this work.

Finally, I extend my thanks to everyone who contributed in any way to the realization of this research.
May Allah send His blessings upon His noble Messenger, his family, and his companions, and grant us success and blessings in our lives.

Dedication

I dedicate this work to my parents, as an expression of my deepest appreciation and gratitude for their constant support, sacrifices, and encouragement.

To my brothers, my grandparents, and my entire family, whose love, care, and presence have been a continuous source of strength and motivation.

To all those who contributed to this work, whether directly or indirectly, and to those who shared the emotional moments throughout its completion, offering support, encouragement, and understanding along the way.

To my friends, whose encouragement and confidence have always inspired me, and to whom I sincerely wish continued success in all their endeavors.

Thanks!

الملخص

لقد شهد التحكم في الأنظمة ناقصة التشغيل تطورًا ملحوظًا خلال العقود القليلة الماضية، ويُعدّ حاليًا أحد المواضيع البحثية الحيوية في مجالات الروبوتات والفضاء والهندسة البحرية. ونظرًا لعدم التوافق بين عدد المحركات ودرجات حرية النظام، تُظهر هذه الأنظمة سلوكيات ديناميكية معقدة تُشكّل تحديات كبيرة، بينما تُحفّز في الوقت نفسه تطوير منهجيات تحكم متقدمة و مبتكرة .

في هذه الأطروحة، طُوّرت عدة استراتيجيات تحكم فعّالة للأنظمة ناقصة التشغيل. أولًا، يُقدّم أسلوب التحكم الانزلاقي مع مرحلة الوصول الحر للأنظمة الميكانيكية ناقصة التشغيل، والذي يُحسّن تتبع المسار والاستقرار من خلال التخلص من طور التذبذب في أسلوب التحكم الانزلاقي. ثانيًا، يُقدّم أسلوب التحكم الانزلاقي السريع مع المنطق الضبابي ، حيث يستخدم المنطق الضبابي لضبط معلمات الانزلاق السريع، مما يُؤدي إلى تقارب أسرع ودقة مُحسّنة في ظل وجود عدم اليقين في النمذجة والاضطرابات الخارجية. علاوة على ذلك، تم تصميم وحدة تحكم انزلاقية طرفية سريعة مع نظام التحكم التكيفي بالمنطق الضبابي من النوع الثاني، للاستفادة من خاصية التقارب في زمن محدود لأنماط الانزلاق الطرفية السريعة، مع توفير تمثيل أكثر فعالية للغموض، مما يعزز بشكل كبير المتانة والقدرة على التكيف. وأخيرًا، تم تقديم مخطط تحكم هجين تكيفي يدمج المنطق الضبابي من النوع الثالث مع التحكم الانزلاقي ذي الرتبة الكسرية دون مرحلة الوصول. يُحسّن هذا النهج سلاسة الاستجابة العابرة، ويُسرّع التقارب، ويُحسّن رفض الاضطرابات، مع التخلص من مرحلة الوصول. تُظهر هذه التحسينات أن التحكم في الأنظمة ناقصة التشغيل في تطور مستمر، دافعًا حدود ما يُمكن تحقيقه في التطبيقات المعقدة في العالم الحقيقي.

كلمات مفتاحية: الأنظمة ناقصة التشغيل، التحكم بالنمط الانزلاقي، التحكم بالنمط الانزلاقي الطرفي السريع الضبابي، منطق ضبابي من النوع الثاني، منطق ضبابي من النوع الثالث، حساب التفاضل والتكامل الكسري، ظاهرة الثرثرة، الاستقرار، المتانة.

Abstract

The control of underactuated systems has advanced significantly in the past few decades, and currently is regarded as a crucial research subject in the domains of robotics, aerospace, and marine engineering. Owing to the mismatch between the number of actuators and system degrees of freedom, these systems exhibit complex dynamic behaviors that pose significant challenges while simultaneously motivating the development of advanced control methodologies.

In this thesis, several robust control strategies are developed for underactuated systems. First, introduces Enhanced Free Reaching Phase Sliding Mode Control (SMC) for underactuated Systems, which enhances trajectory tracking and stability by eliminating the chattering phase of SMC. Subsequently, a fuzzy fast terminal sliding mode control approach is introduced, where fuzzy logic is employed to tune the fast terminal sliding parameters, resulting in faster convergence and improved precision under modeling uncertain-ties and external disturbances. Furthermore, an adaptive fuzzy Type-2 fast terminal sliding mode controller is designed to exploit the finite-time convergence property of fast terminal sliding modes while providing a more effective representation of uncertainty, thereby significantly strengthening robustness and adaptability. Finally, an adaptive hybrid control scheme that integrates Type-3 fuzzy logic with fractional-order sliding mode control without reaching phase is presented. This approach enhances transient smoothness, accelerates convergence, and improves disturbance rejection, while eliminate the reaching phase. These improvements show that controlling under-actuated systems is always changing and growing, pushing the bound-aries of what is achievable in complex, real-world applications.

Key words: *Underactuated System, Sliding Mode Control, Fuzzy Fast Terminal SMC, Fuzzy Type-2, fuzzy Type-3, Fractional-Calculus, Chattering Phenomenon, Stability, Robustness.*

Résumé

La commande des systèmes sous-actionnés a considérablement progressé ces dernières décennies et est actuellement considérée comme un sujet de recherche crucial dans les domaines de la robo-tique, de l'aérospatiale et du génie maritime. En raison du décalage entre le nombre d'actionneurs et les degrés de liberté du système, ces systèmes présentent des comportements dynamiques com-plexes qui posent des défis importants tout en motivant le développement de méthodologies de commande avancées.

Dans cette thèse, plusieurs stratégies de commande robustes sont développées pour les systèmes sous-actionnés. Premièrement, la commande améliorée par mode glissant (SMC) sans phase d'approche pour des systèmes sous-actionnés. Cette commande améliore le suivi et la stabilité de la trajectoire en éliminant la phase d'approche de la SMC. Ensuite, la SMC à terminal rapide flou (FFTSMC) pour UMS a été proposée en combinant la robustesse de la FTSMC avec les performances de la logique floue pour atteindre une convergence rapide et une haute précision en présence d'incertitudes de modèle et des perturbations externes. De plus, on a développé une commande adaptative par mode glissant à terminal rapide flou de type 2 (AFT2-FTSMC) qui combine la capacité de convergence à temps fini de la FTSMC avec la modélisation améliorée des incertitudes de l'AFT-2, ce qui a amélioré considérablement la robustesse et l'adaptabilité du système. Enfin, nous avons proposé un schéma de commande adaptatif hybride en mode glissant d'ordre fractionnaire et à logique floue de type 3. Il intègre des opérateurs d'ordre fractionnaire et une inférence floue de type 3 afin d'améliorer la régularité transitoire, la rapidité de convergence et la robustesse, tout en éliminant la phase d'approche grâce à une surface de commutation innovante dépendante du temps. Ces avancées mettent en évidence la nature dynamique et évolutive de la commande des systèmes sous-actionnés, repoussant les limites de ce qui est réalisable dans des applications complexes du monde réel.

Mots clés: *Systèmes Sous-actionnés, Commande par mode glissant, Mode Glissant Terminale Rapide Floue, Logique Floue de Type 2, Logique Floue de Type 3, Calcul Fraction-naire, Phénomène de Réticence, Stabilité, Robustesse.*

Contents

List of Figures

List of Tables

List of Abbreviations

UMS:	Underactuated Mechanical Systems
SMC:	Sliding Mode Control
FFTSMC:	Fuzzy Fast Terminal Sliding Mode Control
FL:	Fuzzy Logic
FLC:	Fuzzy Logic Control
TORA:	Translational Oscillator with Rotational Actuator
VTOL:	Vertical Take-Off and Landing
LQR:	Linear Quadratic Regulator
ANFIS:	Adaptive Neuro-Fuzzy Inference System
IFOFITSMC:	Improved Fractional-Order Fast Integral Terminal Sliding Mode Control
FOSMC:	Fractional Order Sliding Mode Control
STCL:	Supper-Twisting Control Law
H-GFTSMC :	Hierarchical Global Fast Terminal Sliding Mode Controller
QUAV:	Quadrotor Unmanned Aerial Vehicles
IWP:	Inertia Wheel Pendulum

General introduction

Mechanical systems are often categorized into three principal classes based on their actuation capabilities: fully actuated, overactuated, and underactuated systems. Each class signifies a distinct level of control and complexity, determined by the number of control inputs and degrees of freedom accessible to the system.

Within the broad class of dynamical systems, underactuated systems represent a particularly compelling area of research due to their unconventional structure and behavior. In contrast to fully actuated systems, where a control input directly governs each degree of freedom, underactuated systems operate under a fundamental imbalance between available actuation and degrees of freedom. This inherent limitation introduces both substantial challenges and rich opportunities for the analysis and synthesis of advanced control strategies.

A central research focus in this area lies in understanding the intricate dynamics arising from underactuation and in developing control methodologies that explicitly account for these constraints. Achieving objectives such as trajectory tracking, stabilization, and task execution in underactuated systems requires sophisticated tools drawn from nonlinear control theory, optimization techniques, and dynamical systems analysis. These approaches enable controllers to exploit system structure and internal dynamics rather than relying solely on direct actuation.

Despite their control complexity, underactuated systems offer several notable advantages from a design and implementation perspective. The reduced number of actuators leads to simpler mechanical architectures, which in turn lowers manufacturing costs, decreases maintenance requirements, and improves overall reliability. Moreover, such systems often benefit from improved energy efficiency by taking advantage of passive dynamics and natural motion, thereby reducing the need for continuous control effort and extending component lifespan. Their inherent structural flexibility also allows them to adapt more readily to variations in operating conditions and task requirements, making them well-suited for applications in robotics and aerospace environments where uncertainty and change are common. Additionally, fewer actuated components can enhance fault tolerance, enabling the system to maintain

acceptable performance even in the presence of partial failures.

Nevertheless, the control of underactuated systems remains a demanding problem. Challenges such as strong nonlinearities, parametric uncertainties, and limited sensing and actuation capabilities must be carefully addressed. Overcoming these difficulties requires innovative theoretical developments and practical design solutions. As research in this field continues to advance, underactuated systems are playing an increasingly important role in shaping future technologies in robotics and mechanical engineering, offering efficient, robust, and adaptable solutions for complex real-world applications.

Motivation: Underactuated systems, defined by the presence of fewer control inputs than degrees of freedom, constitute a significant and intellectually demanding class of dynamical systems. The interest in their study arises from a convergence of economic considerations, practical design requirements, theoretical challenges, and application-oriented demands. From an engineering perspective, the reduced number of actuators often leads to simpler and more cost-effective mechanical structures, while also offering improved energy efficiency and operational flexibility. At the same time, the intrinsic limitations imposed by underactuation introduce complex dynamic behaviors that cannot be addressed using conventional control techniques. These challenges have stimulated substantial progress in modern control theory, encouraging the development of advanced nonlinear, adaptive, and robust control methodologies. The need to achieve stability, accurate motion control, and reliable performance under limited actuation remains a driving force for innovation in multiple research disciplines. Due to their advantageous properties and distinctive dynamic characteristics, underactuated systems have found widespread application in areas such as robotics, aerospace systems, marine vehicles, and assistive technologies. Ongoing research in this domain is expected to play a pivotal role in future technological advancements, enabling the design of efficient, resilient, and adaptable systems capable of operating in complex and uncertain environments.

- Reduction of cost and complexity (economic efficiency): Underactuated system architectures contribute to improved economic efficiency by reducing both initial implementation costs and long-term maintenance requirements. The use of fewer actuators results in simplified mechanical structures that are easier to manufacture and assemble. In addition, the number of components reduces the likelihood of mechanical failure, thus improving overall system reliability.

- Improved energy efficiency: Limiting the number of actuators directly reduces power consumption, which leads to more energy-efficient system operation. This characteristic

is particularly advantageous for applications operating under strict energy constraints, where efficient power utilization and sustainability are critical performance factors.

- Weight reduction and enhanced mobility: The absence of excessive actuation hardware enables lighter system designs, which significantly improves mobility, maneuverability, and dynamic responsiveness. Such lightweight configurations are essential in applications including unmanned aerial vehicles, mobile robots, and portable autonomous platforms.

- Enhanced safety and operational reliability: Systems with reduced actuation complexity tend to exhibit greater robustness and fault tolerance. The simplified structure decreases the probability of actuator-related failures, while a deeper understanding of underactuated dynamics facilitates the development of effective fail-safe control strategies and improved safety mechanisms, ensuring dependable performance in practical operating conditions.

Objectives of the thesis: The main objective of this thesis is to develop robust control methodologies for underactuated systems that effectively address the inherent challenges arising from the mismatch between the number of actuators and the system degrees of freedom. In particular, the proposed approaches aim to enhance system performance and stability under uncertain conditions, enabling underactuated systems to operate reliably in partially or fully unknown environments while accomplishing predefined control objectives.

Contributions: The contributions of this thesis project can be summarized as follows: Development of a new sliding mode controller without a reaching phase by constructing a time-varying sliding surface that intersects the initial error state, ensuring immediate sliding motion and significantly reducing chattering while preserving system stability. Next, a fuzzy fast terminal sliding mode control structure is introduced, where fuzzy logic–based tuning enhances control precision and accelerates the convergence of system states toward their desired values. Subsequently, an adaptive fuzzy Type-2 fast terminal sliding mode control (AFT2-FTSMC) strategy is proposed, combining the finite-time convergence property of fast terminal sliding mode control with an adaptive fuzzy estimator that adjusts the control input online, thereby improving robustness and further mitigating chattering in the presence of uncertainties. Finally, an adaptive hybrid Type-3 fuzzy fractional-order sliding mode control strategy is presented, incorporating a novel time-varying switching surface that intersects the sliding manifold with the system's initial error, effectively eliminating the reaching phase and substantially reducing chattering. In this framework, the fractional-order operator acts as a

tunable gain to improve convergence speed and smooth transient behavior, while an adaptive Type-3 fuzzy logic system is employed to accurately approximate unknown nonlinearities and external disturbances in real time.

Organization of the manuscript :

This thesis is organized around five chapters as follows:

In **chapter 1**, we give a general overview of underactuated mechanical systems. The background and motivation to study underactuated mechanical systems are given. Then, a Brief state of the art of the subject is given. We compiled and summarized several noteworthy works in the field. Furthermore, essential and basic notions on nonlinear systems, stability, fuzzy logic, and sliding mode control are explained.

In **chapter 2**, our contribution related to enhanced free reaching phase SMC for UMS is addressed. The dynamic modeling of the UMS is presented first. Then, new robust control inputs for UMS are developed. Moreover, the Lyapunov theory is used to prove the suggested control scheme's convergence and stability. Compared to other controllers this proposed control laws can achieve better tracking, with a chattering-free and robust control performance.

The **chapter 3** is dedicated to the next contribution dealing with the design of a Fuzzy Fast Terminal Sliding Mode Control (FFTSMC) scheme for underactuated mechanical systems. The proposed approach achieved fast convergence, robust performance, and reduced chattering by integrating the benefits of fast terminal sliding mode control and fuzzy logic tuning. The performance of the control method is evaluated through simulations that demonstrate the superiority of the proposed controller.

The **chapter 4** introduces a proposition of an adaptive fuzzy Type-2 fast terminal sliding mode control (AFT2-FTSMC) technique. The chapter details the design of this controller, including the adaptive fuzzy estimator for online control input adjustment and its role in enhancing robustness, reducing chattering, and ensuring fast finite-time convergence. In addition, stability proofs and simulation results demonstrate the capabilities of the proposed controller to obtain improved tracking performance under uncertainties and external disturbances.

In **chapter 5**, we present an adaptive hybrid type-3 fuzzy fractional-order sliding mode control strategy. This chapter first introduces the fractional-order operator, followed by a description of the adaptive Type-3 fuzzy logic system. Building upon these components, the adaptive hybrid type-3 fuzzy fractional-order sliding mode controller is formulated, combining the advantages of fractional-order control and adaptive type-3 fuzzy estimation while eliminating the reaching phase through a novel time-varying switching surface. Subsequently,

stability analysis and Lyapunov-based proofs are conducted to guarantee the closed-loop system stability. Finally, simulation results are provided to demonstrate the superior tracking performance, robustness, and overall effectiveness of the proposed control strategy under uncertainties and external disturbances.
The manuscript ends with general conclusions and some perspectives for future work.

Scientific production:
Publications:

1. A. N.-E. Bendenidina, K. Guesmi, A. Rebai, A. Damani, B. Nail, I. Tibermacine, A. Ma'arif, Adaptive Fuzzy Type-3 Fractional-Order Sliding Mode Controller without Reaching Phase for Underactuated Mechanical Systems. *International Journal of Robotics and Control Systems*, 6(1), 2026.
   https://pubs2.ascee.org/index.php/IJRCS/article/view/2241

International Conferences:

1. A. N.-E. Bendenidina, K. Guesmi, A. Rebai, Fuzzy fast terminal SMC for underactuated mechanical systems, *International Conference on Advances in Electronics, Control and Communication Systems (ICAECCS'23)*, 2023.

2. A. N.-E. Bendenidina, K. Guesmi, A. Rebai, Adaptive Fuzzy type-2 SMC for UMS, *Electrical Engineering International Conference (EEIC'25)*, 2025.

Chapter 1

Underactuated systems: an overview

1.1 Introduction

In this chapter, an overview of underactuated systems is presented. The chapter begins with a description of their essential properties, including the mismatch between the number of actuators and degrees of freedom, which distinguishes them from fully actuated systems. Representative engineering examples are presented to demonstrate the widespread occurrence of such systems in practical applications. These examples also highlight the underlying factors that lead to their natural emergence, including simplified mechanical design, reduced system weight, and energy efficiency requirements. While these attributes offer notable advantages, they simultaneously introduce significant control challenges. Consequently, the development of advanced and innovative control methodologies becomes essential, particularly those capable of ensuring stability and high performance under these constraints.
Subsequently, the rationale for selecting underactuated systems as the central subject of investigation is examined. The interest in these systems stems from their importance in both applied engineering and fundamental control research. From an application-oriented perspective, underactuated dynamics frequently appear in practical systems such as overhead lifting mechanisms, marine platforms, unmanned aerial vehicles, and robotic manipulators. In these contexts, limited actuation often leads to reduced structural weight, improved energy efficiency, and lower implementation costs. From a theoretical standpoint, the nonlinear behavior, intrinsic coupling, and potential instability of underactuated systems present substantial challenges, making them well-suited for the development and assessment of advanced control strategies. Effectively managing these characteristics necessitates control approaches that can guarantee stability, robustness, and performance despite modeling uncertainties and

external disturbances. Consequently, advancing the understanding of underactuated systems not only enhances their practical operation but also supports broader developments in modern control theory, autonomous systems, and intelligent robotics.
Furthermore, this chapter provides a comprehensive review of contemporary control methodologies that have been extensively applied to underactuated systems. The discussion emphasizes the underlying principles of these approaches. In order to support the subsequent controller development, the chapter also introduces several foundational theoretical concepts relevant to underactuated system control. These include key aspects of nonlinear system dynamics, fundamental stability criteria, and other essential notions that form the basis for the analysis and synthesis of control strategies for systems with limited actuation.
Through this comprehensive introduction, we aim to establish a strong basis for the subsequent chapters. By outlining the fundamental concepts and presenting the key challenges associated with underactuated systems, this section equips the reader with the essential background required to appreciate the complexities of their control. In doing so, it prepares the ground for the advanced methodologies that will be developed later, ensuring that the reader can fully grasp both the theoretical significance and the practical implications of the proposed control strategies.

1.2 Background

1.2.1 Underactuated systems

Underactuated systems are a class of complex dynamical systems that have gained significant attention in the field of control engineering due to their challenging nature, these systems have fewer control inputs than degrees of freedom [1], in other words, these systems have more degrees of freedom than control inputs, which results in non-intuitive dynamics and complicates the control design process, leading to interesting and complex behavior, and they are commonly found in robotics, mechanical systems, and control theory such as: cart-pole system [2], marine systems [3], quad-rotor [4], wheeled mobile robot [5], vertical takeoff and landing (VTOL) [6], wheeled inverted pendulum [7].
There are numerous factors that contribute to the underactuation of a system, which are outlined succinctly as follows:

- Natural System Dynamics: Some systems naturally have fewer control inputs (actuators) than degrees of freedom, leading to underactuation, e.g., aircraft, spacecraft, crane.

- Cost and Practical Considerations: Underactuation, such as in satellites equipped with only two thrusters, can be a purposeful design decision to lower system complexity and cost.

- Actuator failure: Underactuation can function as a redundancy mechanism in systems where actuators are prone to failure, such as surface vessels and vertical takeoff and landing aircraft.

- Artificial induction for research and experimental purposes: In certain cases, underactuation is intentionally introduced into mechanical or electromechanical systems to create experimental platforms for research. This allows researchers to study and develop control strategies for managing the challenges posed by underactuated systems, e.g., the cart-pole setup, the ball and beam apparatus, the rotary inverted pendulum, the translational oscillator with rotational actuator system, as well as the Acrobot, among others.

In general, underactuation may result from intrinsic system dynamics, intentional design decisions, actuator malfunctions, or the deliberate creation of experimental scenarios for research purposes. Underactuated mechanical systems provide a range of notable advantages, including:

– Reduction of weight: By requiring fewer actuators compared to fully actuated systems, underactuated systems can be lighter in weight. This weight reduction can lead to improved efficiency, performance, and maneuverability, particularly in applications where weight is a critical factor, such as aerospace and robotics.

– Reduced propensity to breakdown: With fewer moving parts and components, underactuated systems generally have a reduced propensity to breakdown. Simplifying the mechanical structure by using fewer actuators can decrease the likelihood of mechanical failures, leading to increased reliability and uptime.

– Lower energy cost of control: Underactuated systems often rely on exploiting natural dynamics or passive control strategies, which can result in lower energy consumption for control purposes. By leveraging the inherent dynamics of the system, underactuated systems can achieve desired behaviors with minimal energy input, reducing overall energy costs.

These benefits render underactuated mechanical systems highly appealing across a wide range of applications, providing notable improvements in system weight, operational reliability, and energy efficiency.
The focus on modeling and control of underactuated mechanical systems has increased considerably in recent years. This is due, at least in part, to the fact that many modern robotic systems are underactuated, for example, an autonomous underwater vehicle, or a walking robot subject to intermittent ground contact. It is known that modeling the natural dynamics of such systems and exploiting their inherent underactuation is key to building control strategies that are truly effective, efficient, and suited to the application. In addition to robotics, there are important underactuated mechanical systems in aerospace, for example, satellites with a single-axis rotational control and atmospheric entry vehicles. These factors make it important that the control community has a good understanding of the specific characteristics of underactuated systems and tailored methods to control them.

1.2.2 Classification of UMSs

Developing a classification framework for underactuated mechanical systems (UMSs) is a crucial step for analyzing their dynamic behavior and designing effective control strategies. Given the wide range of engineering applications in which these systems appear, several classification schemes have been proposed based on factors such as structural configuration, dynamic characteristics, and application context. Establishing a clear and organized taxonomy not only supports systematic investigation but also highlights the unique challenges associated with each category of underactuated system
A widely used method for categorizing underactuated systems focuses on the source of underactuation. In many engineered systems, underactuation is intentionally incorporated to reduce overall weight, lower costs, or minimize energy consumption. This design choice is particularly prevalent in aerospace and marine applications, where adding additional actuators may be impractical due to physical or operational limitations. Conversely, underactuation can also arise unintentionally as a consequence of actuator faults, mechanical damage, or saturation. Such fault-induced underactuated systems are of particular interest in fault-tolerant control research, where the primary objective is to maintain stability and ensure safe operation despite adverse or unexpected conditions.
Another important classification is according to the degree of underactuation, which is typically defined as the difference between the number of degrees of freedom and the number of available actuators. Systems with a small degree of underactuation, such as the classi-

cal cart–pendulum system, are often used as benchmarks in control theory. By contrast, systems with a high degree of underactuation, such as multi-link flexible manipulators or autonomous underwater vehicles with limited actuation, present more severe challenges due to the increased number of unactuated dynamics.

A further perspective distinguishes UMSs based on their dynamic characteristics. Some systems are described by nonholonomic constraints, such as wheeled mobile robots or underactuated surface vessels, where the restrictions arise from rolling or hydrodynamic interactions. Others exhibit strong nonlinearities or chaotic behaviors, as in the case of the Acrobot and Pendubot, where stabilization and trajectory tracking require advanced nonlinear control designs. In addition, certain UMSs display hybrid dynamics, combining continuous motion with discrete switching events, which complicates both modeling and control tasks.

Finally, underactuated systems may be classified according to their application domains. In robotics, examples include legged robots, aerial drones, and manipulators with passive joints. In aerospace engineering, spacecraft with partially failed thrusters or satellites with limited attitude control actuators represent typical cases. Marine and offshore engineering provide further examples, including ships, underwater vehicles, and floating platforms, where environmental forces contribute to underactuated dynamics. Each domain imposes distinct performance requirements and constraints, shaping the choice of the control methodology.

In conclusion, underactuated mechanical systems can be classified along multiple complementary dimensions, including the source of underactuation, the extent or degree of underactuation, intrinsic dynamic characteristics, and their specific application domains. This comprehensive framework not only guides the selection of appropriate control strategies but also emphasizes the significant role that UMSs play in contemporary engineering applications. By employing such a multidimensional classification, researchers and engineers can gain a clearer understanding of the diversity among underactuated systems and develop control solutions tailored to the particular challenges presented by each category.

1.2.3 Application areas of UMS

Underactuated mechanical systems (UMSs) hold significant theoretical appeal while also playing a vital role in numerous engineering applications. The defining feature of having fewer actuators than degrees of freedom allows these systems to achieve lighter and more compact designs, reduced energy consumption, and simplified mechanical structures. At the same time, this inherent limitation introduces considerable control challenges that necessitate sophisticated and robust control strategies. Consequently, UMSs are commonly employed in

advanced technological systems where efficiency, adaptability, and reliable performance are essential.

A major area where UMSs play a central role is aerospace systems. Many spacecraft and satellites are underactuated by design to reduce fuel consumption and hardware complexity. Precise attitude control must therefore be achieved with a limited number of actuators. Similarly, unmanned aerial vehicles such as quadrotors and tilt-rotor drones are inherently underactuated, since not all translational and rotational motions can be controlled independently.

Robotics provides another rich field of application. Numerous robotic platforms deliberately adopt underactuation to enhance flexibility and reduce system weight. Examples include walking robots, robotic arms with passive joints, and modular snake robots. These systems often operate in unstructured or dynamic environments, which makes the design of reliable controllers crucial.

In marine applications, underactuation naturally arises due to hydrodynamic constraints. Ships, underwater robots, and autonomous surface vehicles typically lack actuation in all directions of motion. This limitation necessitates the use of advanced nonlinear controllers for tasks such as trajectory tracking, path following, and stabilization in the presence of ocean disturbances.

Industrial and transportation systems also make use of underactuated designs. Classic case studies include inverted pendulum systems, self-balancing vehicles, and overhead cranes. The latter, for instance, must ensure safe and efficient movement of loads while suppressing undesired oscillations, despite the fewer control inputs they have.

Emerging interest has also been observed in biomedical engineering, particularly in wearable robotics and prosthetic devices. Exoskeletons designed with fewer actuators achieve reduced power consumption and increased comfort, making them more practical for rehabilitation and assistive purposes.

Overall, the ubiquity of UMSs across aerospace, robotics, marine, industrial, and biomedical fields underscores their importance. At the same time, it highlights the need for sophisticated control strategies capable of ensuring performance, stability, and satisfactory performance despite the inherent limitations in actuation.

1.2.4 Examples of UMS

This section introduces a selection of widely studied examples of UMS. All the examples are chosen due to some analysis and control purposes. Indeed, the complexity of their control

design is of great interests by researchers. These examples include the cart-pole system, the crane system, the Acrobot, the Pendubot, the rotating pendulum, the surface vessel, the beam and ball system. Each example will be described, in what follows, briefly:

1.2.4.1 Cart-pole and crane systems

The cart–pole system illustrated in Fig. (1.1) aims to move the pendulum from its stable downward configuration ($q_1 = 0$ and $q_2 = \pi$), to the upright unstable position ($q_2 = 0$), while maintaining the cart at the reference position($q_1 = 0$). In contrast, the crane system shown in Fig. (1.2) has a different control objective. The goal is to suppress payload oscillations by appropriately regulating the motion of the trolley.

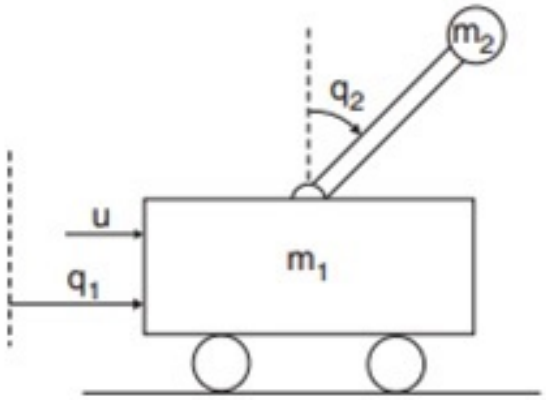

Figure 1.1: Cart-pole system

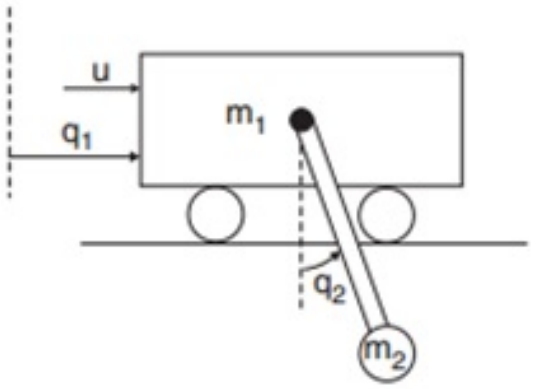

Figure 1.2: Crane system

1.2.4.2 Acrobot and Pendubot

The Acrobot and Pendubot are two-link robotic systems driven by a single actuator, located at the elbow and shoulder joints, respectively, as illustrated in Fig. (1.3). Although both systems share identical dynamic equations, they differ in the form of the input distribution matrix $F(q)$ Specifically, $F = \begin{bmatrix} 0 & 1 \end{bmatrix}^T$ corresponds to the Acrobot, while $F = \begin{bmatrix} 1 & 0 \end{bmatrix}^T$ represents the Pendubot. The control objective in both cases is to drive and stabilize the manipulator at the upright equilibrium position ($q_1 = \pi/2$, and $q_2 = 0$), starting from arbitrary initial conditions.

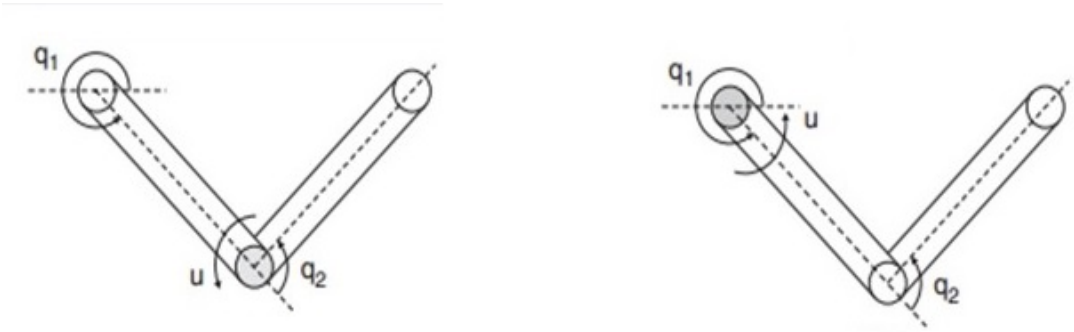

(a) Acrobot (b) Pendubot

Figure 1.3: Two-link manipulators

1.2.4.3 Rotating pendulum

The rotating pendulum, commonly known as the Furuta pendulum (see Fig. 1.4), is composed of a passive pendulum that swings in a vertical plane, mounted at the tip of a horizontally rotating arm actuated by a DC motor.

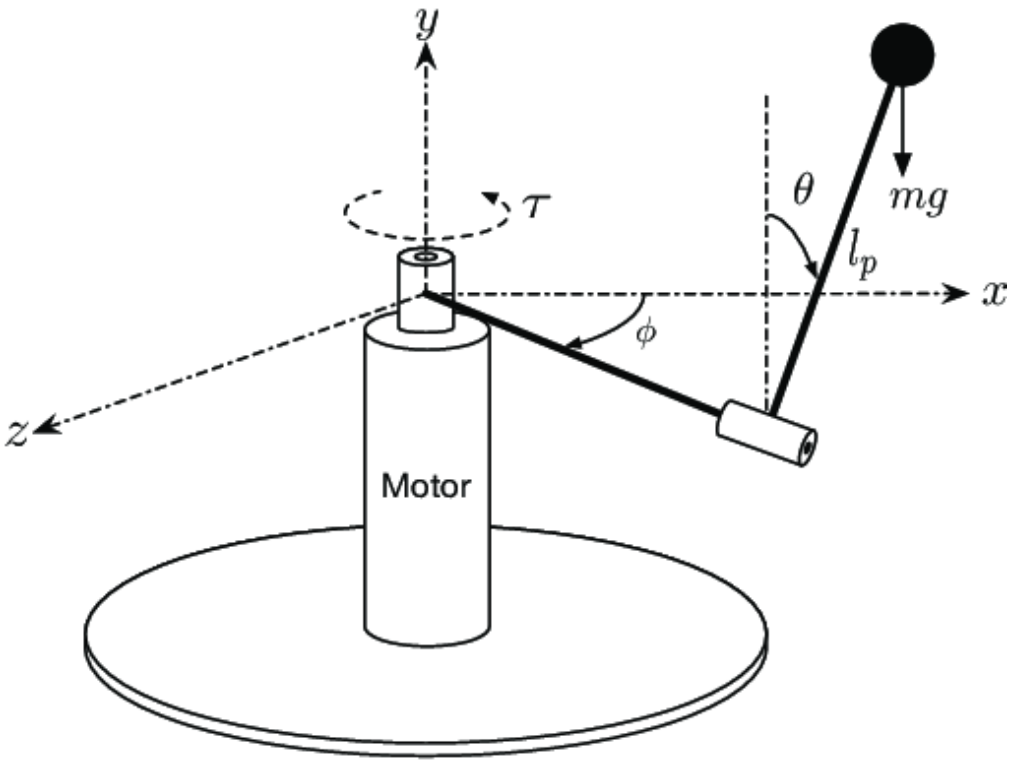

Figure 1.4: Furuta pendulum

1.2.4.4 Surface vessel

The surface vessel depicted in Fig. 1.5 represents a simplified model of underactuated ships, featuring three degrees of freedom and two independent thrusters. Such systems have recently attracted significant interest in the control research community.

1.2.4.5 Beam and ball system

The ball-and-beam system, illustrated in Fig. 1.6, consists of a beam capable of pivoting in the vertical plane at its center and a ball that moves along the beam. The control objective is to position the ball at the center of the beam by appropriately adjusting the beam's angle.

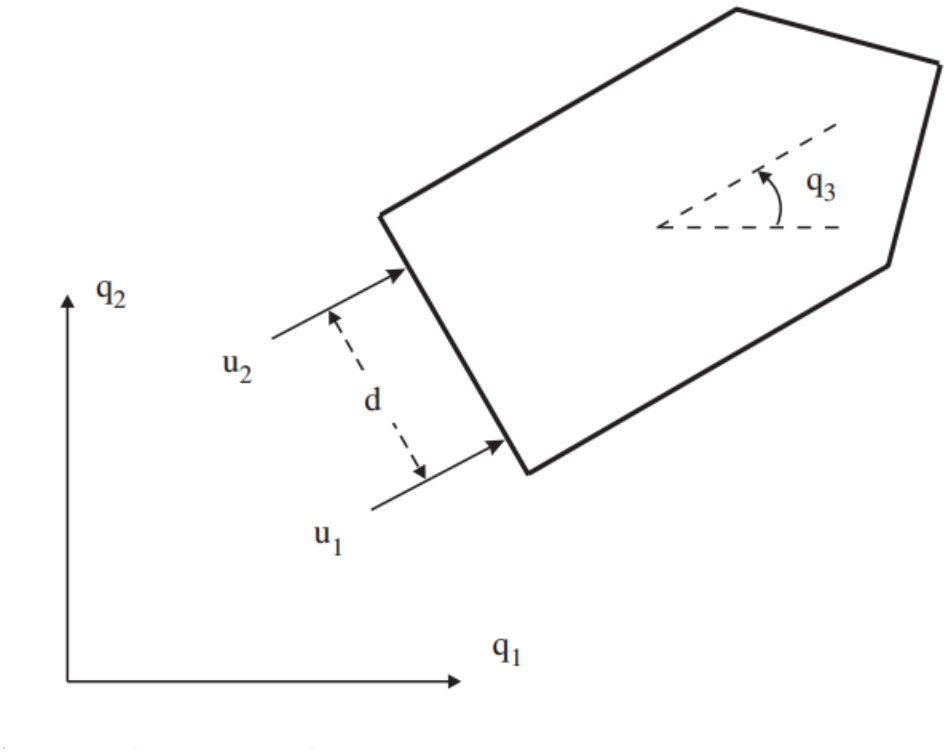

Figure 1.5: Surface vessel

1.2.4.6 Underactuated mobile robots

Wheeled mobile robots shown in figure 1.7 provide another important category of underactuated systems. A differential-drive robot with nonholonomic rolling constraints can move forward and rotate, but it cannot move laterally due to the absence of direct actuation in that direction. This underactuation must be handled through trajectory planning and control algorithms that exploit nonholonomic constraints. Such systems are highly relevant in logistics, service robotics, and autonomous navigation.

1.2.5 Nonlinear dynamics and control

Nonlinear dynamics and control is a branch of applied mathematics and engineering that deals with systems exhibiting nonlinear behavior, where small changes can lead to significant alterations in system dynamics. This field is crucial in various disciplines such as physics, engineering, biology, economics, and more, where systems are often described by nonlinear differential equations.

Nonlinear phenomena are prevalent in nature as the majority of real-world systems inherently exhibit nonlinear behavior. Linear behavior, in contrast, can be considered uncommon

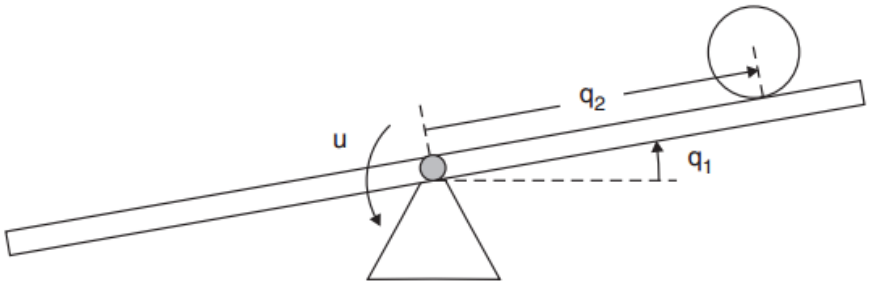

Figure 1.6: Beam and ball system

in the real world because linear systems lack the complexity to accurately describe many phenomena commonly observed in nature.

Describing nonlinear dynamics using linear models was one of the initial approaches scientists took to understand these complex systems. Linear models offer simplicity and tractability, making them easier to analyze mathematically and computationally. By approximating nonlinear systems with linear models, researchers could apply well-established tools from linear systems theory, such as Laplace transforms, eigenvalue analysis, and frequency domain analysis.

Linearization is a common technique used to approximate the behavior of a nonlinear system around an operating point by replacing it with a linear model. This involves finding the tangent or linear approximation of the nonlinear system's dynamics at the operating point. Linear models can be easier to analyze and design controllers for, especially when dealing with small perturbations around a stable operating point. However, linear models have limitations. Indeed, they are only accurate within a certain range of operation and may not capture the full behavior of nonlinear systems, especially under large perturbations or in regions of instability. As systems become more complex, nonlinear effects can become significant, rendering linear models inadequate for describing their behavior accurately.

Despite their limitations, linear models remain valuable tools in understanding and controlling nonlinear systems. They provide insight into system behavior and can serve as a starting point for analysis and controller design. However, as our understanding of nonlinear dynamics has advanced, researchers have developed more sophisticated techniques to model and control nonlinear systems directly, without relying on linear approximations. These approaches include nonlinear control methods, chaos theory, bifurcation analysis, and computational

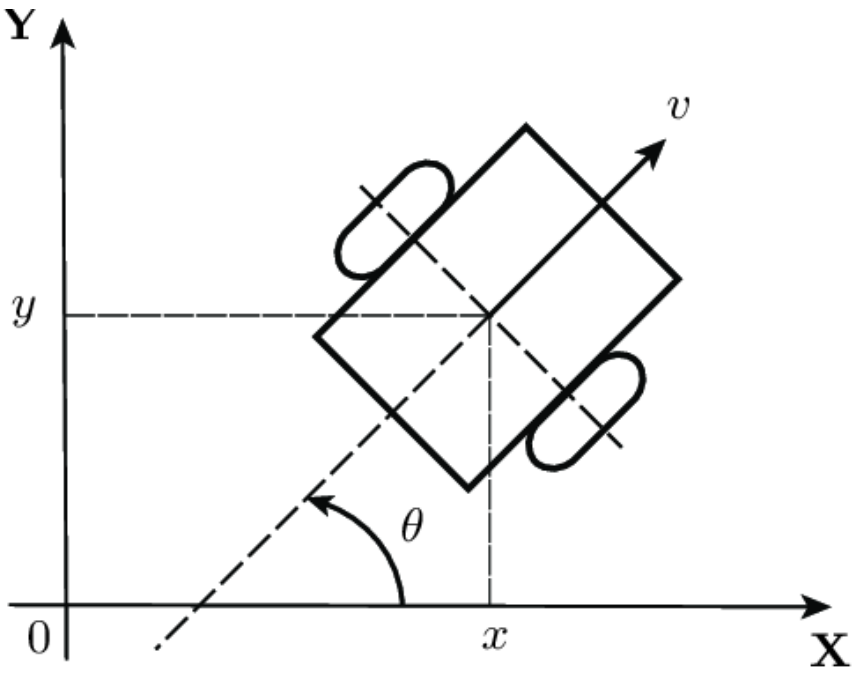

Figure 1.7: Mobile robot

techniques such as numerical simulations and nonlinear optimization.

1.2.6 Motion control of underactuated systems

In addressing the motion control of underactuated systems, researchers aim to develop control strategies that effectively exploit the system's dynamics to achieve desired behaviors. This fact can be extended to the following three problems that can be found in the literature [8]:

- Trajectory tracking: Trajectory tracking involves observing the robot's positions along with the time instances at which it reaches the desired positions. Given a dynamically feasible trajectory $q_d(t)$, the objective is to find a feedback control law that asymptotically stabilizes the tracking error $e(t) = q_d(t) - q(t)$ to zero.

- Trajectory planning: In trajectory planning, the goal is to determine a dynamically feasible trajectory that connects an initial configuration q_0 to a desired final configuration q_d.

- Set-point regulation or stabilization (path planning): Set-point regulation, also known as stabilization or path planning, is similar to trajectory planning, but without considering time constraints. The focus is solely on guiding the robot from an initial

configuration q_0 to a desired configuration q_d. The objective is to find a feedback control law that stabilizes the equilibrium state $q = q_d$ and $\dot{q} = 0$.

Path: The path represents the set of all positions where a robot positions itself while moving from point A to point B. It solely defines the robot's position and does not provide information about its velocity or acceleration. The robot may take any duration, even an entire day, to traverse from point A to point B.
Trajectory: A trajectory is a path with added time information. It not only specifies the positions but also includes velocity and acceleration values along the path. A trajectory indicates the specific time it takes for the robot to move from point$A$ to point B.
In the literature, plenty of papers have been devoted to these problems in underactuated systems. The problems of swinging up and stabilization have been extensively studied, inverted pendulums [9], under-actuated rotary inverted pendulum systems [10], the cart-pole [11], and other works address the trajectory tracking problem for instance [12], and [13] for underactuated two-wheeled mobile robot, and other works address the trajectory tracking problem in this class of systems, like in two-link underactuated manipulators in vertical plane [14], and underactuated marine surface vessels [15].

1.3 Motivations

Underactuated systems are a complex yet fascinating field of study within the realm of robotics and control systems. Control challenges associated with underactuated systems also motivate research and innovation in this field. Designing effective control strategies for underactuated systems requires innovative approaches that account for the system's unique dynamics and constraints. These control challenges provide opportunities for advancing the state-of-the-art in control theory and engineering practice.
Underactuated systems, characterized by having fewer actuators than degrees of freedom, have emerged as a compelling area of research and development in various engineering disciplines. The motivations driving the exploration and utilization of underactuated systems are diverse and multifaceted, encompassing several key factors.
A key driving factor for employing underactuated systems is their inherent efficiency. With a reduced number of actuators and control inputs relative to fully actuated systems, these systems can achieve lower energy consumption, decreased implementation costs, and enhanced overall performance. Such efficiency is especially valuable in scenarios where resources are constrained or energy conservation is a critical design objective.

Robustness represents a further key reason for utilizing underactuated systems. By leveraging passive dynamics alongside well-designed feedback control strategies, these systems can maintain stable and reliable operation even in dynamic or uncertain environments. Harnessing the system's inherent behavior allows underactuated mechanisms to tolerate disturbances and model uncertainties, making them particularly well-suited for applications that demand resilience, adaptability, and dependable performance.
Adaptability is a key characteristic of underactuated systems that motivates their exploration and development. By leveraging their inherent flexibility and agility, underactuated systems can adapt to changes in operating conditions and perform a wide range of tasks with minimal control inputs. This adaptability is particularly valuable in applications where the environment is unpredictable or where tasks require complex and dynamic motion.
Overall, the motivations of underactuated systems stem from their potential to offer efficiency, robustness, adaptability, and new challenges in control design. By understanding and addressing these motivations, researchers and engineers can continue to unlock the full potential of underactuated systems in a wide range of applications.

1.4 Brief state-of-the-art on the UMSs control

In recent decades, considerable progress has been achieved in the control of underactuated mechanical systems (UMSs). Numerous control methodologies have been developed to address the distinctive challenges posed by these systems, which feature fewer actuators than degrees of freedom. The primary objectives of these approaches are to stabilize the system, regulate its motion, and ensure the realization of desired performance, even under dynamic conditions and in the presence of uncertainties. Control strategies for underactuated mechanical systems can generally be categorized into linear and nonlinear approaches. In recent years, there has been growing interest in hybrid methods that combine the strengths of both linear and nonlinear control techniques. By integrating these approaches, researchers aim to design controllers that achieve enhanced performance, increased robustness, and greater adaptability, particularly in practical, real-world applications. The current state of UMS control thus encompasses a wide spectrum of methodologies, each with distinct advantages and associated challenges. Research in this area continues to expand our understanding of underactuated dynamics and fosters the development of innovative control solutions that improve efficiency, stability, and responsiveness across a variety of engineering applications. The following section presents a summary of several notable contributions in the field:

1.4.1 Linear control

Authors of [16] utilized linearization of the equations of motion of the rotary pendulum system around an operating point and implemented a robust LQR-based ANFIS to control the system. The integration of ANFIS was prompted by the robustness limitations of LQR.
Paper [17] has devised a hybrid controller, merging two distinct controllers: one derived from input-output linearization and the other derived from the system's energy function. This approach was applied to control the Rotary Inverted Pendulum.
In [18], the authors applied the Jacobian linearization method to linearize the ball and beam system around an operating point. They then compared the performance of two control strategies: a linear quadratic regulator (LQR) and a hybrid Proportional-Integral-Derivative (PID) combined with LQR. The study aimed to assess the effectiveness of these controllers in regulating the ball and beam system.

1.4.2 Nonlinear control

In paper [19], a nonlinear disturbance observer was developed to estimate the nonlinear terms within the Furuta model. Following this, a sliding mode control strategy was designed to regulate the system, utilizing the linear quadratic regulator (LQR) technique to determine the sliding coefficient.
In [20], the dynamics of the system are transformed, at first, into a normal form using input and state transformations. Then, a nonlinear sliding manifold and sliding mode control are introduced for the reduced-order nonlinear subsystem, commonly referred to as the Lagrangian zero dynamics.
In [21], a hierarchical sliding mode control method employing state-dependent switching gain is proposed for stabilizing underactuated mechanical systems. This controller utilizes both first-level and second-level sliding surfaces to achieve stabilization. In the same context, the paper [22] introduced a multiple-layer sliding mode controller designed for a category of underactuated systems. Initially, the system is partitioned into several subsystems. Then, one subsystem is chosen to form the first-layer sliding mode surface. This surface is then used to construct the second-layer sliding mode surface. This iterative process continues until all states of all subsystems are encompassed.
The paper [23] presents a nonlinear sliding mode observer for a category of second-order UMS. The observer is used to estimate all the states of the system. This controller ensures a good tracking performance, where the errors converge to zero asymptotically, and minimizes

the chattering phenomenon in the control signal.

The authors of [24] proposed a controller composed of a high-order sliding-mode observer to estimate the corresponding velocities, and a super-twisting controller to stabilize the origin of the system asymptotically, in the presence of coupled disturbances.

The paper [25] proposed a nonlinear sliding mode tracking controller, which can realize satisfactory tracking performance and effective swing suppression. The nonlinear dynamics without any linearization can eliminate the tracking errors rapidly in finite time by introducing an elaborately constructed sliding mode surface and simultaneously suppressing the swing. In [26], the authors first construct a coupled sliding surface to guarantee the asymptotic stability of the closed-loop dynamics. Subsequently, a fuzzy logic system is incorporated to validate and demonstrate the efficiency of the designed control strategy.

In paper [27], the approach involves combining a fast terminal sliding mode with fractional derivatives and integrals. Furthermore, the controller is enhanced by integrating an adaptation estimator, which approximates the required knowledge through a uniquely equivalent component. In the same context, authors of [28] propose a fast terminal sliding mode, and to address the chattering problem, the switching gain is adaptively tuned based on fuzzy rules. The tracking error and its differential are utilized as inputs, while the switching gain serves as the output of the fuzzy logic system.

In [29], the proposed is an improved fractional-order fast integral terminal sliding mode (FOFITSMC) technique for regulating the attitude/position of the QUAV. Additionally, adaptive laws are employed to address disturbances affecting the QUAV's position and attitude. In [30], an initial conventional Sliding Mode Control (SMC) was developed to manage the uncertainties in satellite attitude dynamics. To enhance the performance of attitude control, a Fractional Order Sliding Mode Control (FOSMC) was subsequently designed. The classical chattering problem was mitigated by incorporating the hyperbolic tangent function.

In paper [31], a two-loop control architecture was proposed. In the outer-loop, virtual velocity commands are determined to guide the subsequent work. Meanwhile, in the inner-loop, actual control inputs are designed to achieve trajectory tracking. Additionally, a novel direct adaptive neural network controller, coupled with a conditional integrator, is introduced. This controller offered robustness and adaptation capabilities for the vehicle.

The paper [32] presented a double closed-loop layered integral terminal sliding mode control method with a sliding mode observer. Initially, a sliding mode observer is developed based on the system structure. Subsequently, the outer loop controller is designed using the estimated state provided by the observer. Finally, the inner loop controller is designed using

a hierarchical sliding mode control method. In [33], a novel Fast Terminal Sliding Mode Manifold (FTSMM) is developed to address the control system's challenges. Subsequently, a supper-twisting control law (STCL) is applied to mitigate the effects of unknown nonlinear functions within the system. In [34], a Hierarchical Global Fast Terminal Sliding-Mode Controller (H-GFTSMC) is designed according to the underactuated characteristics of the system to handle the problem of large cargo swing during the operation of the bridge crane system. The authors of [35] introduced a fast terminal sliding mode control approach procedure according to the disturbance observer in the presence of external perturbations. A robust controller design is developed, ensuring that the switching manifolds converge to the equilibrium within finite time.

Overall, the state-of-the-art in UMS control encompasses a diverse range of control strategies, spanning classical and modern techniques, passive dynamics exploitation, biomimetic control, and machine learning approaches. Ongoing research in this field continues to advance our understanding of underactuated systems and develop innovative control solutions that enhance their performance, efficiency, and adaptability in various applications.

1.5 Preliminaries

In this section, some important preliminaries about the fundamentals of nonlinear systems, concepts of stability, sliding mode control, and fuzzy logic will be discussed.

1.5.1 Fundamentals of nonlinear systems

A nonlinear system is defined as a system in which the output is not directly proportional to the input, violating the principle of superposition. This means that in nonlinear systems, the combined effect of two inputs is not equal to the sum of their individual effects. Nonlinear systems are characterized by equations that involve nonlinear terms, such as products or powers of the variables. These systems exhibit complex behaviors such as bifurcations, chaos, and limit cycles. Nonlinear systems are prevalent in many fields due to their ability to describe complex and realistic behaviors. A nonlinear dynamic system can be characterized by a finite

set of nonlinear differential equations in what is known as the state-space form:

$$\begin{cases} \dot{x}_1 = f_1(x_1, x_2, ..., x_n) \\ \dot{x}_2 = f_2(x_1, x_2, ..., x_n) \\ . = . \\ . = . \\ \dot{x}_n = f_n(x_1, x_2, ..., x_n) \end{cases} \tag{1.1}$$

where $x_1, x_2, ..., x_n$ stand for the states of the system. These variables offer a comprehensive description of the system at any given moment, and $f_1, f_2...f_n$ are nonlinear functions that characterize the overall system dynamics. In this notation, the state-space system can alternatively be expressed in vector form:

$$\dot{x} = f(x) \tag{1.2}$$

where x is a $n * 1$ state vector and f is a $n * 1$ nonlinear vector function. The number of states, denoted by n, is called the order of the system. The nonlinear system (1.2) is called an autonomous system or "time-invariant system" where the evolution of the system depends only on its current state and is not explicitly influenced by time. In other words, the system's behavior is entirely determined by its internal dynamics, and there are no external inputs explicitly affecting its evolution over time.
On the other hand, a non-autonomous system (2.11) is characterized by dynamics that explicitly depend on time. This means that the behavior of the system changes over time due to external inputs, forcing functions, or time-varying parameters. The evolution of a non-autonomous system cannot be solely determined by its current state; it also depends on external factors or time-dependent functions.

$$\dot{x} = f(t, x) \tag{1.3}$$

Additionally, it's significant to mention that the state equations (1.2) and (2.11) are formulated without explicitly including an input variable u, known as the "unforced state" equation. There are two motives for employing an unforced state equation:
1- Zero Input Assumption: It provides insights into the system's behavior when the input to the system is assumed to be zero, which is relevant for understanding natural or autonomous processes.
2- Closed-loop dynamics: In the context of feedback control systems, the unforced state equation illustrates the closed-loop dynamics when the control input is determined by feedback mechanisms based on the system's current state or time. This allows for a clearer

examination of how the system responds to feedback control strategies without the influence of external inputs.

In summary, the distinction between autonomous and non-autonomous systems lies in whether the system's behavior is solely determined by its internal dynamics (autonomous) or if external factors or time explicitly influence its evolution (non-autonomous).

A broader depiction of a nonlinear system, denoting the system's plant, is a vector differential equation with n dimensions :

$$\dot{x} = f(t, x, u) \tag{1.4}$$

with $f \in R^n$ vector of nonlinear functions depending on the time variable $t \in R^+$, the input vector $u \in R^p$ and the state vector $x \in R^n$.

Most systems are nonlinear by nature, and here are some key fields where nonlinear systems play a crucial role:

Physics: Nonlinear dynamics are fundamental in various physical systems, including fluid dynamics (turbulence) [36], plasma physics [37], and nonlinear optics (such as laser dynamics) [38].

Engineering: Nonlinear systems are critical in control engineering (adaptive and robust control), mechanical engineering (vibrations and structural dynamics) [39], and electrical engineering (nonlinear circuits and signal processing) [40].

Biology: biological systems often exhibit nonlinear behavior, such as in population dynamics (predator-prey models) [41], neural networks (brain activity) [42], gene regulation, and the spread of diseases (epidemiology) [43].

Economics: economic models frequently involve nonlinear relationships, such as in market dynamics [44], and models of consumer behavior [45].

Chemistry: Nonlinear chemical dynamics can be observed in reaction kinetics (autocatalytic reactions) [46], oscillating chemical reactions (like the Belousov-Zhabotinsky reaction) [47], and complex formation processes [48].

Medicine: nonlinear dynamics are important in modeling the human body's physiological processes, such as heart rhythms (cardiac dynamics) [49], brain activity (neurodynamics) [50], and the spread of infectious diseases (epidemiological models) [51].

Ecology: ecological systems exhibit nonlinear behavior in population dynamics [52], and ecosystem stability[53]. Models often include nonlinear terms to describe the effects of carrying capacity, competition, and symbiosis.

Climate science: The climate system is highly nonlinear, with interactions between the atmosphere, oceans, ice, and land. Nonlinear models are used to predict weather patterns,

climate change [54], and extreme weather events.

Robotics: Nonlinear systems are essential in robotics because most robots depend on nonlinear dynamics such as industrial robots [55] medical robots [56], service robots [57] underactuated robotics [58].

Social Sciences: Nonlinear models are used to study social dynamics, including the spread of information or behaviors through populations, opinion formation, and group decision-making processes [59].

These fields leverage the unique capabilities of nonlinear models to capture and predict the intricate behaviors and interactions that linear models cannot adequately describe.

1.5.2 Concepts of stability

Stability is a fundamental concept in the analysis and design of dynamic systems, playing a critical role in control theory and system dynamics. It describes a system's ability to maintain its state or return to a desired condition following disturbances or perturbations. A thorough understanding of stability is essential for ensuring that systems operate predictably and safely under a variety of conditions. This section examines the fundamental principles of stability, with particular emphasis on nonlinear systems, which frequently arise in practical applications and exhibit more complex behavior than their linear counterparts. Conducting stability analysis is key to designing systems that are both robust and reliable across multiple domains, including engineering and robotics. By guaranteeing that a system can tolerate external perturbations and return to equilibrium, we ensure its safe and effective operation. The discussion that follows addresses different forms of stability and the analytical methods employed to assess stability in nonlinear dynamic systems.

1.5.2.1 Equilibrium stability

Equilibrium stability is a crucial aspect of stability analysis in dynamic systems. It focuses on the behavior of a system when it is at or near an equilibrium point, often chosen to be the origin in state-space. Here are the key concepts related to equilibrium stability:

1.5.2.2 Stable equilibrium

A stable equilibrium point x_e indicates that the system's state remains proximate to x_e despite small perturbations.

Definition 1.5.1. *For every $\epsilon > 0$, there exists a $\delta > 0$ such that :*

$$||x_e|| < \delta \Rightarrow ||x(t)|| < \epsilon, \forall t \geq 0 \tag{1.5}$$

1.5.2.3 Asymptotically stable equilibrium

An asymptotically stable equilibrium point $x_e$not only withstands small perturbations but also facilitates the system's return to x_e over time.

Definition 1.5.2.

$$||x_e|| < \delta \Rightarrow \lim_{x \to \infty} x(t) \tag{1.6}$$

1.5.2.4 Exponentially stable equilibrium

Exponential stability of an equilibrium pointx_e denotes its asymptotic stability with a rapid rate of convergence towards x_e

Definition 1.5.3. *(Exponentially Stable Equilibrium): There exist positive constants α, γ such that*

$$||x(t)|| < \alpha||x_e||e^{-\gamma t}, \forall t \geq 0 \tag{1.7}$$

1.5.2.5 Global stability

An equilibrium point x_e is considered globally stable (asymptotically or exponentially) if it satisfies the stability conditions given in Definitions (1.5.1) (1.5.3) for all initial states $x(t)$. Otherwise, the behavior of the system is characterized only locally.
The theory of equilibrium stability provides a structured approach to analyzing and ensuring the stability of systems. By defining stable, asymptotically stable, exponentially stable, and globally stable equilibrium points, this theory helps in designing systems that can withstand perturbations and maintain or return to their desired states efficiently and reliably. Understanding these stability concepts is essential for creating robust and resilient dynamic systems across various applications.

1.5.2.6 Lyapunov stability

Lyapunov stability is named after Russian mathematician Aleksandr Lyapunov, who introduced the theory in the late 19th century. Lyapunov stability can be used to study the stability of systems in a local or global form. The global analysis describes the stability properties in the whole state-space, and the local analysis deals with stability in a neighborhood of the equilibrium point.

Theorem 1. *let x_e be an equilibrium point of the system (1.2) and $V(x)$ be a continuously differentiable function such that: $V(0) = 0$ and $V(x) > 0$ if $x \neq 0$. The derivative of V along the trajectories of (1.2) denoted by $\dot{V}$ is given by :*

$$\dot{V} = \sum_{n}^{i=1} \frac{\partial V}{\partial x_i} \dot{x}_i \tag{1.8}$$

Theorem 2. *If the Lyapunov function V is positive definite and its time derivative $\dot{V}$ is negative semidefinite, the equilibrium at the origin x_e is stable. When these conditions are satisfied over the entire state space, the stability is said to be global.*

1.5.2.7 Stability

The system remains close to x_e when perturbed

Theorem 3. *If V is positive definite and $\dot{V}$ is negative definite, then the origin is asymptotically stable.*

1.5.2.8 Asymptotic stability

The system not only remains close to x_e but also returns to it over time, as long as the initial state is within this neighborhood. Furthermore, if $V(x) \to \infty$ as $||x|| \to \infty$ and V is radially unbounded, then the origin is globally asymptotically stable.

1.5.2.9 Exponential stability

Theorem 4. *If $\alpha||x||^2 \leq V(x) \leq \beta||x||^2$ and $\dot{V} \leq \gamma||x||^2$ with α, β, γ positive constants, then the origin is exponentially stable. If the conditions in the theorem are satisfied in the whole state space, then the origin is globally exponentially stable.*

Exponential stability is stronger than the stability that not only ensures that the system's state converges to an equilibrium point but also specifies that this convergence occurs at an

exponential rate. This type of stability is important for systems where rapid convergence is critical.

If such a function V exists and satisfies the conditions in Theorems (1.5.2.7), (1.5.2.8), or (4), it is referred to as a Lyapunov function for the system (1.2). This function demonstrates that the system's origin is stable, asymptotically stable, or exponentially stable, respectively. For more comprehensive and detailed studies on Lyapunov's direct method for general systems, refer to [60].

1.6 Conclusion

In this chapter, we have conducted an in-depth examination of underactuated mechanical systems (UMSs), highlighting both their theoretical importance and the practical difficulties they pose. By definition, UMSs are characterized by having fewer control inputs than degrees of freedom, a feature that renders their modeling, analysis, and control considerably more challenging than fully actuated systems. This inherent limitation gives rise to complex issues, including pronounced nonlinearities, strong internal coupling, and the risk of instability, which have served as the impetus for extensive research within the control systems community over the past several decades.

We began by outlining the fundamental background and classification of underactuated systems, supported by illustrative examples drawn from robotics, aerospace, and marine engineering. These examples demonstrated the practical significance of UMSs, particularly in modern applications where cost reduction, energy efficiency, and design constraints often necessitate systems with fewer actuators. The discussion also highlighted how the inherent underactuation creates both theoretical challenges and opportunities for innovation in advanced control methodologies.

Following this, we examined a range of control architectures and advanced techniques designed to manage systems with fewer actuators than degrees of freedom. Key theoretical concepts, including Lyapunov's direct method, were also introduced to provide a solid analytical foundation. This groundwork establishes the necessary understanding of underactuated systems and their associated control strategies, serving as a basis for the discussions and developments presented in the subsequent chapters.

Overall, this chapter has provided the groundwork for the more advanced developments presented in the following chapters. By establishing the fundamental properties, challenges, and control considerations of UMSs, it sets the stage for the design and evaluation of innovative

control strategies tailored to underactuated dynamics.
In the subsequent chapter, an enhanced sliding mode control strategy without a reaching phase will be developed for underactuated mechanical systems. By preserving the inherent robustness of sliding mode control while removing the reaching phase, the proposed approach will offer an effective and practically viable solution for contemporary engineering applications.

Chapter 2

Enhanced free reaching phase SMC for UMS

2.1 Introduction

In this chapter, a free-reaching phase sliding mode control (SMC) is developed for underactuated mechanical systems (UMS). Initially, the dynamic model of underactuated systems is introduced, derived by employing the Euler-Lagrange equation while taking into consideration the presence of disturbances and uncertainties. Then, an overview and structure of sliding mode control is presented to establish the foundation for the subsequent development. Followed by the development of free-reaching phase sliding mode control (SMC) for underactuated mechanical systems (UMS). The control law is constructed such that the system states are constrained to remain on the designed sliding surface from the very beginning of operation. This design choice effectively suppresses transient errors and ensures smooth convergence. Then the stability and convergence properties of the scheme are rigorously analyzed through Lyapunov theory, demonstrating that all system trajectories are bounded and asymptotically approach the desired states. Finally, to further validate the effectiveness of the method, a comparative study is carried out to evaluate the performance of the suggested control strategy against other control techniques. The results of this analysis confirm the superiority of the proposed strategy in terms of robustness, precision, and overall capability to manage the inherent complexities of underactuated mechanical systems.

As discussed in the previous chapter, the control of underactuated systems has been widely studied due to the inherent challenges they present. Various control techniques have been employed to address these challenges, ranging from classical methods to modern, sophisti-

cated approaches. To name a few: in [61], the sliding surface function comprises two parts to eliminate the reaching phase of the SMC, a temporary and a classical sliding surface. The controller is designed in a way that guarantees the temporary sliding surface's exponential convergence to the classical sliding surface. Based on [61], the study in [62] expands the method to use the state-dependent Ricci equation to provide an ideal sliding surface for a class of nonlinear systems.

In [63] and for arbitrary beginning circumstances, the tracking errors are adjusted to guarantee that the system response starts on the sliding surface. Authors of [64] suggested a sliding mode controller with a time-varying surface to improve the uncertain dynamical systems' second-order tracking behavior. To expand the method to n^{th} order systems, an efficient version of [64] is described in [65], and in [66]. The sliding surface is modified to enable the system to get started on the surface, effectively eliminating the chattering phenomenon. To approximate the unknown dynamics of the system, the authors then suggested a Type-2 fuzzy system.

Authors of [67] and [68] proposed adjusting the slope of the sliding surface based on the tracking error, and then to compensate for the effect of the unknown dynamics, they developed an improved version of the wavelet neural network technique. In [69], to drive the pendubot system in the direction of the sliding surface, a sliding mode controller is introduced. In [70], a Lyapunov function with suitable criteria for SMC was constructed in terms of linear matrix inequalities (LMI) to avoid the chattering phenomenon. Sliding modes and optimum nonlinear control are combined in the suggested control. An optimal sliding surface is defined by the optimal controller. Then, by combining the benefits of optimality and robustness from both control methodologies, the optimal surface is used to synthesize a super-twisting controller.

The key contribution of this chapter is the development of a free-reaching phase sliding mode control (SMC) strategy for underactuated mechanical systems. Unlike conventional sliding mode control, where robustness is only guaranteed after the system trajectories reach the sliding manifold, the proposed approach ensures that the system states remain on the designed sliding surface from the initial instant of operation. This eliminates the reaching phase, thereby maintaining invariance against uncertainties and external disturbances throughout the entire system response. By integrating this formulation into the context of underactuated systems, the proposed method enhances stability, improves transient performance, and provides a more reliable framework for controlling systems characterized by nonlinear dynamics and limited actuation.

2.2 UMS modeling

Over the past three decades, the analysis and modeling of underactuated mechanical systems (UMSs) have become a central topic in control engineering and robotics. By definition, these systems feature fewer independent control inputs than degrees of freedom, creating an intrinsic imbalance that distinguishes them from fully actuated systems. This underactuation is not merely a technical limitation; it is a fundamental structural property that affects every aspect of system modeling, analysis, and control design. Such a feature often arises naturally in practical applications due to design simplifications, actuator constraints, cost considerations, or operational limitations. For example, aerospace vehicles may be underactuated because it is impractical to install actuators along all rotational axes, while robotic manipulators may include passive joints to reduce weight and energy consumption. The inherent characteristics of UMSs present both theoretical challenges and practical significance, as they embody the trade-offs between system complexity, controllability, and performance. Consequently, precise mathematical modeling is essential, providing the foundation for rigorous stability analysis and enabling the development of control strategies specifically tailored to the unique dynamics of these systems.

Several modeling methods can be applied to complete mechanical systems, including the Newton-Euler approach[71], Kane's method[72], the principle of virtual work [73], and the Lagrange method[74]. Nevertheless, when dealing with underactuated systems, researchers often favor the Lagrangian or Euler–Lagrange framework. This preference arises because these formalisms provide a systematic and compact way to derive equations of motion while naturally incorporating constraints and nonlinear couplings. They also produce structured models that clearly separate inertia, Coriolis, and gravitational effects, which is particularly useful for control design and stability analysis.

2.2.1 Lagrangian system

The Lagrangian formulation of mechanics provides a systematic framework for deriving the equations of motion of complex systems, making it one of the most widely used approaches in modern engineering and control research. Unlike the Newtonian method, which focuses on individual forces and accelerations, the Lagrangian perspective is based on scalar energy functions that capture the overall dynamics of the system in a compact form. This not only simplifies the modeling of systems with multiple interconnected components but also offers a more general way of incorporating constraints and nonlinear interactions.

By employing the Lagrangian equation of motion as the underactuated mechanical system model, let $q \in Q$ be the vector of generalized coordinates, representing the system's configuration, and the kinetic energy K of the system is typically a function of the generalized coordinates and their time derivatives $\dot{q}$:

$$K = \frac{1}{2}\dot{q}^T M(q)\dot{q} \tag{2.1}$$

where $M(q) \in R^{n*n}$ is the inertia matrix.
V is a function of the generalized coordinates $V = V(q)$. The Lagrangian L is defined as the difference between the kinetic and potential energies as [75]:

$$L(q, \dot{q}) = K - V = \frac{1}{2}\dot{q}^T M(q)\dot{q} - V(q) \tag{2.2}$$

The Euler-Lagrange equations are used to derive the equations of motion from the Lagrangian. For each generalized coordinate q_i, the Euler-Lagrange equation is given by:

$$\frac{d}{dt}(\frac{\partial L}{\partial q}) - \frac{\partial L}{\partial q} = F(q)u \tag{2.3}$$

$u \in R^m$ is the input vector and $F(q) = (f_i(q), -..., f_m(q)) \in R^{n*m}$ is the matrix of external forces.
One of the main advantages of adopting the Lagrangian formalism lies in the invariance of the Euler–Lagrange equations, which retain their structure regardless of the chosen coordinate system. This property makes the approach particularly powerful. It allows obtaining the equation describing the evolution of mechanical systems as a function of the applied forces. Using this approach, the equations of motion can be expressed as:

$$\sum_j m_{kj}(q)\,\ddot{q}_j \;+\; \sum_{i,j} \Gamma^k_{ij}(q)\,\dot{q}_i\,\dot{q}_j \;+\; g_k(q) \;=\; e_k^T F(q)u, \qquad k = 1, \ldots, n, \tag{2.4}$$

where e_k is the k^{th} standard basis in R^n,$g(q) \in R^n$ is the generalized gravitational, and $\Gamma^k_{ij}(q)$ corresponds to the Christoffel symbols defined as:

$$\Gamma_{kij}(q) = \tfrac{1}{2}\left(\frac{\partial m_{kj}(q)}{\partial q_i} + \frac{\partial m_{ki}(q)}{\partial q_j} - \frac{\partial m_{ij}(q)}{\partial q_k}\right), \qquad i, j, k = 1, \ldots, n. \tag{2.5}$$

The vector form can be rewritten as:

$$M\ddot{q} + C(q, \dot{q})\dot{q} + G(q) = F(q)u + d(t) \tag{2.6}$$

where $C(q, \dot{q} \in R^{n*n})$ contains Coriolis and centrifugal terms, $G(q) \in R^{n*1}$ is the gravitational term, and $d(t) \in R^m$ is the uncertainty term that encompass unknown external disturbances.

Definition 2.2.1. *Assuming that $F(q)$ is an invertible matrix and that $m = rankF(q) = n$, we refer to (2.6) as a fully-actuated mechanical system. The number of control inputs for fully-actuated systems is equal to the configuration manifold's dimension.*

Definition 2.2.2. *If $m = rankF(q) < n$, then the system is called an Underactuated Mechanical System (UMS)*

Definition 2.2.3. *If $m = rankF(q) > n$, then the system is called an over-actuated system.*

Assuming $F(q) = [0\ I_m]^T$ we denote the unactuated and actuated configuration as $q_u \in R^{n-m}$ and $q_a \in R^m$, respectively. The configuration vector can be partitioned as $q = [q_u\ q_a]^T$ and the UMS motion equations can be re-expressed as:

$$\begin{bmatrix} M_u \\ M_a \end{bmatrix} \begin{bmatrix} \ddot{q}_u \\ \ddot{q}_a \end{bmatrix} + \begin{bmatrix} C_u(q,\dot{q}) \\ C_a(q,\dot{q}) \end{bmatrix} \begin{bmatrix} \dot{q}_u \\ \dot{q}_a \end{bmatrix} + \begin{bmatrix} G_u(q) \\ G_a(q,) \end{bmatrix} = \begin{bmatrix} 0 \\ u \end{bmatrix} \tag{2.7}$$

with $M_u \in R^{(n-m)*n}$, $M_a \in R^{m*n}$, $C_u(q,\dot{q}) \in R^{(n-m)*n}$, $C_a(q,\dot{q}) \in R^{m*n}$, $G_u(q) \in R^{n-m}$ and $G_a(q) \in R^m$. where the subscripts u and a denote the unactuated and actuated parts of the system, respectively. In, [76, 77], the partitioned model was written as:

$$\begin{bmatrix} M_{11} & M_{12} \\ M_{21} & M_{22} \end{bmatrix} \begin{bmatrix} \ddot{q}_u \\ \ddot{q}_a \end{bmatrix} + \begin{bmatrix} F_1 \\ F_2 \end{bmatrix} = \begin{bmatrix} 0 \\ u \end{bmatrix} \tag{2.8}$$

where F_1F_2 contains centripetal, Coriolis, and gravitational terms. By considering $q = [q_1\ q_2]^T$, dynamics of the underactuated system takes the form:

$$\begin{aligned} M_{11}(q)\ddot{q}_1 + M_{12}(q)\ddot{q}_2 + F_1 = 0 \\ M_{21}(q)\ddot{q}_1 + M_{22}(q)\ddot{q}_2 + F_2 = u \end{aligned} \tag{2.9}$$

The cascaded form of the underactuated system model can be expressed using state variables x. This formalism simplifies the analysis and design of control laws by separating the dynamics of the system into more manageable components. Let the state variables be defined as follows$x = [x_1\ x_2\ ...\ x_m]^T$ with $x_1 = q_1$, $x_2 = q_2$,..., $x_m = q_m$, to obtain the following cascaded representation [21]:

$$\begin{pmatrix} \dot{x}_1 \\ \dot{x}_2 \\ \dot{x}_3 \\ \dot{x}_4 \\ . \\ \dot{x}_{2m-1} \\ \dot{x}_{2m} \end{pmatrix} = \begin{pmatrix} x_2 \\ f_1(x) \\ x_4 \\ f_2(x) \\ . \\ x_{2m} \\ f_{2m}(x) \end{pmatrix} + \begin{pmatrix} 0 \\ g_1(x) \\ 0 \\ g_2(x) \\ . \\ 0 \\ g_m \end{pmatrix} U + \begin{pmatrix} 0 \\ d_1(x) \\ 0 \\ d_2(x) \\ . \\ 0 \\ d_m(x) \end{pmatrix} \tag{2.10}$$

The terms $d_1(x)$ ... $d_m(x)$ represent the uncertainties and disturbances assumed to be bounded.
The global cascaded state model is given as [21]:

$$\begin{pmatrix} \dot{x}_{2k-1} \\ \dot{x}_{2k} \end{pmatrix} = \begin{pmatrix} x_{2k} \\ A_k(x) \end{pmatrix} + \begin{pmatrix} 0 \\ B_k(x) \end{pmatrix} U + \begin{pmatrix} 0 \\ d(x)_k \end{pmatrix} \tag{2.11}$$

Taking into consideration the two UMS degrees of freedom, $n = 2$ and $m = 1$, the dynamics in (2.10) change to:

$$\begin{cases} \dot{x}_1 = x_2 \\ \dot{x}_2 = f_1(x) + g_1(x)u + d_1(x) \\ \dot{x}_3 = x_4 \\ \dot{x}_4 = f_2(x) + g_2(x)u + d_2(x) \end{cases} \tag{2.12}$$

Assumption 1. *The uncertain terms are bounded by:* $|d_1(x)| \leq \rho_1$ *and* $|d_2(x)| \leq \rho_2$ *, where* ρ_1 *and* ρ_2 *are known positive constants.*

Definition 2.2.4. *(Degree of underactuation): The degrees of freedom in a system that are not directly controllable are referred to as its degree of underactuation.*

In table 2.1, we present a summary of the dynamic models for several representative underactuated systems, offering a foundation for understanding their intrinsic complexities and the challenges involved in their control. In the design of controllers, the primary goal is to develop a control law capable of guiding the system states to the desired equilibrium efficiently and reliably. Special attention is given to ensuring that this convergence is maintained in the presence of external disturbances and uncertainties in the system model, thereby providing both robust performance and overall stability.

2.3 Sliding mode control

Sliding Mode Control (SMC), also known as Variable Structure Control with a Sliding Mode [78], is a robust control methodology specifically developed to manage nonlinear dynamic systems. Its strength lies in its ability to maintain performance and stability even when the system is subject to modeling uncertainties or external disturbances, which makes it particularly valuable for engineering applications that demand high reliability and precision.
Since its initial development in the late 1950s as a variable structure control method [79],

System	$M(q)$	$C(q,\dot{q})$	$G(q)$	$F(q)$
crane system	$\begin{bmatrix} M+m & -ml\cos(\theta) \\ -ml\cos(\theta) & ml^2 \end{bmatrix}$	$\begin{bmatrix} 0 & ml\sin(\theta)\dot{\theta} \\ 0 & 0 \end{bmatrix}$	$\begin{bmatrix} 0 \\ -mgl\sin(\theta) \end{bmatrix}$	$\begin{bmatrix} 1 \\ 0 \end{bmatrix}$
Inverted pendulum	$\begin{bmatrix} M+m & -ml\cos(\theta) \\ -ml\cos(\theta) & ml^2 \end{bmatrix}$	$\begin{bmatrix} 0 & ml\sin(\theta)\dot{\theta} \\ 0 & 0 \end{bmatrix}$	$\begin{bmatrix} 0 \\ -mgl\sin(\theta) \end{bmatrix}$	$\begin{bmatrix} 1 \\ 0 \end{bmatrix}$
TORA	$\begin{bmatrix} M+m & ml\cos\theta \\ ml\cos\theta & J+ml^2 \end{bmatrix}$	$\begin{bmatrix} 0 & -ml\dot{\theta}\sin\theta \\ 0 & 0 \end{bmatrix}$	$\begin{bmatrix} 0 \\ -mgl\sin\theta \end{bmatrix}$	$\begin{bmatrix} 1 \\ 0 \end{bmatrix}$
VTOL	$\begin{bmatrix} m & 0 & 0 \\ 0 & m & 0 \\ 0 & 0 & J \end{bmatrix}$	$\begin{bmatrix} 0 & 0 & 0 \\ 0 & 0 & 0 \\ 0 & 0 & 0 \end{bmatrix}$	$\begin{bmatrix} 0 \\ mg \\ 0 \end{bmatrix}$	$\begin{bmatrix} -s_3 & nC_3 \\ C_3 & nS_3 \\ 0 & 0 \end{bmatrix}$
Beam-and-Ball System	$\begin{bmatrix} I+mr^2 & -mr\cos(\theta) \\ -mr\cos(\theta) & m \end{bmatrix}$	$\begin{bmatrix} 0 & mr\sin(\theta)\dot{\theta} \\ 0 & 0 \end{bmatrix}$	$\begin{bmatrix} -mgr\sin(\theta) \\ 0 \end{bmatrix}$	$\begin{bmatrix} 1 \\ 0 \end{bmatrix}$
Acrobot	$\begin{bmatrix} I_1+I_2+m_1l_{c1}^2+m_2(l_1^2+l_{c2}^2+2l_1l_{c2}\cos(\theta_2)) & I_2+m_2(l_{c2}^2+l_1l_{c2}\cos(\theta_2)) \\ I_2+m_2(l_{c2}^2+l_1l_{c2}\cos(\theta_2)) & I_2+m_2l_{c2}^2 \end{bmatrix}$	$\begin{bmatrix} -m_2l_1l_{c2}\sin(\theta_2)\dot{\theta}_2 & -m_2l_1l_{c2}\sin(\theta_2)(\dot{\theta}_1+\dot{\theta}_2) \\ m_2l_1l_{c2}\sin(\theta_2)\dot{\theta}_1 & 0 \end{bmatrix}$	$\begin{bmatrix} (m_1l_{c1}+m_2l_1)g\cos(\theta_1)+m_2l_{c2}g\cos(\theta_1+\theta_2) \\ m_2l_{c2}g\cos(\theta_1+\theta_2) \end{bmatrix}$	$\begin{bmatrix} 0 \\ 1 \end{bmatrix}$
Pendubot	$\begin{bmatrix} I_1+I_2+m_1l_{c1}^2+m_2(l_1^2+l_{c2}^2+2l_1l_{c2}\cos(\theta_2)) & I_2+m_2(l_{c2}^2+l_1l_{c2}\cos(\theta_2)) \\ I_2+m_2(l_{c2}^2+l_1l_{c2}\cos(\theta_2)) & I_2+m_2l_{c2}^2 \end{bmatrix}$	$\begin{bmatrix} -m_2l_1l_{c2}\sin(\theta_2)\dot{\theta}_2 & -m_2l_1l_{c2}\sin(\theta_2)(\dot{\theta}_1+\dot{\theta}_2) \\ m_2l_1l_{c2}\sin(\theta_2)\dot{\theta}_1 & 0 \end{bmatrix}$	$\begin{bmatrix} (m_1l_{c1}+m_2l_1)g\cos(\theta_1)+m_2l_{c2}g\cos(\theta_1+\theta_2) \\ m_2l_{c2}g\cos(\theta_1+\theta_2) \end{bmatrix}$	$\begin{bmatrix} 1 \\ 0 \end{bmatrix}$

Table 2.1: Dynamic modeling of several representative underactuated systems

and later its application to robotic systems by Slotine and Asada in 1986 [80], sliding mode control (SMC) has emerged as a powerful framework for addressing the control of uncertain and nonlinear dynamical systems [81]. Its capacity to maintain stability and robust performance in the presence of modeling inaccuracies and external disturbances has made it a widely adopted strategy across various engineering disciplines.
The fundamental idea behind SMC is to force the system's state to reach and remain on a predefined surface, known as the sliding surface. Once the state is on this surface, the system exhibits desired dynamic behaviors that are robust to disturbances and model uncertainties. By transforming a higher-order system into a first-order system, SMC simplifies the control problem, ensuring the system's performance is maintained even in the presence of uncertainties.

2.3.1 Fundamentals of a sliding mode controller

The fundamental concept of SMC lies in the design of a control law that drives system trajectories toward the sliding surface and maintains them on it thereafter. The sliding surface is typically defined as a linear or nonlinear function of the system states, and its design reflects the desired closed-loop behavior. The control strategy is generally divided into two phases:"sliding mode" and "reaching mode" [82].

2.3.1.1 Reaching phase

When the sliding surface is non-zero. During this stage, the control law ensures that trajectories are driven toward the sliding manifold (see figure 2.1).

2.3.1.2 Sliding phase

When the sliding surface equals zero, and once on the manifold, the system evolves according to the reduced-order dynamics, which are insensitive to matched uncertainties and disturbances (see figure 2.1).

2.3.2 Structure of a sliding mode controller

The design methodology of a Sliding Mode Controller (SMC) is typically organized into three fundamental stages: defining the sliding surface in the first phase to ensure that the necessary criteria are satisfied, determining the sliding condition, and calculating the control

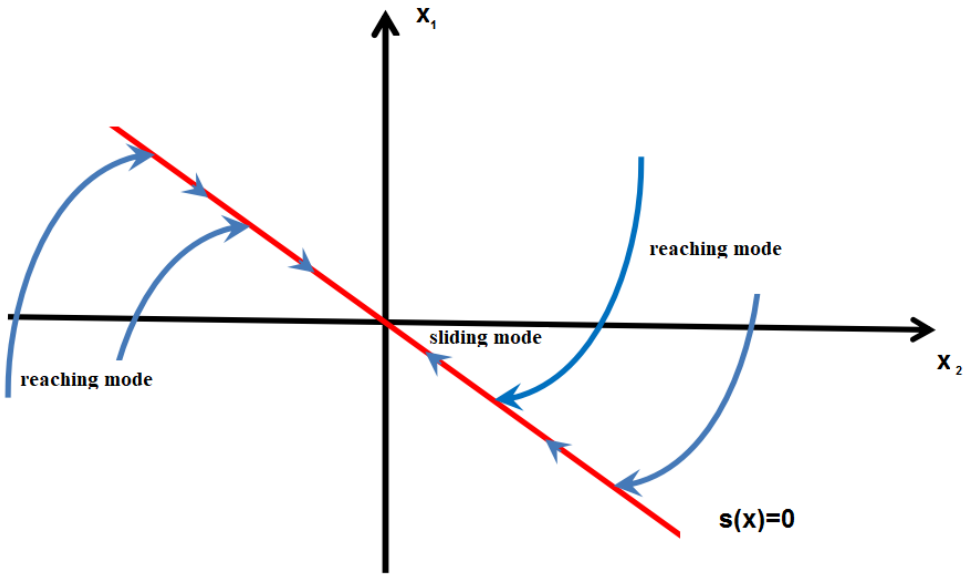

Figure 2.1: Sliding surface

input. The figure 2.2 illustrates the block diagram representing the design framework of the sliding mode control (SMC) scheme.

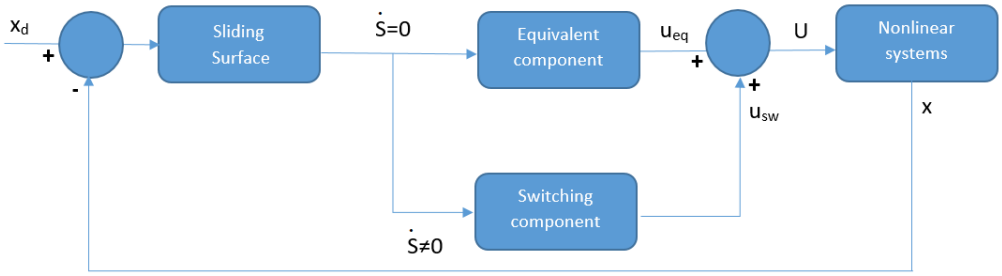

Figure 2.2: Block diagram of SMC

2.3.3 Define the sliding surface

To design a sliding mode surface S so that the desired design requirements are met, the following criteria should be satisfied:

- The order of S should be less than the order of the plant.
- The derivative of S should be continuous and contains the control input u.

As S approaches zero, the tracking error e should also approach zero, ensuring that the system's performance meets the desired specifications. Usually a time-varying sliding surface $s(t)$ is simply defined in the state-space R^n by the scalar equation, given by [83]:

$$S = (\frac{d}{dt} + c)^{n-1}x = c_1x + c_2\dot{x} + .. + c_{n-1}x^{n-2} + x^{n-1} \tag{2.13}$$

where c_i are positive constants. x is the system state or tracking error, and n denotes the order of the system.

2.3.4 Determining the sliding condition

To guarantee that trajectories reach the sliding surface, a convergence condition must be imposed. This requirement, often called the sliding or reaching condition, ensures that the sliding variable diminishes consistently. A common mathematical form is:

$$S\dot{S} < 0 \tag{2.14}$$

This inequality establishes that the surface is attractive, meaning the system states are directed toward it despite disturbances or model uncertainties. The sliding condition thus plays a crucial role in ensuring accessibility of the manifold.

2.3.5 Design the control law

The final stage involves designing the control input that enforces both the reaching condition and invariance of the trajectories on the sliding surface. The control law typically contains two components:

2.3.5.1 Equivalent Control

It represents the continuous part of the control input, and it is derived by setting the sliding variable derivative to zero ($s(x,t) = 0$) under the assumption that the system remains on the sliding surface. This term is responsible for ensuring that the system dynamics follow the desired trajectory when sliding occurs.

2.3.5.2 Switching control

It introduces a discontinuous term designed to drive the system toward the sliding surface during the reaching phase, and it ensures robustness against matched disturbances and

parameter uncertainties. Typically, this term is expressed as a signum or saturation function,e.g.:

$$u_{sw} = -ksign(S) \tag{2.15}$$

where K is a positive gain that guarantees the reaching condition.
Thus, the total control law is expressed as:

$$u = u_{eq} - u_{sw} \tag{2.16}$$

where u_{eq} is called the equivalent control input.
This structure ensures that the system converges to the sliding surface and remains there, achieving the dual objectives of accuracy and robustness. However, the discontinuous nature of u_{sw} can lead to chattering 2.3 , a practical limitation that requires mitigation strategies such as boundary layers, higher-order SMC, or smooth approximation functions.

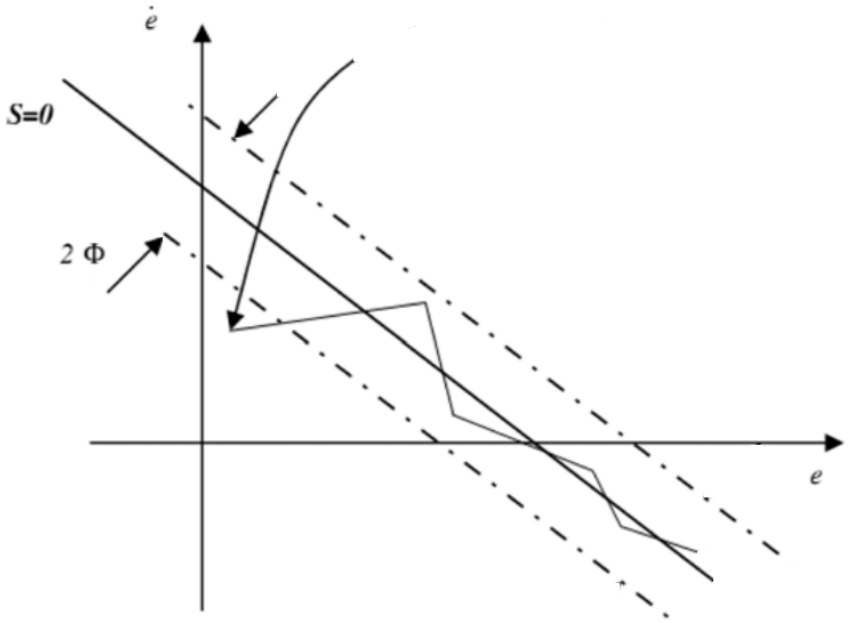

Figure 2.3: Chattering phenomenon

2.3.6 Robustness and chattering phenomenon

A key advantage of sliding mode control (SMC) lies in its intrinsic robustness to variations in system parameters and matched external disturbances. Because the system's behavior on the sliding manifold is largely independent of such uncertainties, SMC can maintain desired

performance without requiring precise knowledge of all model parameters. Nevertheless, the discontinuous switching inherent to conventional SMC often produces a high-frequency oscillation known as chattering. This phenomenon can inadvertently excite unmodeled dynamics and, in practical implementations, may result in actuator wear or reduced control effectiveness. To address these limitations, numerous enhancements have been developed, including boundary layer approaches, higher-order sliding mode techniques, and intelligent control strategies.

1. **Boundary-layer methods**: The most common approach replaces the $sign(.)$ function with a smoother function, thereby reducing oscillations near the sliding manifold while maintaining robustness. Some representative approaches include:

   - Saturation function: This function ensures a linear transition close to the sliding surface, reducing abrupt switching and smoothing the control signal:

$$sat(\frac{s}{\varphi}) = \begin{cases} sign(\frac{s}{\varphi}) if |\frac{s}{\varphi}| \geq 1 \\ \frac{s}{\varphi} if |\frac{s}{\varphi}| < 1 \end{cases} \tag{2.17}$$

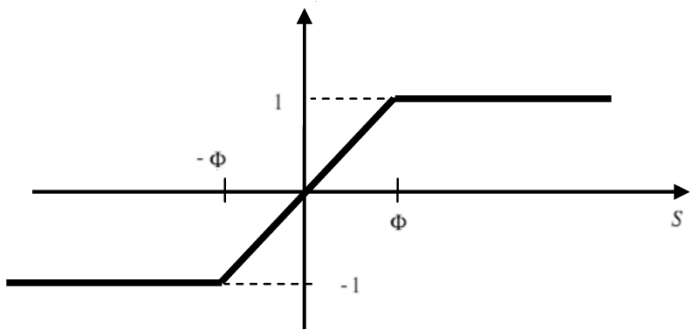

Figure 2.4: Saturation function

   - Hyperbolic tangent function: continuous approximation given by:

$$\tanh(s) = \frac{e^s - e^{-s}}{e^s + e^{-s}} \tag{2.18}$$

     The $tanh(.)$ function (2.5) provides a continuous and smooth transition around the sliding surface, effectively reducing chattering by smoothing out the control signal.

   - Sigmoid-type function:

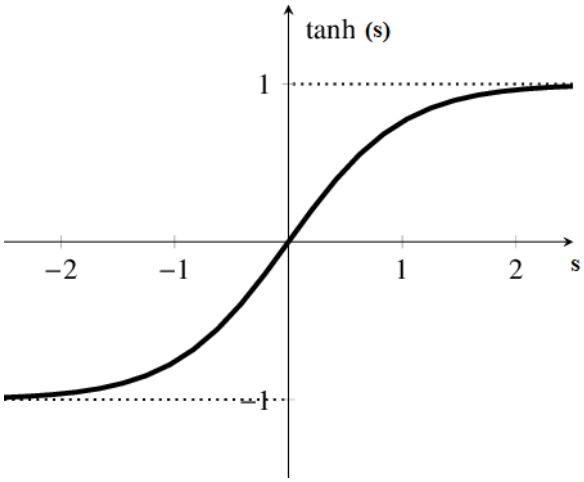

Figure 2.5: Hyperbolic tangent function

- According to the different system, we can design the various approach law, such as:
  Constant plus proportional rate reaching [84]:

$$u_{sw} = -k_1 sign(S) - k_2 S \qquad with \qquad k_1, k_2 > 0 \tag{2.19}$$

  The power rate reaching law is expressed as [84]:

$$u_{sw} = -q|s(t)|^{\varphi} sign[s(t)] \qquad with \qquad q > 0 \qquad and \qquad 0 < \varphi < 1 \tag{2.20}$$

  Author of article [85] proposed the following reaching law:

$$u_{sw} = k[s(t)]s(t) \qquad with \qquad k_1 > 0 \tag{2.21}$$

$$k[s(t)] = \frac{-k_1 s_0}{s_0 + |s(t)|} \tag{2.22}$$

2. **Higher-order SMC:** Unlike conventional SMC, where discontinuity is directly applied to the control input to enforce $s = 0$, HOSMC extends this idea by constraining not only the sliding variable but also its derivatives. This ensures that the switching effect appears in higher derivatives rather than the control input itself, leading to smoother actuation.

3. **Integration with other methods:** Techniques such as fuzzy logic systems, neural networks, and adaptive approximators are integrated with SMC to estimate uncertainties and disturbances smoothly. These methods reduce the amplitude of the switching control, thereby suppressing chattering while maintaining robustness.

2.3.7 Extensions of sliding mode control

Sliding mode control (SMC) has several extensions and refinements since its original introduction. These developments aim to enhance robustness and reduce practical challenges such as chattering. The most notable variants include conventional first-order SMC, higher-order SMC, integral SMC, terminal SMC, and fast terminal SMC.

- **Integral sliding mode control (ISMC):** Integral sliding mode control addresses the problem of the reaching phase inherent in conventional SMC. In standard approaches, uncertainties may affect the system before the states arrive at the sliding surface. ISMC eliminates this issue by embedding integral terms in the surface design, ensuring that the system trajectory lies on the sliding manifold from the initial moment. A typical integral sliding surface is expressed as:

$$(\frac{d}{dt} + \gamma)^{n-1} e(t) + K_i \int_0^t e(\tau) d\tau \tag{2.23}$$

  $K_i$is integral positive gain,$\gamma$is positive constant. This formulation incorporates both differential and integral components of the error. The differential part ensures responsiveness and dynamic performance, while the integral term improves accuracy by compensating for constant disturbances and model uncertainties.

- **Terminal sliding mode control (TSMC):** To address the relatively slow convergence of traditional sliding mode control, Terminal Sliding Mode Control (TSMC) was developed. Unlike conventional SMC, which ensures only asymptotic convergence of tracking errors, TSMC employs nonlinear sliding surfaces that drive the system states to their desired values within a finite time. This rapid convergence is achieved by embedding nonlinear error terms—frequently expressed as fractional powers—directly into the sliding manifold design. A typical expression for a terminal sliding surface can be formulated as follows:

$$S = \dot{x} + \beta x^{(q/p)} \tag{2.24}$$

  where $\beta > 0$ and p, q are odd integers such that $\frac{q}{p} < 1$. This nonlinear structure accelerates convergence as the trajectory approaches the equilibrium point, ensuring faster stabilization compared to standard SMC.

- **Fast terminal sliding mode control (FTSMC):** To address the singularity issues and further enhance convergence performance, Fast Terminal Sliding Mode Control

(FTSMC) was proposed. This method refines the sliding surface design to achieve finite-time convergence without singularity problems. By combining both linear and nonlinear error terms, FTSMC ensures fast convergence both far from and near the equilibrium point. An example of a fast terminal sliding surface is:

$$S = \dot{x} + \alpha x + \beta x^{(q/p)} \tag{2.25}$$

where $\alpha, \beta > 0$ and p, q are odd integers such that $\frac{q}{p} < 1$. This design not only eliminates the singular behavior observed in TSMC but also ensures faster settling time compared to both SMC and TSMC. FTSMC has demonstrated strong robustness, reduced chattering effects, and superior transient performance in numerous applications, ranging from robotic manipulators and mobile robots to aerospace and marine vehicles.

2.4 Controller design

In general, under-actuated systems are more difficult to control due to their limited number of control inputs compared to the degrees of freedom in the system dynamics. The objective is to synthesize a controller that guides the system's output to follow the desired path accurately. This necessitates a sophisticated control strategy that can effectively manage the system's dynamics and constraints to achieve precise tracking performance. To solve this issue, an SMC (Sliding Mode Control) without the reaching phase technique is proposed in this chapter. This method aims to robustly stabilize the underactuated system despite its inherent complexity. To this end, we define the tracking error as:

$$e = x - x_d \tag{2.26}$$

The choice of the sliding surface, as expressed in equation (5.9), leads us to the specified control input outlined in equation (2.16). However, employing this control input entails several constraints and drawbacks, including:

- Chattering Problem: One of the main drawbacks of SMC is chattering, which refers to high-frequency oscillations around the sliding surface, especially in the presence of uncertainties and disturbances. Chattering can lead to mechanical wear and tear, as well as undesirable noise in the system.
- Control energy and response trade-off: There's often a trade-off between achieving a quick response from the system and minimizing control energy. Setting high gains

(values of c_i) can lead to a fast reaction from the controller, but it may also introduce chattering and require a large amount of control effort. On the other hand, lower gains may reduce chattering but might result in slower responses, potentially leading to overshoot or instability if the system dynamics are not well understood or modeled accurately.

2.4.1 Proposed approach

Our main goal is to obtain an expression that enables us to start the system on the sliding surface. We accomplish this by redefining the tracking error vector found in (2.26) as:

$$e = x - x_d - \delta(x_0 - x_{d0}) \tag{2.27}$$

We propose the following exponential form of δ:

$$\delta = e^{-\frac{2}{\pi}atan(t)} \tag{2.28}$$

Then the new form of the error becomes:

$$e = e - \delta e_0 \tag{2.29}$$

The following is the selection of the sliding surface of second-order UMS systems with two degrees of freedom:

$$S = k_1(c_1 e_1 + \dot{e}_1) + k_2(c_2 e_2 + \dot{e}_2) \tag{2.30}$$

where k_1, k_2 are positive constants. e_1, e_2 are the errors of the first and second degrees of freedom.

Consequently, the proposed surface avoids the approaching phase and the related shortcomings.

The time derivative of (2.30) is:

$$\dot{S} = k_1(c_1 \dot{e}_1 + \ddot{e}_1) + k_2(c_2 \dot{e}_2 + \ddot{e}_2) \tag{2.31}$$

By employing the new error expression provided by (2.29), equation (2.31) becomes:

$$\dot{S} = k_1(c_1 \dot{e}_1 - \dot{\delta} e_{10} + [\ddot{e}_1 - \ddot{\delta} e_{10}]) + k_2(c_2 \dot{e}_2 - \dot{\delta} e_{20} + [\ddot{e}_2 - \ddot{\delta} e_{20}]) \tag{2.32}$$

Hence,

$$\dot{S} = k_1(c_1 \dot{e}_1 - \dot{\delta} e_{10} + [\ddot{x}_1 - \ddot{x}_{d1} - \ddot{\delta} e_{10}]) + k_2(c_2 \dot{e}_2 - \dot{\delta} e_{20} + [\ddot{x}_2 - \ddot{x}_{d2} - \ddot{\delta} e_{20}]) \tag{2.33}$$

Using (2.12), the expression (2.32) becomes:

$$\begin{aligned}\dot{S} = k_1(c_1\dot{e}_1 - \dot{\delta}e_{10} + [f_1 + g_1U - \ddot{x}_{d1} - \ddot{\delta}e_{10}]) + \\ k_2(c_2\dot{e}_2 - \dot{\delta}e_{20} + [f_2 + g_2U - \ddot{x}_{d2} - \ddot{\delta}e_{20}])\end{aligned} \tag{2.34}$$

By setting $\dot{S} = 0$, the equivalent control term can be written as:

$$\begin{aligned}U_{eq} = -(k_1g_1 + k_2g_2)^{-1}[k_1(c_1\dot{e}_1 - \dot{\delta}e_{10} + f_1 - \ddot{x}_{d1} - \ddot{\delta}e_{10}) \\ +k_2(c_2\dot{e}_2 - \dot{\delta}e_{20} + f_2 - \ddot{x}_{d2} - \ddot{\delta}e_{20})]\end{aligned} \tag{2.35}$$

Using $u_{sw} = -K_1S - K_2sgn(S)$ as the switching control, the control input may be expressed as follows:

$$\begin{aligned}U = -(k_1g_1 + k_2g_2)^{-1}[k_1(c_1\dot{e}_1 - \dot{\delta}e_{10} + f_1 - \ddot{x}_{d1} - \ddot{\delta}e_{10}) + \\ k_2(c_2\dot{e}_2 - \dot{\delta}e_{20} + f_2 - \ddot{x}_{d2} - \ddot{\delta}e_{20}) - K_3S - K_4sgn(S)]\end{aligned} \tag{2.36}$$

where the signum function is denoted by $sign(S)$, and the constants k_3, k_4 are positive.

2.5 Stability analysis

Theorem 5. *Employing the sliding surface specified in equation (2.30), the controller outlined in equation (2.36) drives the system described in equation (2.12) to asymptotically converge towards the reference trajectory. Consequently, the tracking errors described in equation (2.29) will converge to zero asymptotically.*

Proof. Consider the Lyapunov function candidate defined in equation (2.37):

$$V = \frac{1}{2}S^2 \tag{2.37}$$

Its time derivative is:

$$\dot{V} = S\dot{S} \tag{2.38}$$

Substituting (2.31) and (2.12) in (2.38), leads to:

$$\begin{aligned}\dot{V} = S(c_1\dot{e}_1 + \ddot{e}_1 + c_2\dot{e}_2 + \ddot{e}_2) \\ = S(c_1\dot{e}_1 - \dot{\delta}e_{10} + [f_1 + g_1U - \ddot{x}_{d1} - \ddot{\delta}e_{10}] + c_2\dot{e}_2 - \dot{\delta}e_{20} + [f_2 + g_2U - \ddot{x}_{d2} - \ddot{\delta}e_{20}])\end{aligned} \tag{2.39}$$

Substituting (2.35) in (2.39) gives:

$$\dot{V} = S(k_1d_1(x) + k_2d_2(x)) - k_3S^2 - k_4|S| \tag{2.40}$$

We have $k_1d_1(x) + k_2d_2(x) \leq |k_1d_1(x)| + |k_2d_2(x)|$, so the expression (2.40) becomes:

$$\dot{V} \quad \leq |S|(k_1d_1(x) + k_2d_2(x)) - k_3S^2 - k_4|S| \tag{2.41}$$

Then,

$$\dot{V} \quad \leq |S|[k_1 d_1(x) + k_2 d_2(x) - k_4] - k_3 S^2 \tag{2.42}$$

By setting $\gamma = k_1\rho_1 + k_2\rho_2$, equation (2.42) becomes:

$$\dot{V} \quad \leq |S|[\gamma - k_4] - k_3 S^2 \tag{2.43}$$

By selecting the switching controller gain k_4 as follows:

$$k_4 > \gamma \tag{2.44}$$

We conclude that the UMS (2.12) is asymptotically stabilised using the controller (2.36) and the tracking error converges asymptotically to zero. □

2.6 Simulation results

To provide a more comprehensive validation of the proposed control design, a detailed comparative analysis is carried out. In this study, the performance of the suggested sliding mode controller is directly compared with the results obtained in [66] without fuzzy approximation. The comparison focuses on key performance indicators such as robustness to parameter uncertainties, accuracy of trajectory tracking, convergence speed, and the ability to minimize chattering effects. By contrasting these results, it becomes possible to highlight the advantages introduced by the suggested controller framework.

For this purpose, the benchmark system selected for evaluation is the crane system, a representative example of underactuated mechanical systems that poses significant challenges due to its nonlinear dynamics and inherent underactuation. Both control strategies were applied to this system under identical simulation conditions to ensure a fair and objective comparison. The outcomes demonstrated that the proposed controller exhibited superior tracking performance, with enhanced robustness against disturbances and modeling errors.

Overall, this comparative study not only validates the efficacy of the proposed controller in addressing the target task but also provides strong evidence of its superiority over existing approaches. The results clearly indicate that the suggested controller offers a more reliable and efficient solution for controlling underactuated mechanical systems, thus reinforcing its potential for broader applications in complex engineering systems.

2.6.1 Crane system

Cranes are widely used around the world [86] and may be found in many places, including shipyards, construction sites, warehouses, and construction sites. Cranes come in a variety

of forms [87], with figure 5.2 displaying the most common type. Reducing the unwanted payload swings while moving the load is the control goal. It is possible to write these dynamic

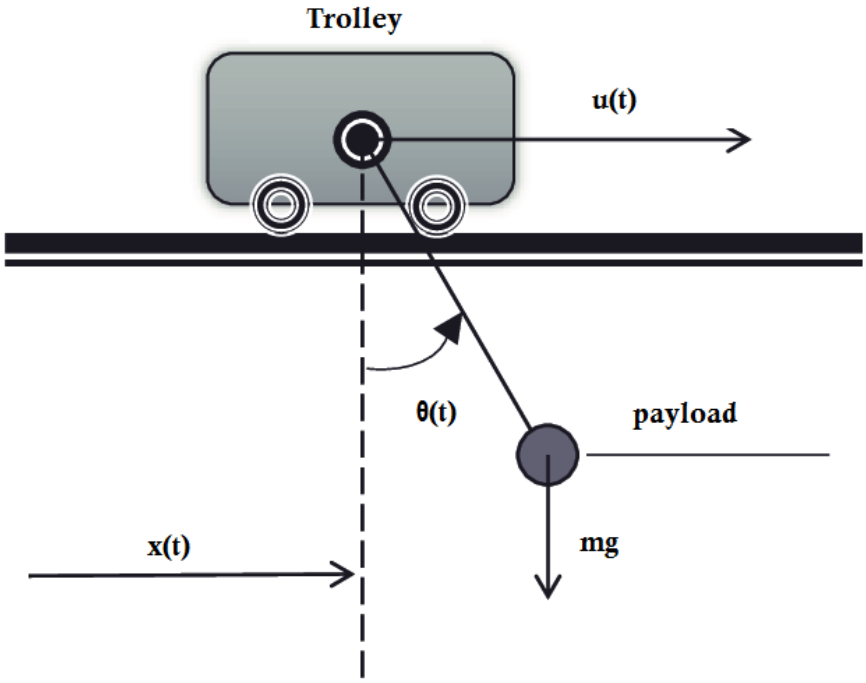

Figure 2.6: Crane system

equations in state space (2.12) with the state vector $\begin{bmatrix} x_1 & x_2 & x_3 & x_4 \end{bmatrix}^T = \begin{bmatrix} x & \dot{x} & \theta & \dot{\theta} \end{bmatrix}^T$ and the nonlinear functions f_1, g_1, f_2, g_2 defined as [88]:

$$\begin{cases} f_1 = \frac{(-m^2L^2gcos(\theta)sin(\theta+mL^2(mL\dot{\theta}^2sin(\theta)-d\dot{x})}{mL^2(M+m(1-cos(\theta)^2))} \\ g_1 = \frac{mL^2}{mL^2(M+m(1-cos(\theta)^2))} \\ f_2 = \frac{(m+M)mgLsin(\theta)-mLcos(\theta)(mL\dot{\theta}^2sin(\theta)-d\dot{x})}{mL^2(M+m(1-cos(\theta)^2))} \\ g_2 = \frac{mLcos(\theta)}{mL^2(M+m(1-cos(\theta)^2))} \end{cases} \tag{2.45}$$

The parameters and variables of the crane system are summarized in table 2.2. The simulation parameters are given in table 2.3. The initial and the desired values are selected as: $x = \begin{bmatrix} 0 & 0 & 0 & 0 \end{bmatrix}^T$, $x_d = \begin{bmatrix} 3 & 0 & 0 & 0 \end{bmatrix}^T$.

Figure 2.7 presents the dynamic response of the proposed controller, highlighting its effectiveness in simultaneously stabilizing the payload and controlling the trolley's motion. The results indicate that the controller rapidly suppresses oscillations of the suspended load while ensuring precise tracking of the trolley to the prescribed target positions. The smooth

Symbols	Description
x	Position of the cart
$\dot{x}$	Velocity of the cart
θ	Angle of the payload
$\dot{\theta}$	Angular velocity of the payload
m	Mass of the payload
M	Trolley's mass
L	Rope length
g	Gravity acceleration
d	Damping factor

Table 2.2: Description of the variables and parameters

Parameters	Values	Parameters	Values
m	5 kg	M	8kg
L	2m	g	-10m/s
d	1 kg/m	k1	1.7
k2	2.4	k3	11
c1	.6	c2	12

Table 2.3: Simulation parameters

and prompt convergence of the system states reflects the robustness and reliability of the proposed control strategy in managing the coupled translational and pendular dynamics of the underactuated system.

The proposed control strategy effectively governs the faster dynamics of the system, as illustrated in figures 2.8 and 2.9. For comparison, the responses obtained in [66] are depicted by the trajectories (x, $\dot{x}$) for the trolley and (θ, $\dot{\theta}$) for the payload, whereas the corresponding results achieved using the proposed method are represented by (x_p, $\dot{x}_p$) and (θ_p, $\dot{\theta}_p$). The figures demonstrate that the proposed approach provides improved transient performance, ensuring rapid convergence of both trolley displacement and payload swing while maintaining accurate tracking and overall system stability.

The suggested technique strategy achieves superior tracking performance, as evidenced by

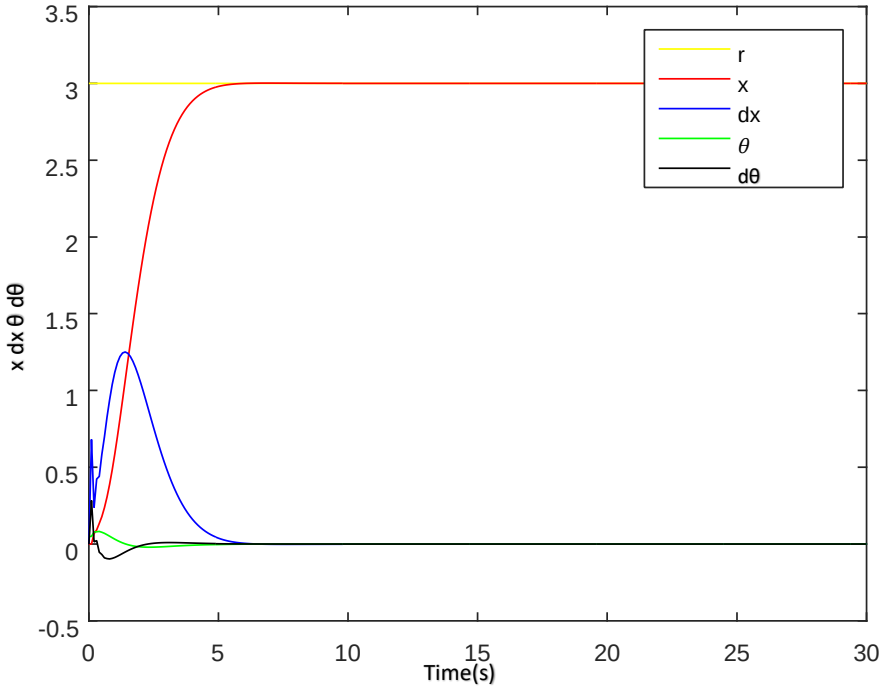

Figure 2.7: Results of the proposed control method, states x, $\dot{x}$, θ and $\dot{\theta}$

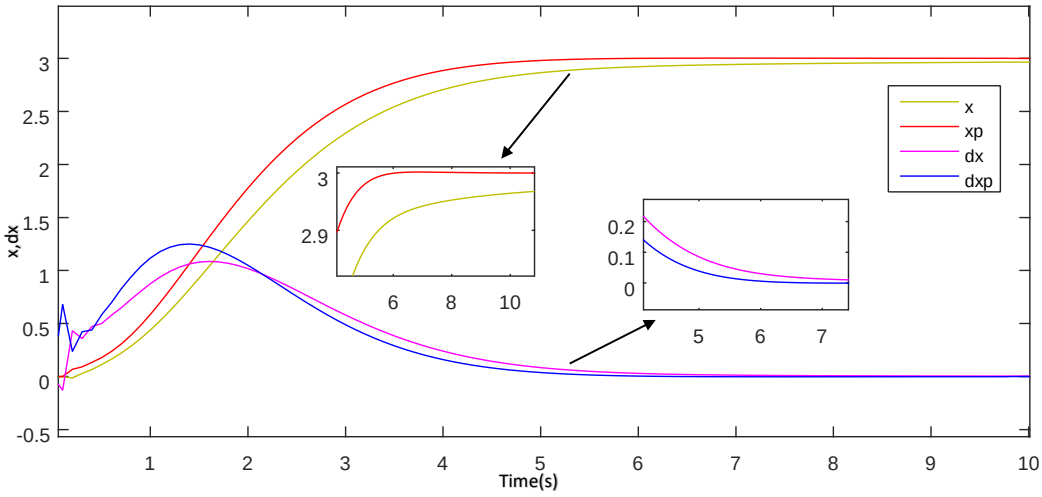

Figure 2.8: Comparison between the two controllers, x and $\dot{x}$

the analysis of the tracking error responses depicted in Figures 2.10 and 2.11. In these figures, the trajectories denoted by (e_{p1}, e_{p2}) correspond to the errors associated with the outputs of the proposed approach. The results demonstrate that the tracking errors converge rapidly to zero, highlighting the accuracy and reliability of the controller in maintaining precise

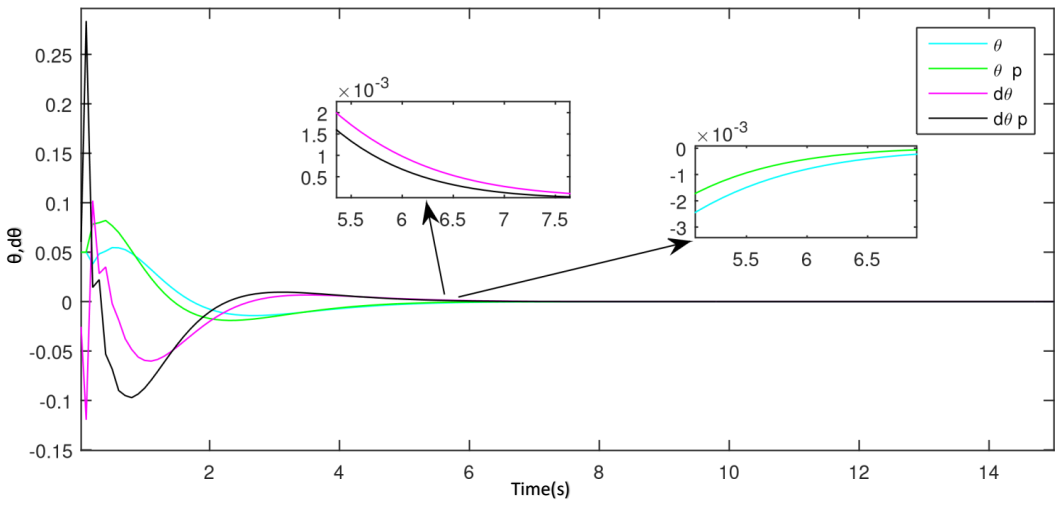

Figure 2.9: Comparison between the two controllers, θ and $\dot{\theta}$

trajectory tracking under the considered operating conditions.

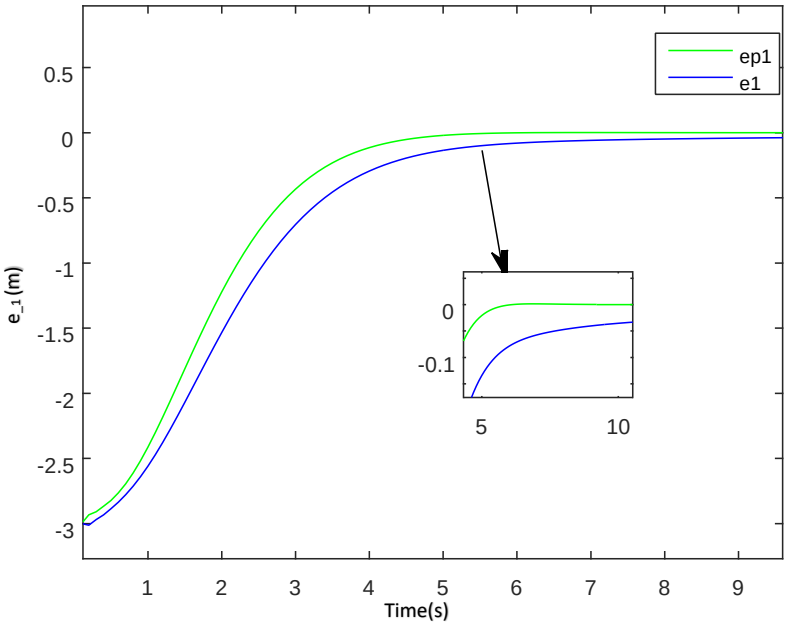

Figure 2.10: Comparison between the two controllers, the tracking error e_1

Figure 2.12 illustrates the evolution of the sliding surfaces, while Figure 2.13 depicts the corresponding control inputs. A comparative analysis reveals that both controllers exhibit similar overall behavior; however, the proposed approach demonstrates a faster convergence toward the origin compared to the method presented in [66]. This indicates that the suggested

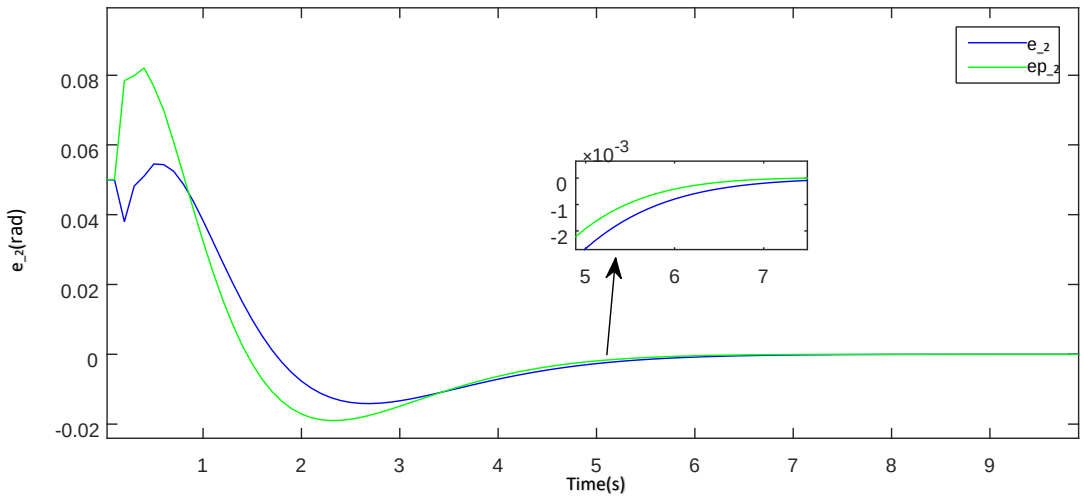

Figure 2.11: Comparison between the two controllers, the tracking error e_2

controller not only maintains the desired sliding motion but also enhances the transient response, leading to quicker stabilization of the system states.

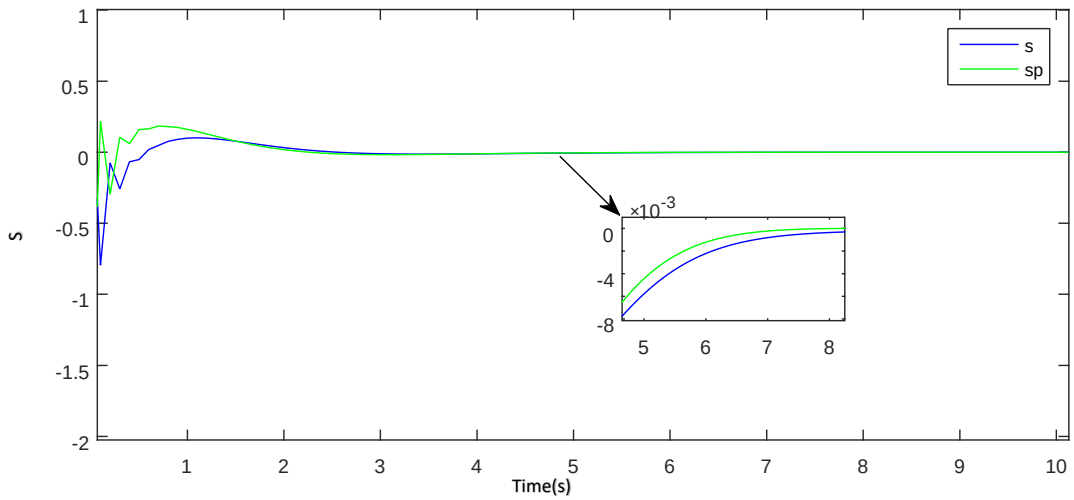

Figure 2.12: Comparison between the two controllers, the surface S

To evaluate the robustness of the proposed control strategy against external disturbances, we consider:

$$d_1 = 1.9 * cos(t) d_2 = 1.7 * sin(t) \tag{2.46}$$

introduced into the system at $t = 15s$. This allows for the assessment of the controller's capability to maintain accurate performance and stabilize the system in the presence of unforeseen external influences.

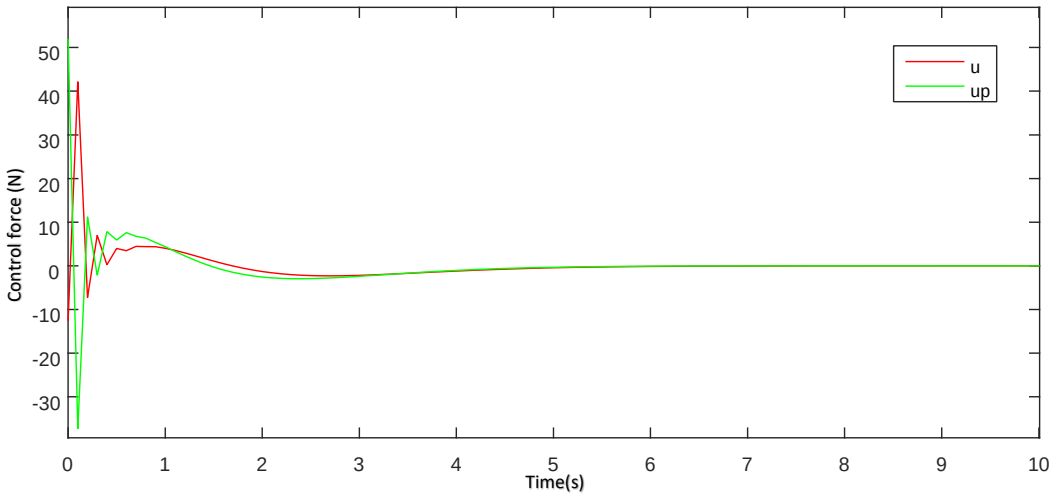

Figure 2.13: Comparison between the two controllers, the control action U

As illustrated in figures 2.14 and 2.15, the proposed control strategy exhibits enhanced robustness against external disturbances. The results indicate that the system is able to maintain stable and accurate performance despite the presence of perturbations, demonstrating the effectiveness of the suggested approach in handling external uncertainties.

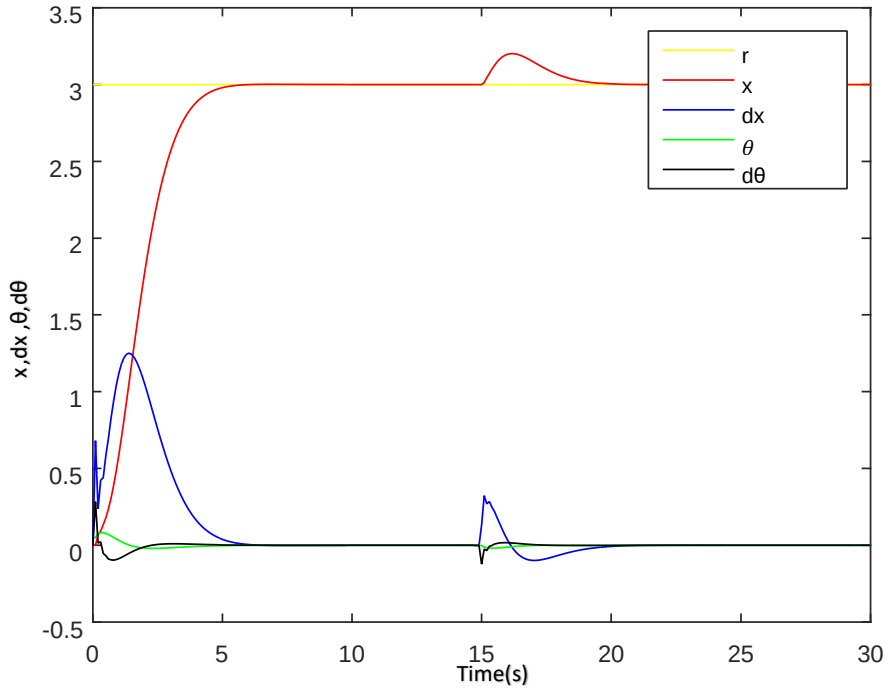

Figure 2.14: States with external disturbances

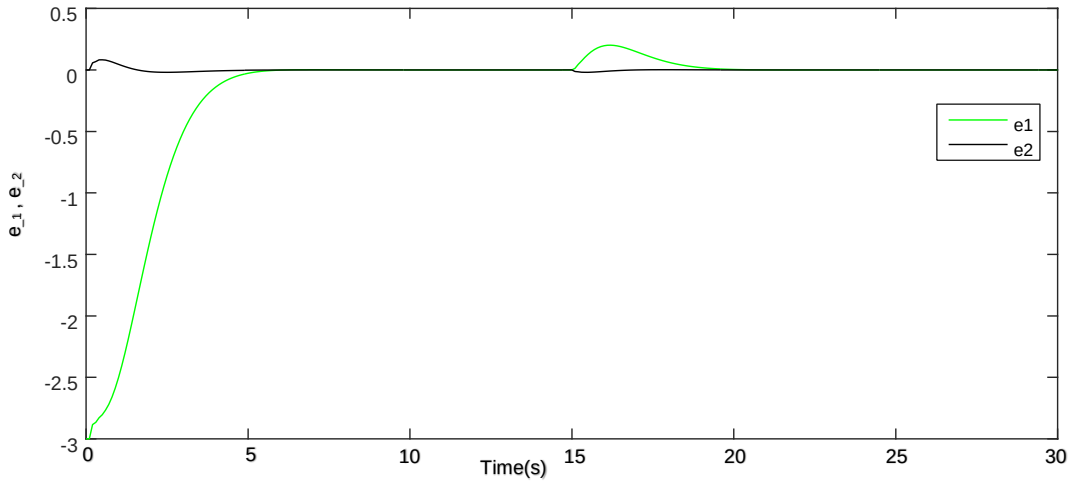

Figure 2.15: Tracking errors with external disturbances

The analysis of the sliding surfaces in figure 2.17 and the control inputs in figure 2.16 reveals that both the sliding variable and the control signals remain largely unaffected by the presence of external disturbances. This observation reinforces the conclusion regarding the superiority of the proposed control strategy, demonstrating its ability to maintain stable, robust performance while effectively handling perturbations without significant deviation in the system's behavior.

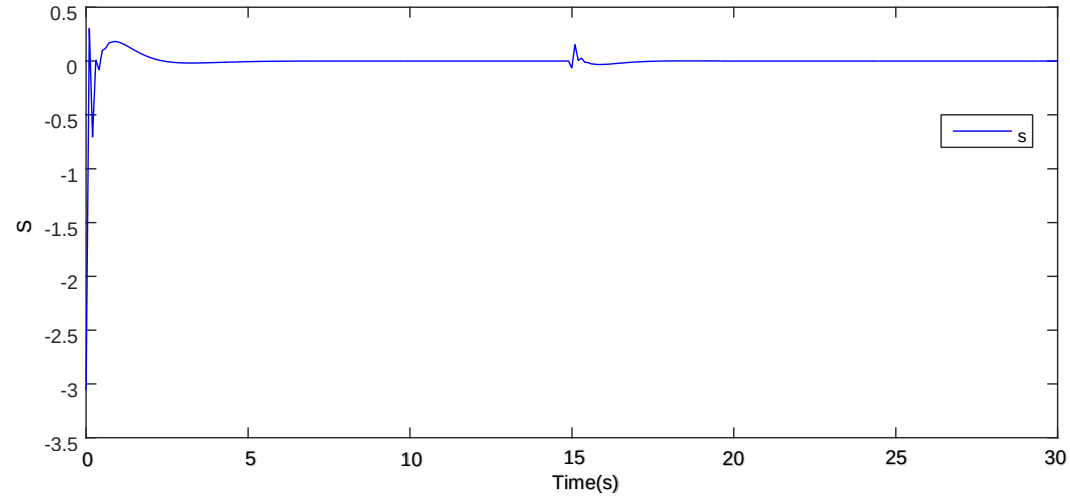

Figure 2.16: Sliding surfaces with external disturbances

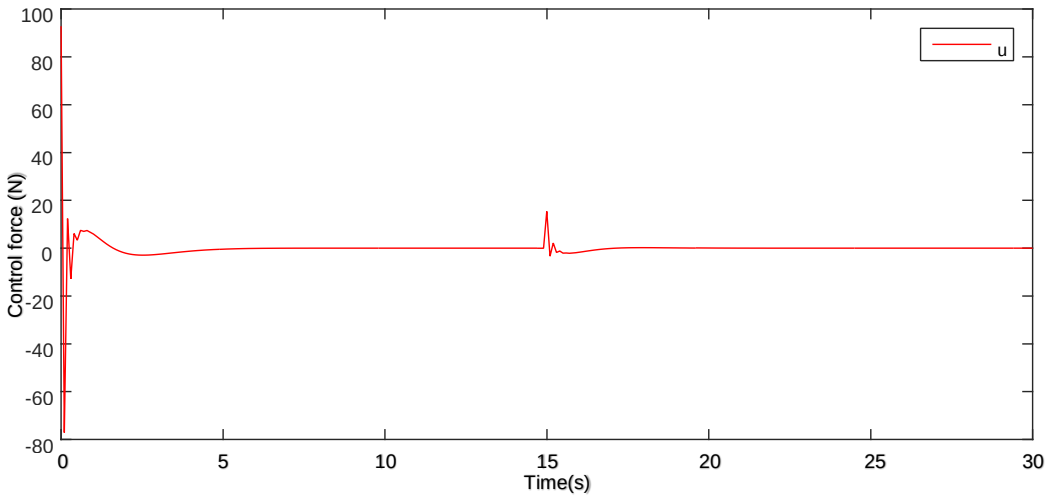

Figure 2.17: Control actions with external disturbances

2.7 Conclusion

This study presents a novel sliding mode control approach specifically developed for nonlinear underactuated mechanical systems, aiming to achieve fast and robust tracking while entirely removing the conventional reaching phase inherent in classical SMC schemes. In traditional sliding mode control, the reaching phase represents a key limitation, as system trajectories are not immediately robust against disturbances or uncertainties until they reach the sliding manifold. To overcome this limitation, the proposed method employs a redefined sliding surface constructed through transformations of the tracking error. This ensures that, from the outset of operation, the system trajectory lies directly on the sliding manifold, independent of initial conditions, thereby providing immediate robustness and improved performance.

The proposed control scheme guarantees that the tracking error asymptotically approaches zero while effectively minimizing undesirable effects, such as chattering. By removing the traditional reaching phase, the method enhances both robustness and the reliability of the control action, which is especially critical in systems requiring rapid stabilization. Furthermore, the approach offers a systematic framework for deriving sliding domain equations directly from tracking error formulations, thereby streamlining the control design process for complex underactuated mechanical systems.

The effectiveness of the proposed approach has been validated through simulation studies. The results demonstrate that the suggested controller achieves superior performance in terms of convergence speed, steady-state accuracy, and robustness against modeling uncertainties when compared with more conventional methods. Furthermore, the simulations confirm the

controller's ability to handle nonlinearities and external disturbances efficiently, without sacrificing smoothness or control effort.

Overall, the developed Free Reaching Phase SMC framework represents a significant advancement in the control of underactuated mechanical systems. By combining the robustness of sliding mode control with the elimination of the reaching phase, the methodology provides a powerful and practical tool for modern engineering applications.

In the next chapter, a fuzzy fast terminal sliding mode control (FFTSMC) scheme will be developed for underactuated mechanical systems. The approach will combine the finite-time convergence properties of fast terminal sliding mode control with the adaptive tuning capability of fuzzy logic. By embedding a fuzzy inference mechanism within the FFTSMC framework, the controller parameters are adjusted online, leading to improved tracking accuracy and faster convergence of the system states to their reference trajectories.

Chapter 3

Fuzzy Fast Terminal SMC for UMS

3.1 Introduction

This chapter develops a Fuzzy Fast Terminal Sliding Mode Control (FFTSMC) technique for Underactuated Mechanical Systems. Using the Euler-Lagrange equation, the dynamical model of Underactuated Mechanical Systems is first constructed, which considers the presence of disturbances and uncertainties in practical applications. While the previous chapter introduced the Free Reaching Phase of SMC, which enhanced robustness with free reaching; however, this approach still relied on traditional SMC. In this chapter, hierarchical Terminal Sliding Mode Control (TSMC) has been introduced, enhancing traditional SMC by ensuring finite-time convergence and incorporating it with fuzzy tuning. This integrated approach, known as Fuzzy Fast Terminal Sliding Mode Control (FFTSMC), ensures rapid and robust convergence to desired states and offers superior control performance compared to traditional SMC and TSMC, especially in challenging and uncertain environments.

Using Lyapunov's theory, we demonstrate the convergence and stability of the suggested control method. We offer, in such a way, a mathematical framework to guarantee that the system's states will remain stable and converge to the desired equilibrium. In the last section, we provide some simulation results to illustrate the improved effectiveness and performance of the proposed control method. These results will demonstrate the robustness and efficiency of the proposed FFTSMC method and confirm its potential for enhancing the control of underactuated mechanical systems in practical applications.

As discussed in Chapter 1, the hybrid controller, combining features from different controllers, has been widely used recently due to its ability to leverage the strengths of each component controller. By integrating the benefits of multiple control strategies, hybrid con-

trollers can provide enhanced performance, robustness, and adaptability in complex control scenarios. Indeed, [26] presented a hybrid fuzzy moving sliding mode control to adjust the effective gains of the sliding surface in an underactuated container crane system using a fuzzy mechanism. The authors in [89] proposed a finite-time, robust control strategy for an underactuated, uncertain system. They created two-layer hierarchical FTSM surfaces after presenting the suggested controller. A fuzzy system is used in [90] to estimate the unknown non-linear functions for the multi-input/multi-output underactuated systems. The authors suggested combining SMC with adaptive PI to prevent the chattering phenomena and ensure precise monitoring of the intended trajectory. The authors in [91] suggested an adaptive fuzzy integral terminal SMC to drive a nonholonomic robot by combining the system's kinematic and dynamic models and using a fuzzy approximator for the system uncertainties.

The adaptive fuzzy SMC of an underactuated oscillatory plant was the main emphasis of the authors' work in [92]. In order to improve the performance of the system, the sliding surface is adjusted using the adaptive term. The asymptotic stability and resilience of the entire system are ensured by synthesizing the SMC law. The content in [93] discusses the combination of an SMC scheme with an adaptive fuzzy system. This resulted in a unique intelligent sliding mode controller, which uses a switching parameter in place of state variables, reducing the amount of fuzzy rules and simplifying the controller design.

The key contribution of this chapter is the development of a Fuzzy Fast Terminal Sliding Mode Control (FFTSMC) strategy for underactuated mechanical systems. This approach combines the finite-time convergence property of fast terminal sliding mode control with the tuning capability of fuzzy logic, resulting in a controller that is both robust and efficient. Specifically, fuzzy logic is utilized to approximate the fast terminal parameters, allowing real-time adjustment of control gains based on system behavior.

Unlike conventional sliding mode designs that may suffer from chattering and slow convergence near equilibrium, the proposed method ensures rapid error elimination, smoother control signals, and strong resilience against uncertainties. By embedding fuzzy logic into the sliding mode framework, the control gains are adaptively adjusted in real time, thereby improving precision and reducing the need for extensive manual tuning. This chapter not only introduces the theoretical formulation of the FFTSMC but also establishes its stability using Lyapunov-based analysis and validates its performance through simulations on representative underactuated systems. The proposed contribution, therefore, provides a solid foundation for advancing the control of nonlinear, underactuated dynamics where robustness and fast convergence are critical.

3.2 Dynamical modeling of UMS

As indicated in the previous chapter, there are many modeling techniques. just like we did in the previous chapter. We have applied the Euler-Lagrange approach in this chapter. The system (2.12) can be split into the following two subsystems:

$$\begin{cases} \dot{x}_1 = x_2 \\ \dot{x}_2 = f_1(x) + g_1(x)u + d_1(x) \end{cases} \tag{3.1}$$

$$\begin{cases} \dot{x}_3 = x_4 \\ \dot{x}_4 = f_2(x) + g_2(x)u + d_2(x) \end{cases} \tag{3.2}$$

The control methodology developed for a second-order system can be extended and generalized to systems of arbitrary order, following a similar design procedure.

3.3 Fuzzy logic

Fuzzy logic (FL), introduced by Lotfi Zadeh in the 1960s [94], is an extension of classical Boolean logic designed to handle the concept of partial truth. Unlike traditional binary sets where variables must be either 0 or 1 (false or true), fuzzy logic allows for a range of truth values between 0 and 1. This makes fuzzy logic particularly useful for dealing with uncertain, imprecise, or vague information.

3.3.1 Linguistic fuzzy modeling

Linguistic fuzzy modeling refers to fuzzy modeling where the focus is on high interpretability but low accuracy. This form uses linguistic variables and terms to describe the system's behavior, making it intuitive and easily understandable by humans. As an example, we have the Mamdani approach, widely used due to its intuitive and human-like reasoning approach. Named after Ebrahim Mamdani, this method is particularly popular for applications requiring interpretability and simplicity.

3.3.2 Precise fuzzy modeling:

In precise fuzzy modeling, we get low interpretability, but we will be getting high accuracy or precision. For example, we can mention the Takagi-Sugeno (T-S) approach, known for its precision and effectiveness in handling complex control problems. Named after Takagi and

Sugeno, this approach uses fuzzy sets to model systems accurately, often incorporating linear or nonlinear functions in the rule consequent.

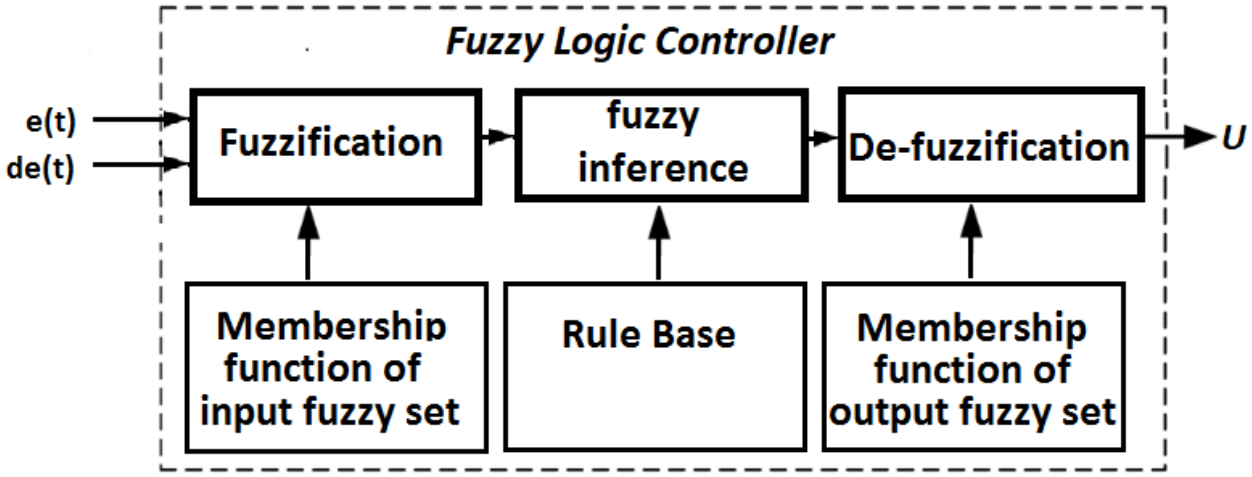

Figure 3.1: Fuzzy logic controller

3.3.3 Structure of a fuzzy logic controller

The FLC is the intelligent controller that emulates the human thinking and decision-making function. It is a well-recognized approach for managing nonlinear, uncertain, and complex systems, especially in cases where obtaining an exact mathematical model is difficult. Unlike conventional control strategies such as PID or state-feedback controllers, which depend on precise knowledge of system parameters, the FLC employs linguistic rules and fuzzy reasoning to transform input variables into corresponding control actions. This makes it a flexible and powerful control method, particularly effective for underactuated mechanical systems (UMSs), where control challenges are intensified by underactuation and nonlinear behaviors. The architecture of a fuzzy logic controller, shown in Figure (3.1), generally comprises four core components: fuzzification, rule base, inference engine, and defuzzification. Each of these modules serves a distinct purpose in converting precise input data into fuzzy reasoning and subsequently transforming the fuzzy output into a definitive control signal suitable for implementation in the plant.

1. **Fuzzification:** The first stage of fuzzy control is the conversion of crisp numeric inputs, such as tracking errors and their derivatives, into fuzzy representations. This is done

with the use of membership functions that assign various numerical values to degrees of membership in [0, 1]. Selection of appropriate membership functions (e.g., triangular, trapezoidal, or Gaussian) is vital in modeling input signals' uncertainty and reflecting the model dynamics in an accurate way.

For instance, if the tracking error is defined within the universe of discourse [-5,5], membership functions might classify this error into linguistic terms such as low (L), medium (M), and high (H). The choice of the type and shape of membership functions—such as trapezoidal(3.2) , Gaussian (3.3), triangular, or bell-shaped—significantly influences the controller's performance. Gaussian functions illustrated in figure (3.3), for example, provide smooth transitions between linguistic terms, whereas triangular functions are computationally simpler and widely used in real-time implementations.

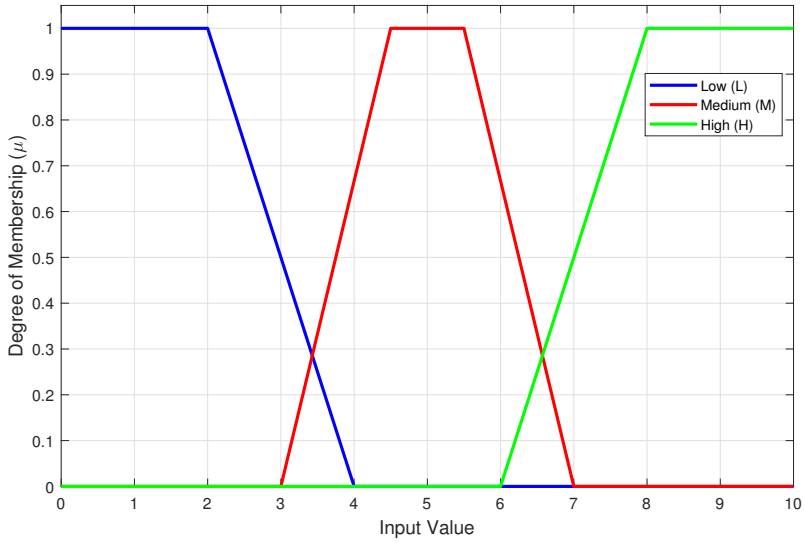

Figure 3.2: Trapezoidal membership functions

2. **Inference:** The inference mechanism, also known as the reasoning engine, combines the information from the fuzzification process and the rule base to derive fuzzy conclusions. This stage determines how the fuzzy rules are evaluated and aggregated to produce fuzzy outputs. The two most widely used inference schemes are:

   - Mamdani inference: in this approach, both the antecedent (if-part) and the consequent (then-part) of the rules are represented as fuzzy sets. It is intuitive, easy to interpret, and closely resembles human reasoning. However, it may require additional computational effort during defuzzification.

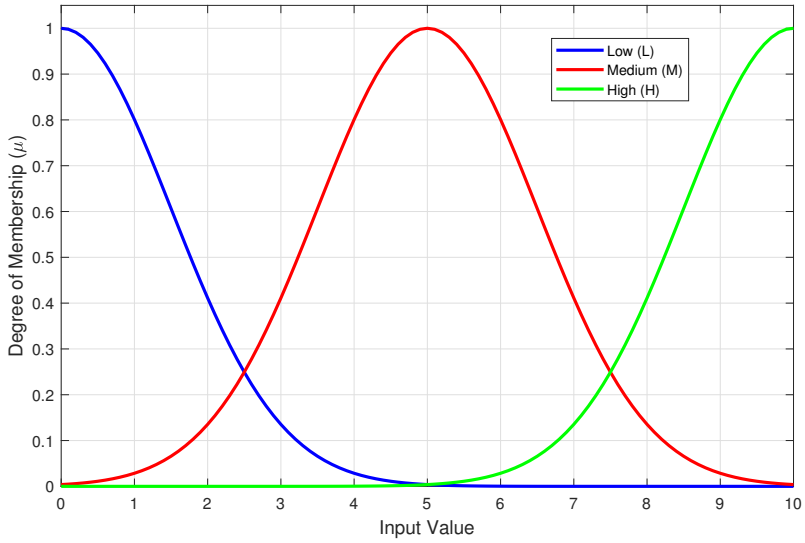

Figure 3.3: Gaussian membership functions

- Takagi–Sugeno (T–S) reasoning: where the antecedent is described using fuzzy sets and a linear or nonlinear mathematical function of the input variables, is used to describe the consequent. It provides better accuracy and is also computationally efficient, which can be applied to real-time control.

The inference engine combines the results from a number of applicable rules using aggregation operators (e.g., min, max, product), resulting in a collection of fuzzy outputs that describes the controller's decision in natural language.

3. **Defuzzification:** Defuzzification Interface: The final stage in a fuzzy logic controller involves converting the fuzzy outputs into precise numerical values that can be directly applied to the system actuators. This process, known as defuzzification, ensures that the controller produces actionable control signals from the linguistic reasoning of the fuzzy inference engine. Several methods exist for performing defuzzification, among which the most commonly used are:

   - Center of Gravity (COG): This method calculates the weighted average of the output fuzzy set, yielding a smooth and balanced control signal that reflects the combined effect of all active rules.
   - Center Average (CA): Particularly effective in Takagi–Sugeno inference systems, this approach computes a weighted average based on the mathematical consequent of the rules, producing a precise and computationally efficient control output.

Among the various defuzzification techniques, the center of gravity (COG) method is the most commonly employed in engineering practice, as it provides smooth, reliable, and consistent control outputs.

3.3.4 Hybrid fuzzy control strategies

Although standalone fuzzy logic controllers offer substantial benefits, their effectiveness can be further improved by integrating them with other control approaches. Such hybrid fuzzy control schemes leverage the strengths of multiple techniques, overcoming challenges like sensitivity to parameter variations, limited adaptability, and slow system convergence.

1. **Fuzzy–sliding mode control:** Sliding mode control is widely recognized for its ability to maintain robust performance in the presence of uncertainties and external disturbances. However, the conventional approach often generates high-frequency oscillations known as chattering, which can degrade system performance. By integrating fuzzy logic into the sliding mode framework, the control law or switching surface can be smoothly modulated, effectively mitigating chattering while retaining the inherent robustness of SMC. This hybrid control strategy has been successfully implemented in a variety of applications, including underactuated mechanical systems, robotic manipulators, and power electronic converters.

2. **Fuzzy–adaptive control:** Adaptive control techniques continuously adjust controller parameters in real time to maintain desired system performance despite uncertainties or disturbances. When combined with fuzzy logic, the controller leverages both human-like reasoning and real-time parameter adaptation, enabling improved handling of modeling inaccuracies and external perturbations. This hybrid approach enhances system stability and robustness, making it particularly effective for complex and nonlinear systems where precise models are difficult to obtain.

3. **Fuzzy–predictive control:** Model predictive control (MPC) is powerful for handling multivariable systems with constraints, but it requires accurate models. By combining MPC with fuzzy models, predictive controllers can handle imprecise dynamics while still optimizing performance over prediction horizons.

The development of hybrid fuzzy strategies represents an important advancement in intelligent control. They are particularly relevant for underactuated mechanical systems, where high nonlinearity, input limitations, and environmental uncertainties demand controllers that are both robust and flexible.

3.4 Design of the hierarchical fast terminal SMC

Sliding Mode Control (SMC) is a robust control strategy well-suited for nonlinear systems with uncertainties. But without applying a sufficient control force, the asymptotical stability might not be able to provide a fast convergence for high-precision control. Terminal sliding modes (TSMs) [95], which are nonlinear switching manifolds, can significantly enhance transient performance. Control designs have effectively employed TSM control in many applications [96]. Its finite time convergence lies in its exponentially growing convergence rate when the state is near the equilibrium, the current TSM control may not deliver the same convergence performance when the system state is far from the equilibrium, when compared to the sliding-mode control. The authors in [97] developed a method that combines the benefits of TSM (finite time) transient convergence at a distance from the equilibrium and conventional sliding-mode control convergence when it is close to the equilibrium. This approach is known as fast terminal sliding mode (FTSM), and it has been used a lot recently [98]. It is expressed as:

$$S = \dot{x} + \alpha x + \beta x^{(q/p)} \tag{3.3}$$

where $\alpha, \beta > 0$ and p, q are odd integers such that $\frac{q}{p} < 1$. From (3.5) we can conclude that the approximate dynamics for x_1 becomes $\dot{x} = -\alpha x$ when it is far from zero and $\dot{x} = -\beta x^{(q/p)}$ when it is near zero.

Lemma 1. *Once the system states converge to the nonlinear sliding manifold such that* $(X) = 0$*, the settling time corresponding to the transition from* $e \neq 0$ *to* $e = 0$ *can be expressed as:*

$$t = \frac{p}{\alpha(p-q)} \left[ln\left(\alpha x(0)^{(p-q)/p} + \beta\right) - ln(\beta) \right] \tag{3.4}$$

Proof. Once the system states arrive at the nonlinear sliding surface, the following equation holds:

$$S = \dot{x} + \alpha x + \beta x^{(q/p)} = 0 \tag{3.5}$$

Equation (3.5) may be expressed as:

$$\dot{x} = +\alpha x + \beta x^{(q/p)} \tag{3.6}$$

$$x^{(-q/p)}\dot{x} + \alpha x^{(1-q/p)} = -\beta \tag{3.7}$$

We may rewrite the equation (3.7) as follows if we assume that $\varrho = x^{(1-q/p)}$:

$$\dot{\varrho} + \frac{p-q}{p}\alpha\varrho = -\beta\frac{p-q}{p} \tag{3.8}$$

The following is the result of solving equation (3.8):

$$\frac{\beta}{\alpha}exp(-\alpha\frac{p-q}{p}t)+\varrho(0)exp(-\alpha\frac{p-q}{p}t)=-\frac{\beta}{\alpha} \tag{3.9}$$

Calculating the logarithm of equation (3.9) yields:

$$t=\frac{p}{\alpha(p-q)}ln\frac{\alpha\varrho(0)+\beta}{\beta} \tag{3.10}$$

The convergence time is finite, provided by: $\varrho(0)=x(0)^{(1-q/p)}$ and given as:

$$t=\frac{p}{\alpha(p-q)}\left[ln\left(\alpha x(0)^{(p-q)/p}+\beta\right)-ln(\beta)\right] \tag{3.11}$$

□

In this chapter, the dynamic control law for the UMS described by (3.1,3.2) is designed using the hierarchical fast terminal SMC. The suggested H-FTSMC technique consists of the following steps: first, it divides the system into several sub-systems; next, it designs the sub-sliding surfaces of the lower layer; and last, from the upper layer, we construct the total sliding. The sliding surfaces are chosen as:

$$\begin{aligned}S_1&=\dot{e}_1+\alpha_1e_1+\beta_1e_1^{(q_1/p_1)}\\S_2&=\dot{e}_2+\alpha_2e_2+\beta_2e_2^{(q_1/p_1)}\end{aligned} \tag{3.12}$$

with x_{id} is the desired trajectory $e_i=x_i-x_{id}, i=1,2$. When (3.12) is differentiated with respect to time, we obtain:

$$\begin{aligned}\dot{S}_1&=\ddot{e}_1+\alpha_1\dot{e}_1+\beta_1(q_1/p_1)\dot{e}_1e_1^{(q_1/p_1)-1}\\&=f_1+g_1U+d_1-\ddot{x}_{1d}+\alpha_1\dot{e}_1+\beta_1(q_1/p_1)e_1^{(q_1/p_1)-1}\dot{e}_1\\\dot{S}_2&=\ddot{e}_2+\alpha_2\dot{e}_2+\beta_2(q_2/p_2)\dot{e}_2e_2^{(q_2/p_2)-1}\\&=f_2+g_2U+d_2-\ddot{x}_{2d}+\alpha_2\dot{e}_2+\beta_2(q_2/p_2)e_2^{(q_1/p_1)-1}\dot{e}_2\end{aligned} \tag{3.13}$$

By putting $\dot{S}_1=0$ and $\dot{S}_2=0$, we can obtain the two equivalent control terms:

$$U_{eq1}=-\frac{1}{g_1}[f_1-\ddot{x}_{1d}+\alpha_1\dot{e_1}+\beta_1\dot{e_1}(q_1/p_1)e_1^{(q_1/p_1)-1}] \tag{3.14}$$

$$U_{eq2}=-\frac{1}{g_2}[f_2-\ddot{x}_{2d}+\alpha_2\dot{e_2}+\beta_2\dot{e_2}(q_2/p_2)e_2^{(q_2/p_2)-1}] \tag{3.15}$$

Next, the total sliding surface of the upper layer is:

$$S=k_1S_1+k_2S_2 \tag{3.16}$$

with k_1, k_2 are positive constants.
By taking the derivative of the equation (3.16), we find:

$$\dot{S} = k_1\dot{S}_1 + k_2\dot{S}_2 \tag{3.17}$$

Based on the H-FTSMC method [99], the control input may be expressed as the total of the equivalent and switching control laws as follows:

$$U = U_{eq1} + U_{eq2} + U_{sw} \tag{3.18}$$

with the switching control denoted by U_{sw} and given as follows:

$$U_{sw} = \frac{-(k_1 g_1 U_{eq2} + k_2 g_2 U_{eq1} + k_3 S + k_4 sign(S))}{k_1 g_1 + k_2 g_2} \tag{3.19}$$

with $k_3, k_4 > 0$.
The expression for the total control law may be obtained by replacing (3.15) (3.16) and (3.19) in (3.18):

$$U = \frac{k_1 g_1 U_{eq1} + k_2 g_2 U_{eq2} - k_3 S - k_4 sign(S)}{k_1 g_1 + k_2 g_2} \tag{3.20}$$

It should be noted that the $sign(.)$ function is discontinuous, and that this is what causes the undesired chattering phenomena [100]. One solution to this issue is to use a smoother and continuous function, such as the hyperbolic tangent function, provided as:

$$\tanh(s) = \frac{e^s - e^{-s}}{e^s + e^{-s}} \tag{3.21}$$

Consequently, the following is the fuzzy fast terminal SMC action:

$$U = \frac{k_1 g_1 U_{eq1} + k_2 g_2 U_{eq2} - k_3 S - k_4 tanh(S)}{k_1 g_1 + k_2 g_2} \tag{3.22}$$

The next section introduces a fuzzy tuning framework aimed at adjusting the parameters α and β. This mechanism allows the controller to dynamically adjust its behavior.

3.5 Fuzzy tuning of the H-FTSMC

The purpose of this section is to construct a fuzzy system to modify the α and β H-FTSMC parameters. The goal is to improve the convergence rate and decrease the system response of the system states [101]. To do this, the fuzzy tuner is made as follows:
The sliding parameters α and β are taken into consideration as the fuzzy system's output vector, while the tracking error e is chosen as the input. Five sets inside the discourse input

	NB	NS	ZO	PS	PB
α	B	M	S	M	B
β	S	M	B	M	S

Table 3.1: Tuning rule base

are designated as follows: NB (Negative Big), NS (Negative Small), Z (Zero), PS(Positive Small), PB (Positive Big), and the fuzzy sets for the outputs are: S (Small), M (Medium), B (Big). To get crisp values at the outputs during defuzzification, the center average approach is employed. The fuzzy rule base is shown in table (3.1), and the membership functions to fuzzify input and outputs are displayed, respectively, in figures (3.5), (3.6), and (3.7).

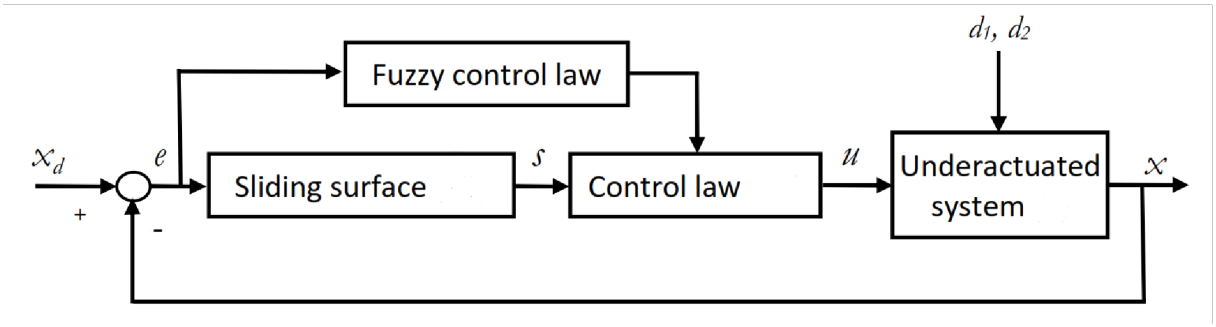

Figure 3.4: Fuzzy-FTSMC control scheme

3.6 Stability analysis

Theorem 6. *The tracking error e converges to the origin along the nonlinear sliding surface in finite time (3.11) while the state variables (3.1) and (3.2) converge to the reference trajectories using the control input defined in (3.22).*

Proof. Consider the Lyapunov function candidate:

$$V = \frac{1}{2}S^2 \tag{3.23}$$

Its time derivative is:

$$\dot{V} = S(k_1\dot{S}_1 + k_2\dot{S}_2) \tag{3.24}$$

Substituting the surface expression (3.13) into the Lyapunov derivative form (3.24), yields:

$$\begin{aligned}\dot{V} = S(k_1(\ddot{e}_1 + \alpha_1\dot{e}_1 + \beta_1(q_1/p_1)\dot{e}_1 e_1^{(q_1/p_1)-1}) \\ +k_2(\ddot{e}_2 + \alpha_2\dot{e}_2 + \beta_2(q_2/p_2)\dot{e}_2 e_2^{(q_2/p_2)-1}))\end{aligned} \tag{3.25}$$

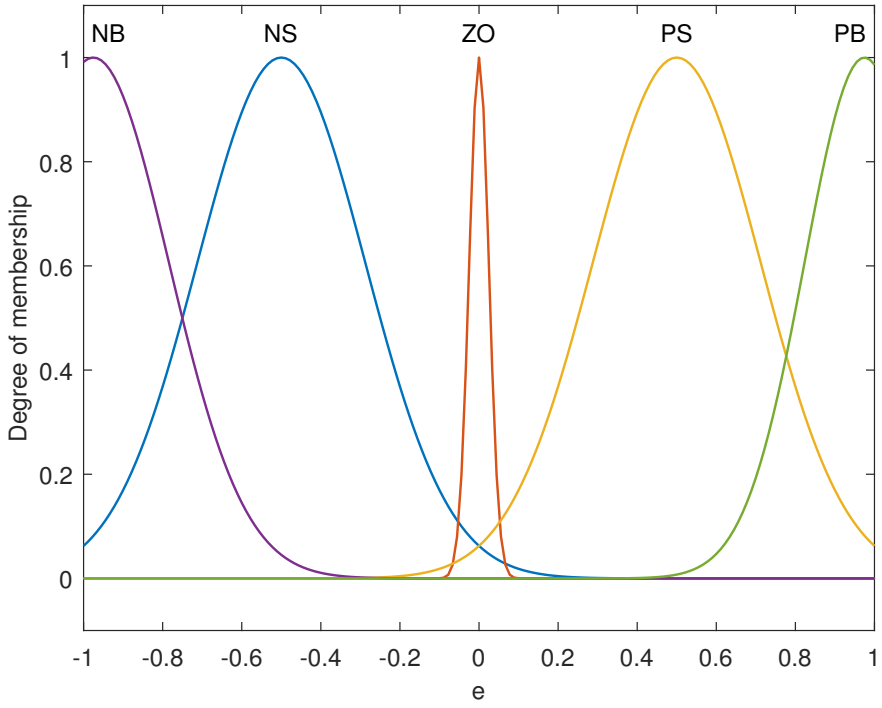

Figure 3.5: Membership functions of e

By substituting the system described by (3.1) in (3.25) we obtain:

$$\begin{aligned}\dot{V} = S[k_1(f_1 + d_1 + \alpha_1\dot{e_1} + \beta_1\dot{e_1}(q_1/p_1)e_1^{(q_1/p_1)-1}) \\ \check{\text{s}} + k_2(f_2 + d_2 + \alpha_2\dot{e_2} + \beta_2\dot{e_2}(q_2/p_2)e_2^{(q_2/p_2)-1}) + (k_1g_1 + k_2g_2)U]\end{aligned} \tag{3.26}$$

Applying the control law (3.22) to (3.25) yields:

$$\dot{V} = S(k_1d_1(x) + k_2d_2(x)) - k_3S^2 - k_4|S| \tag{3.27}$$

We have $S(k_1d_1(x) + k_2d_2(x)) \leq |S|(|k_1d_1(x)| + |k_2d_2(x)|)|)$, so the expression (3.29) becomes:

$$\begin{aligned}\dot{V} &\leq |S|(|k_1d_1(x)| + |k_2d_2(x))|) - k_3S^2 - k_4|S| \\ &= |S|[|k_1d_1(x)| + |k_2d_2(x))| - k_4] - k_3S^2\end{aligned} \tag{3.28}$$

By putting $\gamma = |k_1d_1(x)| + |k_2d_2(x)|$ the resulting formulation becomes:

$$\dot{V} \quad \leq |S|[\gamma - k_4] - k_3S^2 \tag{3.29}$$

Choosing the gain parameter k_4 to satisfy $k_4 > \gamma$, ensures that the system represented by equations (3.1) and (3.2) converges to the origin in finite time, under the control law specified in (3.19). This selection guarantees system stability in the sense of Lyapunov. This condition

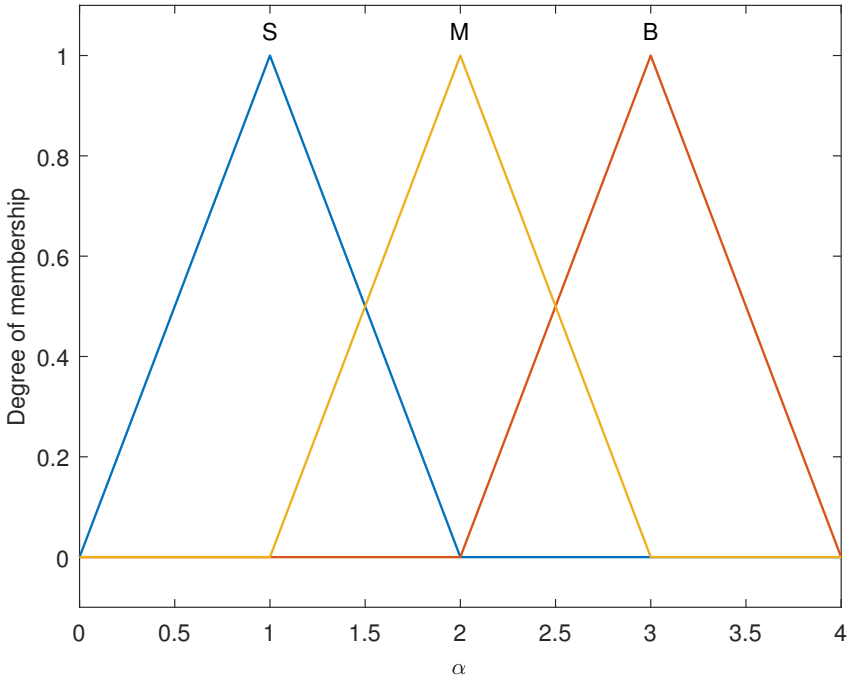

Figure 3.6: Membership functions of α

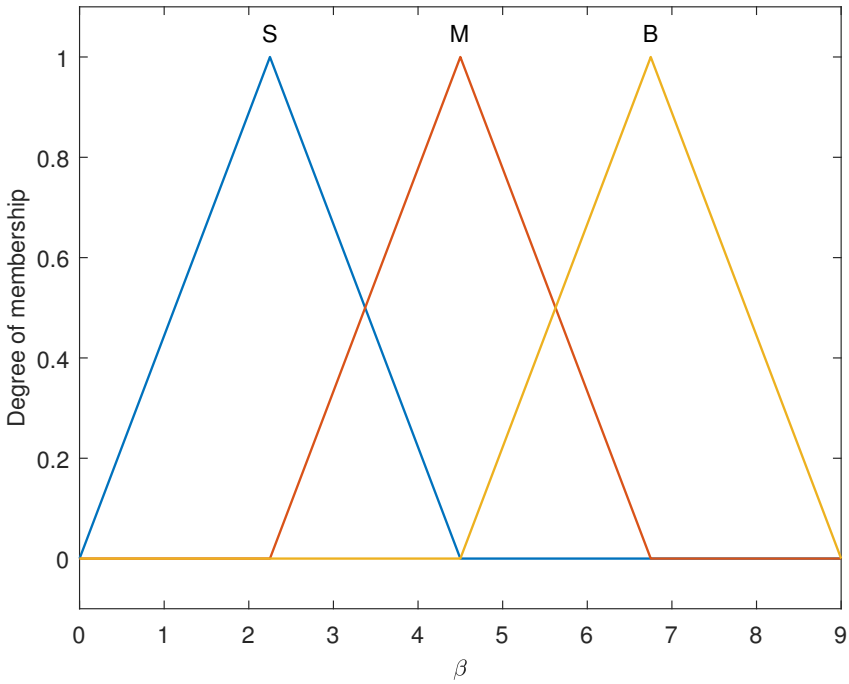

Figure 3.7: Membership functions of β

highlights the critical role of proper gain selection in achieving both rapid convergence and robust stability for the controlled system. □

3.7 Simulation results

To rigorously assess the performance of the proposed control approach and demonstrate its ability to achieve the desired objectives, this section presents an extensive series of simulation studies. These simulations are conducted under diverse operating conditions, including the presence of external disturbances and system uncertainties, which are characteristic challenges in underactuated mechanical systems. By examining both transient and steady-state responses, the analysis provides a comprehensive evaluation of the controller's robustness, convergence speed, and tracking precision.

To highlight the advantages of the proposed methodology, a comparative analysis is performed, in which the performance of the developed Fuzzy Fast Terminal Sliding Mode Control (Fuzzy-FTSMC) is evaluated against that of the conventional Fast Terminal Sliding Mode Control (FTSMC). This comparison aims to quantify improvements in tracking accuracy, convergence speed, and overall system robustness achieved by incorporating fuzzy logic into the control scheme. This comparative analysis provides deeper insight into the contribution of the fuzzy adaptation mechanism, particularly in enhancing convergence speed, minimizing chattering, and improving robustness against uncertainties. The results of this study serve as clear evidence that the integration of fuzzy logic with FTSMC offers superior control performance and reliability compared to its classical counterpart.

The control method is applied to the crane system described in [88], where the state vector $\begin{bmatrix} x_1 & x_2 & x_3 & x_4 \end{bmatrix}^T = \begin{bmatrix} x & \dot{x} & \theta & \dot{\theta} \end{bmatrix}^T$ may be used to express the dynamic equations of the system in the state space (3.1,3.2) and f_1, g_1, f_2, g_2, the nonlinear functions, described in (2.45) and the parameters and variables of the crane system are summarizes in the table **??**. The simulation parameters are given in table 3.2.

Figure 3.4 presents the schematic of the control architecture developed using the fuzzy-based Fast Terminal Sliding Mode Control (fuzzy-FTSMC). The central aim of this control design is twofold: first, to completely suppress the oscillatory motion of the payload by driving the swing angle $\theta$to zero, and second, to simultaneously guide the trolley toward the desired reference position denoted as x_d, That is, $\theta = 0$ and $x = x_d$. The system is initialized with the state vector $x = \begin{bmatrix} 0 & 0 & 0 & 0 \end{bmatrix}^T$, while the reference state is defined as $x_d = \begin{bmatrix} 2 & 0 & 0 & 0 \end{bmatrix}^T$. To further examine robustness, external disturbances are introduced in

Parameters	Values	Parameters	Values
m	5kg	M	8kg
L	2m	g	-10m/s
d	1kg/m	k_1	9.7
k_2	13.9	k_3	1
k_4	2.5	p_1	27
p_2	29	q_1	25
q_2	27		

Table 3.2: Simulation parameters

the form of $d_1 = 0.005 * sin(150 * t)$ and $d_2 = 0.01 * sin(200 * t)$.
Under identical simulation conditions, a comparative evaluation is carried out between the proposed fuzzy-based Fast Terminal Sliding Mode Control (fuzzy-FTSMC) and the conventional FTSMC without fuzzy adaptation. This comparison is intended to highlight the impact of incorporating fuzzy logic into the control design, particularly in terms of adaptability and transient performance. The responses of the system states obtained from both controllers are depicted in Figs. (3.8) and (3.9), providing a clear visualization of their respective behaviors. These results allow for a direct examination of convergence speed, tracking accuracy, and robustness, thereby demonstrating the practical benefits achieved by the fuzzy-tuned FTSMC over its non-adaptive counterpart.

The simulation results depicted in figures (3.8) and (3.9) demonstrate that the proposed Fuzzy-FTSMC achieves a markedly faster dynamic response compared to the conventional FTSMC. In particular, whereas the standard FTSMC requires approximately 8 seconds to reach steady-state, the fuzzy-FTSMC attains convergence in roughly 4 seconds. This improvement indicates that the integration of fuzzy logic significantly enhances the system's response speed, effectively halving the settling time and highlighting the benefits of fuzzy-based tuning in accelerating system performance.
The tracking error responses shown in figures (3.10) and (3.11) provide clear evidence that the proposed fuzzy-FTSMC achieves superior tracking accuracy compared to the conventional FTSMC. The suggested approach ensures faster error convergence, reduced steady-state deviation, and improved robustness in the presence of uncertainties.
Furthermore, figure (3.12) presents the control input signals produced by both control strategies, enabling an evaluation of actuator effort and the smoothness of control actions. Simul-

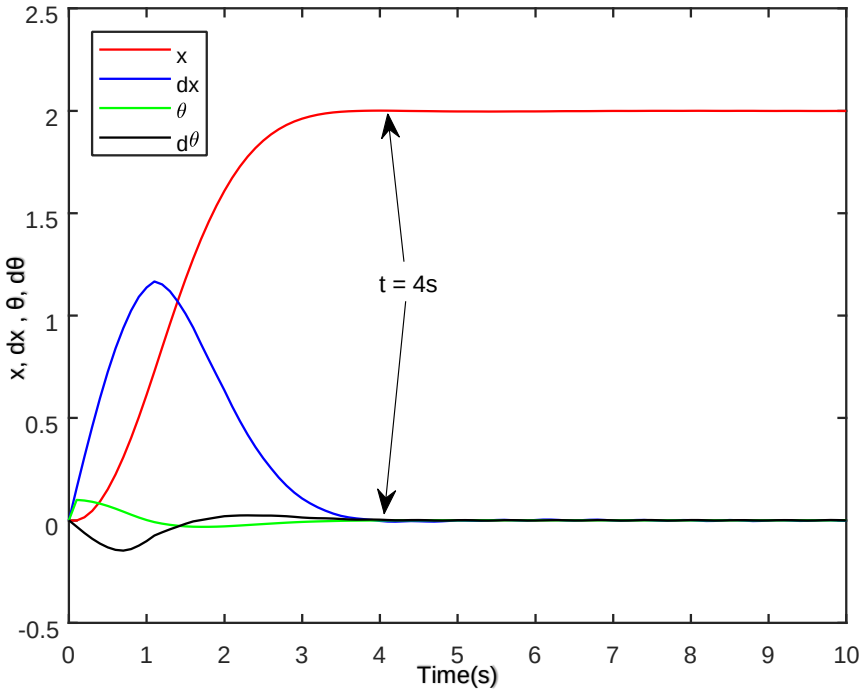

Figure 3.8: States with fuzzy-FTSMC

taneously, figure (3.13) shows the trajectories of the sliding surfaces, which provide insight into the system's stability and convergence behavior under each controller. Collectively, these results demonstrate that the fuzzy-tuned controller not only improves trajectory tracking but also ensures smoother, more efficient actuation while preserving system stability throughout the entire operating range.

To summarize these findings, the comparative simulations clearly demonstrate the effectiveness of the fuzzy-FTSMC framework over the conventional FTSMC. The inclusion of fuzzy tuning substantially accelerates the system dynamics, reducing settling time by nearly half, and enables more precise tracking performance with faster error convergence and diminished steady-state offsets. Furthermore, the evaluation of control inputs highlights that the proposed controller achieves smoother actuation without sacrificing stability. The analysis of sliding surfaces further reinforces the robustness and convergence properties of the fuzzy-FTSMC. Collectively, these results establish that the fuzzy-enhanced controller not only improves responsiveness and accuracy but also ensures efficient and reliable performance in the presence of uncertainties.

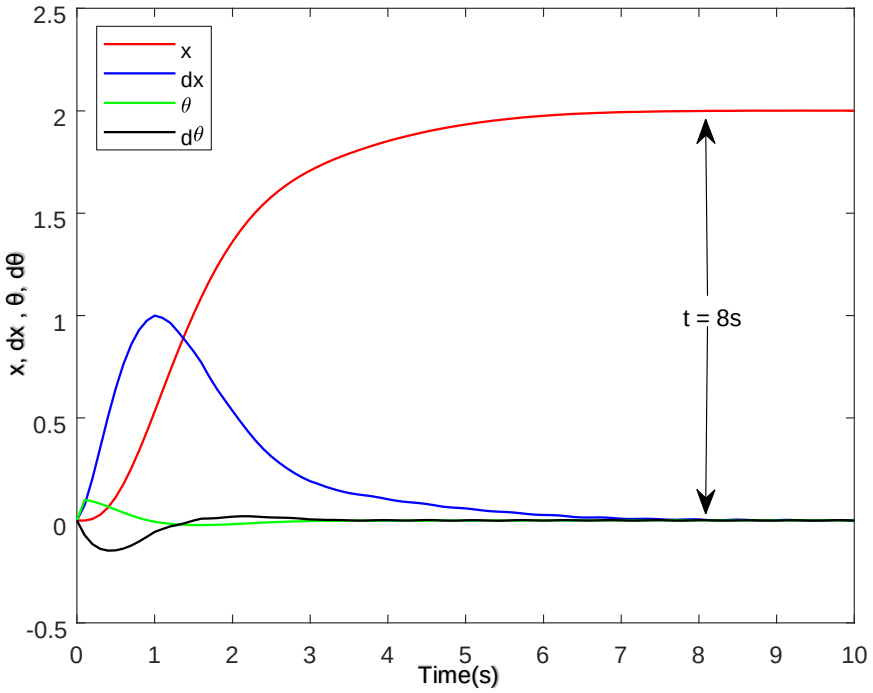

Figure 3.9: States with FTSMC

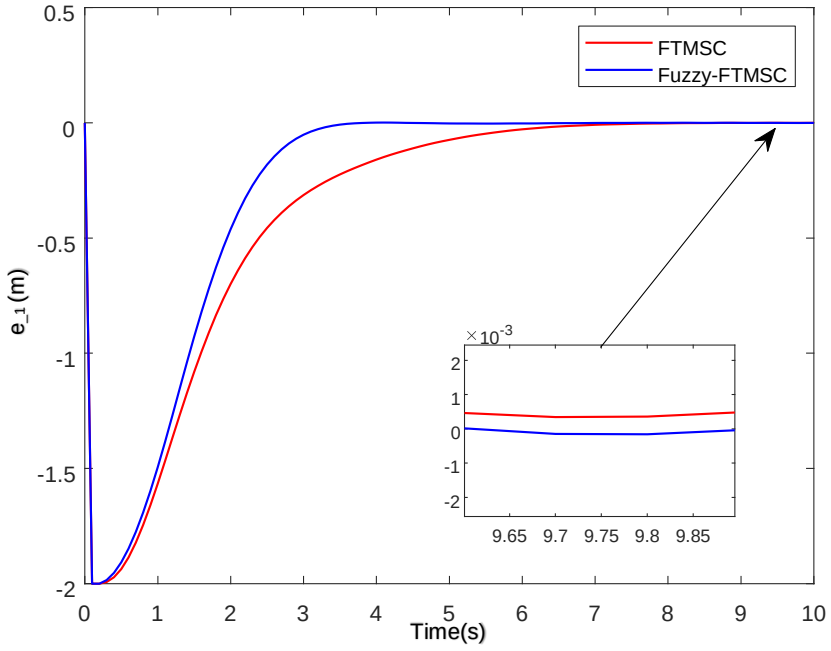

Figure 3.10: Tracking error e_1

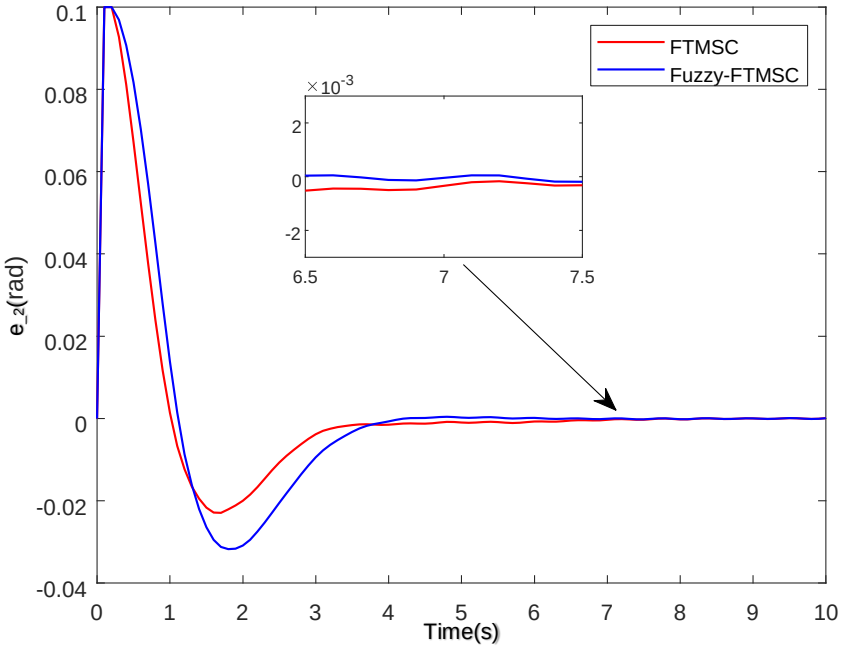

Figure 3.11: Tracking error e_2

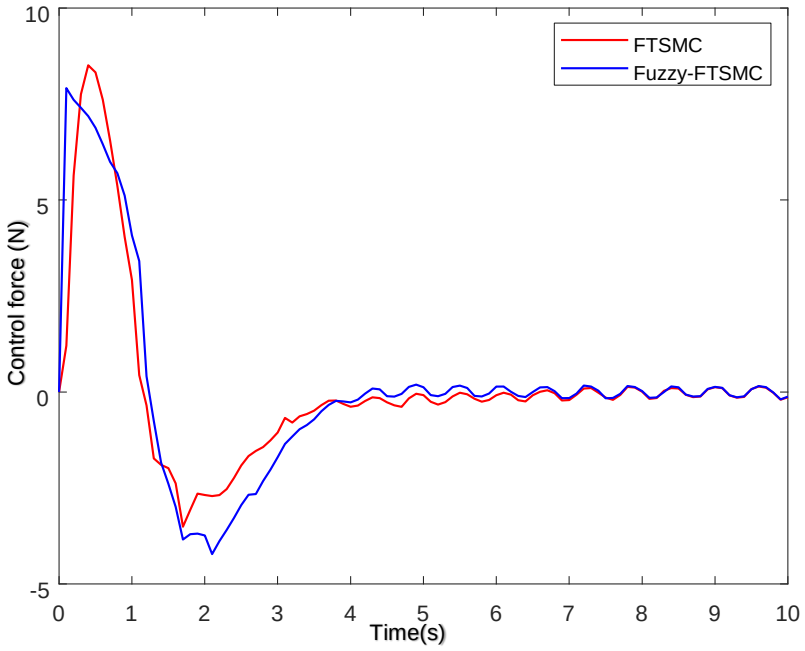

Figure 3.12: Control actions of fuzzy-FTSMC and FTSMC

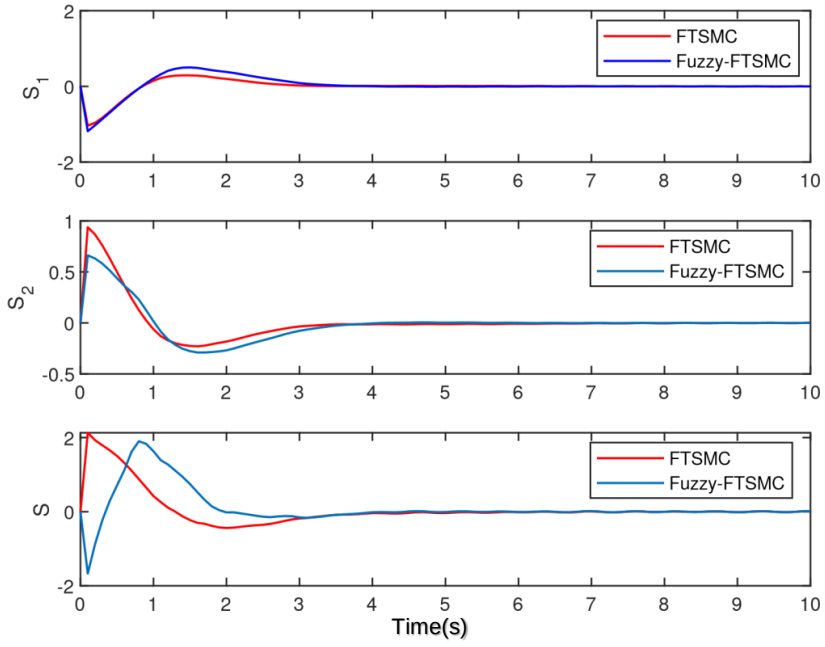

Figure 3.13: Surfaces of fuzzy-FTSMC and FTSMC

3.8 Conclusion

In this chapter, a Fuzzy Fast Terminal Sliding Mode Control (FFTSMC) approach is developed for the stabilization and trajectory tracking of underactuated mechanical systems. The primary aim is to design a control scheme that ensures rapid convergence, high robustness, and minimizes the chattering phenomenon commonly associated with traditional sliding mode controllers. By integrating fast terminal sliding mode control with fuzzy logic, the controller leverages real-time tuning of control parameters, thereby improving precision and accelerating the alignment of system states with their desired trajectories.

The stability and convergence of the proposed control strategy were rigorously examined using Lyapunov stability theory. The analysis demonstrated that the closed-loop system ensures the tracking error converges to zero in finite time, while maintaining robustness against matched uncertainties and external disturbances. This theoretical validation confirms the reliability of the proposed approach and underscores its effectiveness for underactuated systems, where both stability and robustness are critical design requirements.

To validate the performance of the proposed FFTSMC framework, comprehensive simulation experiments were carried out on an overhead crane system. The findings revealed that the controller significantly improved convergence speed while effectively suppressing oscillations

and mitigating chattering, outperforming conventional sliding mode controllers and comparable techniques. Additionally, the incorporation of fuzzy tuning resulted in smoother control signals, emphasizing the practical benefits of the approach.

For the next chapters, the control strategy can be further improved by integrating Type-2 fuzzy logic into the fast terminal sliding mode framework, enabling better handling of uncertainty and enhancing robustness and adaptability under presence of external disturbances.

Chapter 4

Adaptive fuzzy type-2 FTSMC for UMS

4.1 Introduction

This chapter introduces an Adaptive Fuzzy Type-2 Fast Terminal Sliding Mode Control (AFT2-FTSMC) approach for underactuated mechanical systems (UMSs), which are nonlinear, strongly coupled systems characterized by having fewer actuators than degrees of freedom. The primary aim of this strategy is to overcome the challenges inherent in such systems, including nonlinear dynamics, inter-variable coupling, model uncertainties, and external disturbances. The proposed controller combines the finite-time convergence properties of Fast Terminal Sliding Mode Control (FTSMC) with the enhanced uncertainty-handling capability of type-2 fuzzy systems, which surpass conventional type-1 fuzzy logic in dealing with higher levels of imprecision. While the previous chapter presented a Fuzzy Fast Terminal Sliding Mode Control (FFTSMC) framework that improved convergence speed and robustness, its reliance on type-1 fuzzy logic constrained its performance in environments with significant uncertainties and modeling errors.

In the proposed framework, an adaptive fuzzy system is utilized to estimate the control input continuously in real time, providing accurate compensation for model uncertainties and external disturbances. By embedding fuzzy type-2 logic within the FTSMC framework, the controller effectively enhances the system's robustness and stability. Moreover, the adaptive update laws enable the control structure to adjust dynamically in response to varying system conditions, thereby improving tracking accuracy and resilience in highly uncertain environments.

As discussed in Chapter 1, the underactuated mechanical systems (UMSs) have been widely utilized in the literature, and recent studies have explored various hybrid schemes that integrate fuzzy logic with advanced sliding-mode control techniques to enhance robustness and convergence. For example, in [102] A robust control framework for robotic systems is proposed by integrating type-2 fuzzy logic with the nonsingular fast sliding-mode technique. Similarly, the study [103] developed a new PID-FTSM framework integrated with type-2 fuzzy systems, aimed at achieving faster convergence while reducing steady-state deviations, and in [104], an AFT2FTSMC algorithm is integrated to develop robust controllers for robotic manipulator trajectory tracking in the presence of parameter uncertainties, external disturbances, and potential faults. An adaptive type-2 fuzzy logic system is utilized to approximate the time-varying, nonlinear, and uncertain dynamics of the robot in [105].
A novel observer-based direct adaptive type-2 fuzzy sliding-mode control (SMC) approach is introduced in [106]. Initially, a high-gain observer is constructed to estimate the system's tracking errors. Building upon this observer, a fuzzy type-2 is then employed to approximate the equivalent control law. A fault-tolerant position tracking strategy for quadrotor UAVs is proposed in [107], employing a model-reference integral sliding-mode controller enhanced with an interval type-2 fuzzy model.
The study [108] introduces an adaptive interval type-2 fuzzy sliding-mode control (AIT2FSMC) approach that combines sliding-mode control with adaptive interval type-2 fuzzy logic to address the control of chaotic systems. In addition, a control framework is presented for a 6-DOF octorotor aircraft, which integrates interval type-2 fuzzy logic control with sliding-mode control (SMC) employing a proportional–integral–derivative (PID) sliding surface. In this scheme, the interval type-2 fuzzy controller generates the switching control signal, while the output gain of the fuzzy sliding component is adaptively tuned online through a supervisory type-2 fuzzy mechanism, forming an adaptive interval type-2 fuzzy sliding-mode control structure.
In this chapter, the developed AFT2-FTSMC strategy represents a significant step forward in the controller design for underactuated systems. It not only ensures rapid convergence and high control precision, but also establishes a balance between robustness and smooth control action, making it suitable for practical applications such as cranes, robotic manipulators, and other nonlinear systems with limited actuation. The effectiveness and superiority of the proposed approach will be validated through comparative simulation studies against previously introduced methods.

4.2 Type-2 fuzzy logic system

Fuzzy logic has been widely acknowledged as a powerful approach for managing complex nonlinear dynamics and handling uncertain or imprecise information. Traditional Type-1 Fuzzy Logic Systems (T1FLS) have proven effective across numerous control and decision-making scenarios. Nevertheless, because T1FLS employs crisp membership functions, it may fall short in capturing the full extent of uncertainty present in practical applications. To overcome this limitation, Type-2 Fuzzy Logic Systems (T2FLS) were developed, extending the capabilities of type-1 systems to better represent and manage uncertainty.
Type-2 fuzzy logic systems expand upon traditional fuzzy frameworks by incorporating uncertainty directly into the membership grades, providing an additional layer of flexibility. This feature allows T2FLSs to more accurately capture the behavior of highly nonlinear systems, accommodate measurement noise, and account for unmodeled dynamics or parameter variations. Consequently, type-2 fuzzy systems are particularly well-suited for controlling underactuated and uncertain systems, where achieving both robustness and adaptability is essential. Nevertheless, many real-world systems are subject to variations and disturbances that evolve over time, which necessitate the inclusion of adaptation mechanisms. This motivates the development of adaptive type-2 fuzzy logic systems (AT2FLSs), where system parameters are adjusted online to ensure robustness and improved performance in dynamic environments.

4.2.1 Fundamentals of type-2 fuzzy sets

In the literature, type-2 fuzzy sets are commonly categorized into interval type-2 fuzzy logic systems (IT2FLSs) and generalized type-2 fuzzy logic systems (GT2FLSs). In the literature, type-2 fuzzy sets are commonly categorized into interval type-2 fuzzy logic systems (IT2FLSs) and generalized type-2 fuzzy logic systems (GT2FLSs). Interval type-2 fuzzy sets are the most widely employed because they offer a reasonable compromise between computational feasibility and the ability to model uncertainty. In this case, uncertainty in the membership grade is represented by an interval bounded by an upper membership function (UMF) and a lower membership function (LMF), and the region enclosed between them is referred to as the footprint of uncertainty (FOU). As we can see in Figure (4.1), this footprint captures the range of possible membership values and provides a direct description of the uncertainty embedded within the fuzzy model. GT2 fuzzy sets, on the other hand, extend this concept further by allowing the secondary memberships themselves to be fuzzy

sets, As displayed in Figure (4.2), creating a three-dimensional structure capable of modeling more intricate forms of uncertainty, This gives them greater representational power to model complex uncertainty but also introduces significantly higher computational cost, especially during the type-reduction stage.

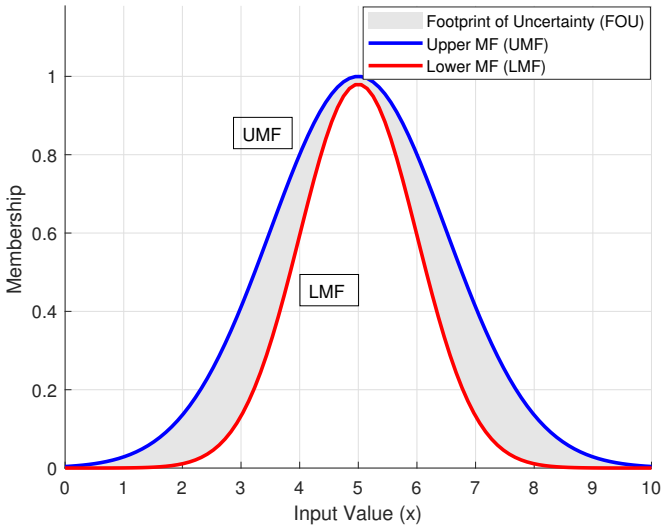

Figure 4.1: Interval type-2 fuzzy logic system (IT2FLSs)

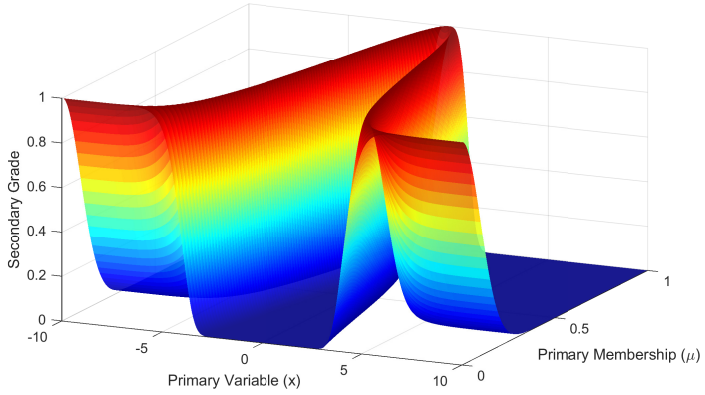

Figure 4.2: Generalized type-2 fuzzy logic system (GT2FLSs)

Mathematically speaking, an interval type-2 (IT2) fuzzy set, denoted as $\tilde{B}$ is described through an interval type-2 membership function $\mu_{\tilde{B}}(x,u)$, defined as:

$$\tilde{B} = \left\{ \Big(x,u\Big),\ \mu_{\tilde{B}}(x,u) \;\middle|\; \forall x \in X,\ \forall u \in J_x \subseteq [0,1] \right\}, \tag{4.1}$$

where X is the universe of discourse, and J_x represents the *primary membership*, which is an interval within $[0,1]$ for each x.

In this case, the secondary membership function takes values of either 0 or 1, which simplifies the representation compared to generalized type-2 fuzzy sets. The uncertainty in the membership function is captured by the so-called *footprint of uncertainty (FOU)*, defined as the union of all primary membership intervals across X by $FOU(B) = \cup_{\forall x \in X}[\underline{\mu}_B(x), \overline{\mu}_B(x)]$ where $\underline{\mu}_B$ is the Upper Membership Function (UMF) corresponds to the upper boundary of the footprint of uncertainty (FOU)B and $\overline{\mu}_B$ the Lower Membership Function (LMF) characterizes the lower boundary of its footprint of uncertainty (FOU)B. This structure makes IT2 fuzzy sets computationally more tractable while still effectively handling uncertainty. In the case of generalized type-2 (GT2), a fuzzy set is expressed as:

$$\tilde{B} = \left\{ \Big(x, u\Big),\ \mu_{\tilde{B}}(x,u) \;\middle|\; \forall x \in X,\ \forall u \in J_x \subseteq [0,1],\ \mu_{\tilde{B}}(x,u) \in [0,1] \right\}, \tag{4.2}$$

where $\mu_{\tilde{A}}(x,u)$ is referred to as the *secondary grade*, representing the degree of membership of u at the primary variable x. Unlike interval type-2 sets, in which the secondary membership values are restricted to either zero or one, GT2 sets allow these values to take any grade in the interval $[0,1]$. This leads to a three-dimensional membership function, offering a more expressive framework for modeling uncertainty. However, this richness comes at the expense of significantly higher computational complexity, especially in the type-reduction stage, which must be performed before defuzzification.

4.2.2 Structure of adaptive type-2 fuzzy logic system

A type-2 fuzzy logic system follows the same general architecture as a conventional type-1 FLS, but it is enhanced to handle higher levels of uncertainty. The overall framework still depends on expert knowledge and is composed of five principal components. These are:

1. **Fuzzification module:** This block transforms crisp numerical inputs into type-2 fuzzy sets. Unlike type-1 fuzzification, the membership functions here have an additional dimension representing uncertainty, typically in the form of a footprint of uncertainty (FOU). Various forms of membership functions can be utilized to model type-2 fuzzy sets, including triangular, trapezoidal, Gaussian, and others. Among these, Gaussian functions are commonly employed due to their smoothness and mathematical tractability. Illustrative examples of an IT2 Gaussian membership function and a GT2 Gaussian membership function are provided in figures (4.1) and (4.2), respectively.

2. **Rule base:** The rule base stores the collection of fuzzy if–then rules defined by domain experts or derived from data. In the case of type-2 systems, the antecedents and

consequents are expressed using type-2 fuzzy sets, thereby extending the flexibility in capturing uncertainty. The structure of the i^{th} type-2 rule is:
R^k : **If** x_1 is $\tilde{\Gamma}_1^k$ and x_2 is $\tilde{\Gamma}_2^k$ ...and x_n is $\tilde{\Gamma}_n^k$ **Then** $y \in \varrho^k$.
Here, $\tilde{\Gamma}_n^k$ denote the type-2 fuzzy sets that characterize the antecedent part of the rules, while ϱ^k corresponds to the consequent fuzzy set of the i^{th} rule, $\varrho^k \in [\omega_l^k, \omega_m^k]$ which specifies the weighting range in the rule's consequent component.

3. **Inference engine** The inference process determines how the rules are activated based on the fuzzified inputs and how they interact. In type-2 FLS, the inference results are themselves fuzzy sets with embedded uncertainty. In our work the product operation [109] will be employed, using either the minimum or the product t-norm for rule evaluation, the firing strength of the i^{th} rule denoted as Γ^i is represented by an interval type-2 fuzzy set and expressed as $\Gamma^i(x) = [\underline{f}^i(x), \overline{f}^i(x)]$, where $\underline{f}^i(x), \overline{f}^i(x)$ denote the lower and upper membership functions, respectively as:

$$\begin{aligned} \underline{f}^i(x) &= \underline{\mu}_{\tilde{\Gamma}_1^k}(x_1) * ... * \underline{\mu}_{\tilde{\Gamma}_n^k}(x_n) \\ \overline{f}^i(x) &= \overline{\mu}_{\tilde{\Gamma}_1^k}(x_1) * ... * \overline{\mu}_{\tilde{\Gamma}_n^k}(x_n) \end{aligned} \tag{4.3}$$

These limits characterize the footprint of uncertainty (FOU) associated with the antecedent of the rule, enabling the firing strength to directly reflect the imprecision present in the membership functions.

4. **Type-Reduction Mechanism:** This is a critical step that differentiates type-2 from type-1 FLS. Since the inference produces type-2 fuzzy sets, they must be reduced to type-1 fuzzy sets before defuzzification. Among the different type-reduction techniques, this work applies Karnik and Mendel[110] method using the center-of-sets, since it achieves faster computation compared to the centroid-based method:

$$Y_c = \frac{\sum_{i=1}^{M} f^i \omega^i}{\sum_{i=1}^{M} f^i} \tag{4.4}$$

where Y_c is the interval set determined by two end points y_l and y_r and $\omega^i \in W^i = [W_L^i, W_R^i]$is the Type-2 interval consequent set.

5. **Defuzzification:** Finally, the type-reduced fuzzy sets are converted back into crisp numerical outputs. This output represents the control signal or decision generated by the system. By applying the center of gravity method, the defuzzification process yields the crisp output for each corresponding output variable, expressed as:

$$y(x) = \frac{y_l + y_r}{2} \tag{4.5}$$

the output y_l and y_r may be formulated as an expansion over fuzzy basis functions (FBFs), which can be written as follows:

$$\begin{aligned} y_l &= \frac{\sum_{i=1}^{M} f_l^i \omega_l^i}{\sum_{i=1}^{M} f_l^i} = \sum_{i=1}^{M} \omega_l^j \Psi_l^j = \Psi_l^T \omega_l(x) \\ y_r &= \frac{\sum_{i=1}^{M} f_r^i \omega_r^i}{\sum_{i=1}^{M} f_r^i} = \sum_{i=1}^{M} \omega_r^j \Psi_r^j = \Psi_r^T \omega_r(x) \end{aligned} \tag{4.6}$$

where,

$$\Psi_l^j = \frac{f_l^i}{\sum_{i=1}^{M} f_l^i}; \Psi_r^j = \frac{f_r^i}{\sum_{i=1}^{M} f_r^i} \tag{4.7}$$

$\Psi_r(x)$,$\Psi_l(x)$is the fuzzy basis functions (FBF) vector of y, such that $\Psi_r(x) = [\Psi_r^1, ..., \Psi_r^m]$ and $\Psi_l(x) = [\Psi_l^1, ..., \Psi_l^m]$.

The output of type-2 fuzzy logic system can be expressed in a linear-in-parameters structure as:

$$y = \frac{\Psi_l^T \omega_l + \Psi_r^T \omega_r}{2} = \Psi^T \omega \tag{4.8}$$

Here, $\Psi^T(x)$ represents the vector of adjustable parameters associated with the fuzzy basis functions. This formulation is incorporated within the adaptive control framework, where it is utilized to approximate the required control input. By doing so, the controller is able to construct an equivalent control law that dynamically adapts to system uncertainties and external disturbances, thereby ensuring robustness and enhanced tracking performance.

4.2.3 Hybrid adaptive fuzzy type-2

Hybrid adaptive fuzzy type-2 control strategies have emerged as a promising direction for addressing complex nonlinear and uncertain systems. Combining type-2 fuzzy logic with advanced control techniques such as sliding mode control, backstepping, model predictive control, or neural networks enable hybrid strategies to leverage the strengths of each method. The interval type-2 fuzzy framework enhances the system's ability to manage uncertainties and measurement noise, surpassing the capabilities of conventional type-1 fuzzy systems in complex and dynamic environments. Simultaneously, the adaptive element allows real-time adjustment of control parameters, ensuring robust performance and precise trajectory tracking despite time-varying disturbances or changes in system parameters. This hybridization not only improves stability and accelerates convergence but also mitigates chattering and reduces control effort, making the approach more practical for real-world applications. Recent research indicates that adaptive fuzzy type-2 hybrid controllers consistently outperform

traditional method schemes, demonstrating their effectiveness for implementation in underactuated mechanical systems, robotics, and other safety-critical engineering domains.

4.3 Design of the adaptive fuzzy type-2 FTSMC

This chapter introduces an adaptive fuzzy type-2 fast terminal sliding mode control (AFT2-FTSMC) framework specifically developed to tackle the control challenges inherent in underactuated mechanical systems (UMSs). The proposed approach combines the inherent robustness of sliding mode control with the finite-time convergence characteristics of fast terminal sliding mode techniques, while utilizing the superior uncertainty-handling and approximation capabilities of type-2 fuzzy logic systems. The main motivation behind this approach is to design a controller that ensures rapid tracking performance, enhances robustness against uncertainties, and simultaneously reduces the chattering problem inherent in conventional sliding mode techniques.

The fast terminal sliding mode control (FTSMC) ensures that the system trajectories converge to the desired states in finite time, which provides faster error dynamics than standard sliding mode controllers, and the type-2 fuzzy logic system (T2FLS) is incorporated to directly approximate the control input in real time. By modeling the footprint of uncertainty (FOU) in the membership functions, the T2FLS achieves more reliable approximations under uncertain and noisy conditions compared to type-1 fuzzy systems.

To formally establish the control framework, the tracking error is defined as the deviation between the system's actual state trajectory $y(t)$ and the desired reference trajectory $y_d(t)$. Mathematically speaking, it can be expressed as:

$$e = y(t) - y_d(t) \tag{4.9}$$

This error variable serves as the basis for designing the sliding surface and deriving the adaptive fuzzy type-2 fast terminal sliding mode control law.

For each scalar error component, the fast terminal sliding surface is selected in such a manner to guarantee the finite-time convergence while retaining desirable transient characteristics. Indeed, the fast terminal sliding surface using a scalar error $e(t)$ is:

$$S = \dot{e} + \alpha e + \beta e^{(q/p)} \tag{4.10}$$

The combination of a linear term αe and a nonlinear terminal term $\beta e^{(q/p)} sign(e)$ accelerates convergence both away from and near the origin and helps avoid singularity issues of simple

terminal surfaces.

To overcome the difficulties associated with limited actuation and the strongly coupled dynamics of underactuated systems, a practical approach involves decomposing the system into multiple interconnected subsystems that reflect its cascaded dynamic structure. For each subsystem, a fast terminal sliding surface is designed to ensure finite-time convergence of the local error dynamics. These local surfaces are then systematically integrated to form a higher-level sliding manifold, coordinating the behavior of the complete system. This hierarchical control framework, commonly known as Hierarchical Sliding Mode Control (HSMC), offers a structured methodology for managing coupled dynamics while guaranteeing robust global stability. The resulting global sliding manifold unifies the dynamics of all subsystems into a single sliding condition, providing the foundation for the overall control law. Mathematically, the global sliding manifold can be represented as:

$$S = k_1 S_1 + k_2 S_2 + ... + k_n S_n = \sum_{i=1}^{n} k_i S_i \tag{4.11}$$

where $k1, ..., k_n$ represent positive control gains.

The corresponding sub-sliding surfaces are defined as follows:

$$\begin{aligned} S_1 &= \dot{e_1} + \alpha_1 e_1 + \beta_1 e_1^{(q_1/p_1)} \\ S_2 &= \dot{e_2} + \alpha_2 e_2 + \beta_2 e_2^{(q_2/p_2)} \\ &... \\ S_n &= \dot{e_n} + \alpha_n e_n + \beta_n e_n^{(q_n/p_n)} \end{aligned} \tag{4.12}$$

Taking the derivative of (4.12) with respect to time yields:

$$\begin{aligned} \dot{S}_1 &= \ddot{e_1} + \alpha_1 \dot{e}_1 + \beta_1 (q_1/p_1) \dot{e}_1 e_1^{(q_1/p_1)-1} \\ \dot{S}_2 &= \ddot{e_2} + \alpha_2 \dot{e}_2 + \beta_2 (q_2/p_2) \dot{e}_2 e_2^{(q_2/p_2)-1} \\ &... \\ \dot{S}_n &= \ddot{e_n} + \alpha_n \dot{e}_n + \beta_n (q_n/p_n) \dot{e}_n e_n^{(q_n/p_n)-1} \end{aligned} \tag{4.13}$$

By substituting the dynamic equations into (2.11), we arrive at the following representation:

$$\begin{aligned} \dot{S}_1 &= h_1(x) + j_1(x) u_{1eq} + d_1 - \ddot{y}_{1d} + \alpha_1 \dot{e}_1 + \beta_1 (q_1/p_1) \dot{e}_1 e_1^{(q_1/p_1)-1} \\ \dot{S}_2 &= h_2(x) + j_2(x) u_{2eq} + d_2 - \ddot{y}_{2d} + \alpha_2 \dot{e}_2 + \beta_2 (q_2/p_2) \dot{e}_2 e_2^{(q_2/p_2)-1} \\ &... \\ \dot{S}_n &= h_n(x) + j_n(x) u_{neq} + d_n - \ddot{y}_{nd} + \alpha_n \dot{e}_n + \beta_n (q_n/p_n) \dot{e}_n e_n^{(q_n/p_n)-1} \end{aligned} \tag{4.14}$$

For each actuated subsystem, the associated equivalent control input can be formally specified as follows :

$$\begin{aligned} u_{1eq} &= j_1(x)^{-1}(h_1(x) + d_1 - \ddot{y}_{1d} + \alpha_1\dot{e}_1 + \beta_1(q_1/p_1)\dot{e}_1 e_1^{(q_1/p_1)-1}) \\ u_{2eq} &= j_2(x)^{-1}(h_2(x) + d_2 - \ddot{y}_{2d} + \alpha_2\dot{e}_2 + \beta_2(q_2/p_2)\dot{e}_2 e_2^{(q_2/p_2)-1}) \\ &\dots \\ u_{neq} &= j_n(x)^{-1}(h_n(x) + d_n - \ddot{y}_{nd} + \alpha_n\dot{e}_n + \beta_n(q_n/p_n)\dot{e}_n e_n^{(q_n/p_n)-1}) \end{aligned} \tag{4.15}$$

At this point, we arrive at the explicit expression of the equivalent control law for each subsystem, ensuring that the system trajectories are driven toward the defined manifold and converging to the designed sliding surfaces, thereby maintaining robust performance.
Taking the time derivative of the global manifold sliding surfaces in (4.11) yields:

$$\begin{aligned} \dot{S} = k_1(\ddot{e_1} + \alpha_1\dot{e}_1 + \beta_1(q_1/p_1)\dot{e}_1 e_1^{(q_1/p_1)-1}) + \dots k_n(\ddot{e}_n + \alpha_n\dot{e}_n + \beta_n(q_n/p_n)\dot{e}_n e_n^{(q_n/p_n)-1}) \\ = \sum_{i=1}^{n} k_i(\dot{S}_i) \end{aligned} \tag{4.16}$$

When the system dynamics are embedded into (4.16), the expression becomes:

$$\begin{aligned} \dot{S} = k_1(h_1(x) + j_1(x)u_1 + d_1 - \ddot{y}_{1d} + \alpha_1\dot{e}_1 + \beta_1(q_1/p_1)\dot{e}_1 e_1^{(q_1/p_1)-1}) + \dots \\ + k_n(h_n(x) + j_n(x)u_n + d_n - \ddot{y}_{nd} + \alpha_n\dot{e}_n + \beta_n(q_n/p_n)\dot{e}_n e_n^{(q_n/p_n)-1}) \\ = \sum_{i=1}^{n} k_i(h_i(x) + j_i(x)u_{ieq} + d_i - \ddot{y}_{id} + \alpha_i\dot{e}_i + \beta_i(q_i/p_i)\dot{e}_i e_i^{(q_i/p_i)-1}) \end{aligned} \tag{4.17}$$

The control law for the i^{th} subsystem is expressed as the sum of an equivalent component and a switching one, expressed as:

$$u_i = u_{ieq} + u_{isw} \tag{4.18}$$

where the switching term takes the form:

$$u_{isw} = -\kappa_{1i}S - \kappa_{2i}sign(S) \tag{4.19}$$

where κ_{1i} and κ_{2i} are positive design parameters ensuring robustness.
Let $u_{ieq}^{\star}$ represent the ideal control law that compensates for system nonlinearities and guarantees satisfaction of the sliding condition. In the proposed framework, an interval type-2 fuzzy logic system (IT2-FLS) is employed to generate an approximation $\hat{u}_{ieq}$ of $u_{ieq}^{\star}$, where the difference corresponds to the approximation error:

$$\tilde{u}_{ieq} = \hat{u}_{ieq} - u_{ieq}^{\star}, \qquad \|\tilde{u}_{ieq}\| \leq \bar{\varepsilon}. \tag{4.20}$$

with $\bar{\varepsilon}$ constant.
The actual control action associated with each actuated subsystem is determined according to the following expression:

$$u_i = \hat{u}_{ieq} + u_{isw}, \tag{4.21}$$

Hence, the equivalent control signal generated by the Type-2 FLS can be expressed as:

$$\hat{u}_{ieq} = \Psi^T \omega \tag{4.22}$$

This simplified structure will allow us to approximate the control input and exploit the adaptive technique.

4.4 Stability analysis

Theorem 7. *By employing the sliding surface defined in (4.16), the control law in (4.22) ensures that the system dynamics described in (4.13) converge asymptotically to the desired reference trajectory, driving the tracking error e toward zero.*

Proof. To analyze the stability of the proposed control scheme, we introduce the Lyapunov candidate function defined by:

$$V = \frac{1}{2}S^2 + \frac{1}{2}\tilde{\Psi}^T \Gamma^{-1} \tilde{\Psi} \tag{4.23}$$

Since $\Gamma > 0$ is selected as the adaptation gain to guarantee proper adjustment of the fuzzy parameters, differentiating the Lyapunov candidate function V with respect to time provides:

$$\dot{V} = S\dot{S} + \tilde{\Psi}^T \Gamma^{-1} \dot{\Psi} \tag{4.24}$$

Replacing the surface expression of (4.17) into the Lyapunov derivative form in (4.24), leads to:

$$\dot{V} = S(\sum_{i=1}^{n} k_i(h_i(x) + j_i(x)u_i + d_i - \ddot{y}_{id} + \alpha_i \dot{e}_i + \beta_i(q_i/p_i)\dot{e}_i e_i^{(q_i/p_i)-1})) + \tilde{\Psi}^T \Gamma^{-1} \dot{\Psi} \tag{4.25}$$

When the control input described by (4.22) is incorporated into the system equation (4.25), the resulting formulation becomes:

$$\dot{V} = S(\Psi^T \omega + \Delta_r + \sum_{i=1}^{n} u_{isw} + \sum_{i=1}^{n} k_i d_i) + \tilde{\Psi}^T \Gamma^{-1} \dot{\Psi} \tag{4.26}$$

Consequently, the corresponding adaptation laws can be formulated as:

$$\dot{\Psi} = -\Gamma S \omega, \tag{4.27}$$

Inserting the expression given in (4.27) into (4.26), the following expression can be derived:

$$\dot{V} = S(\Delta_r - \sum_{i=1}^{n} \kappa_{1i} S - \sum_{i=1}^{n} \kappa_{2i} sign(S) + \sum_{i=1}^{n} k_i d_i) \tag{4.28}$$

Given that $S\Delta_r \leq |S|\bar{\Delta}_r$ and $S\sum_{i=1}^{n} k_i d_i \leq |S|\sum_{i=1}^{n} k_i \bar{d}_i$, the expression in (4.28) can be reformulated as:

$$\dot{V} \leq -S^2 \sum_{i=1}^{n} \kappa_{1i} + |S|(\bar{\Delta}_r + \sum_{i=1}^{n} k_i \bar{d}_i - \sum_{i=1}^{n} \kappa_{2i}) \tag{4.29}$$

Hence, the equation (4.29) establishes the stability of the global sliding manifold, provided that the control gain condition $\bar{\Delta}_r + \sum_{i=1}^{n} k_i \bar{d}_i \leq \sum_{i=1}^{n} \kappa_{2i}$ is satisfied. □

4.5 Simulation results

This section details the results of numerical simulations performed to assess the performance of the proposed Adaptive Fuzzy Type-2 Fast Terminal Sliding Mode Controller (AFT2-FTSMC) applied to underactuated mechanical systems (UMSs). The evaluation was carried out using MATLAB, with an overhead crane system serving as a representative benchmark. This system was chosen because of its inherent underactuation and strongly coupled nonlinear dynamics, characteristics that make it a standard test case for validating advanced control strategies in the literature.

The simulations are conducted to evaluate the effectiveness of the proposed controller in meeting multiple critical performance criteria simultaneously. In particular, the assessment focuses on the controller's ability to achieve accurate trajectory tracking of the trolley, attenuate oscillations of the suspended payload, ensure finite-time convergence of the tracking errors, and maintain smooth control inputs. The incorporation of type-2 fuzzy logic enhances the system's robustness to modeling uncertainties and external disturbances, while the fast terminal sliding mode component ensures rapid convergence of system states. To validate these capabilities, graphical representations of state trajectories, tracking errors, and control efforts are provided, supporting the theoretical analysis.

Collectively, the simulation results confirm the effectiveness of the proposed AFT2-FTSMC strategy, highlighting its capability to robustly manage the complexities and dynamic challenges inherent in underactuated mechanical systems.

The primary aim of the proposed control strategy is to guide the crane trolley to a desired reference position while concurrently minimizing payload swing, ensuring the pendulum angle remains near zero. To evaluate the controller's performance, simulations were carried out

under clearly specified initial conditions and parameter values. The system was initialized with the following state vector:

$$x = \begin{bmatrix} 0.4 & 0 & 0.1 & 0 \end{bmatrix}^T \tag{4.30}$$

and the desired trajectory for the trolley motion is chosen as:

$$y_d(t) = sin(0.5 * t) \tag{4.31}$$

The physical parameters of the overhead crane model used in the study are specified as follows: payload mass $M_p = 7kg$, trolley mass $M_c = 9kg$, cable length$l = 2m$, gravitational acceleration $g = -9.81m/s$, and damping coefficient $D = 0.3kg/m$.
For the controller design, the gains of the fast terminal sliding mode surfaces are tuned to $k1 = 2.5, k2 = 1.3$, with terminal parameters $\alpha_1 = 1.9, \beta_1 = .2$, $\alpha_2 = 14, \beta_2 = .2$ The shaping exponents of the sliding manifolds are assigned as $p1 = 23, q1 = 21, p2 = 17, q2 = 15$, The reaching term parameters are set to $\kappa_1 = 12, \kappa_2 = 11$.
To evaluate the robustness of the proposed controller, external disturbances are introduced into the system in the form:

$$D1 = D2 = 0.5 * sin(.05 * k) + .3 * exp(-((k - 1120)^2)/(2 * h^2)), h = 55. \tag{4.32}$$

As illustrated in figure 4.3, the proposed control strategy demonstrates a strong ability to guide the crane trolley accurately toward the desired reference position. The system's response closely follows the intended trajectory, exhibiting only minimal deviations during the transient phase. Furthermore, the motion converges with negligible overshoot and a significantly shortened settling time, highlighting the controller's effectiveness in achieving both precision and stability. These results substantiate the applicability of the proposed method for reliable regulation of the crane's translational motion under dynamic operating conditions.

As illustrated in figure 4.4, the proposed control strategy effectively suppresses payload oscillations during crane operation. The swing angle decreases smoothly and converges rapidly toward zero, demonstrating that oscillatory disturbances are efficiently attenuated. This performance underscores the controller's capability to robustly stabilize the underactuated dynamics of the system, even under demanding motion conditions. Moreover, the observed response highlights the controller's role in ensuring overall system safety and reliable operation, which are essential considerations in practical crane applications.

As shown in figure 4.5, the tracking error responses for both the trolley displacement and

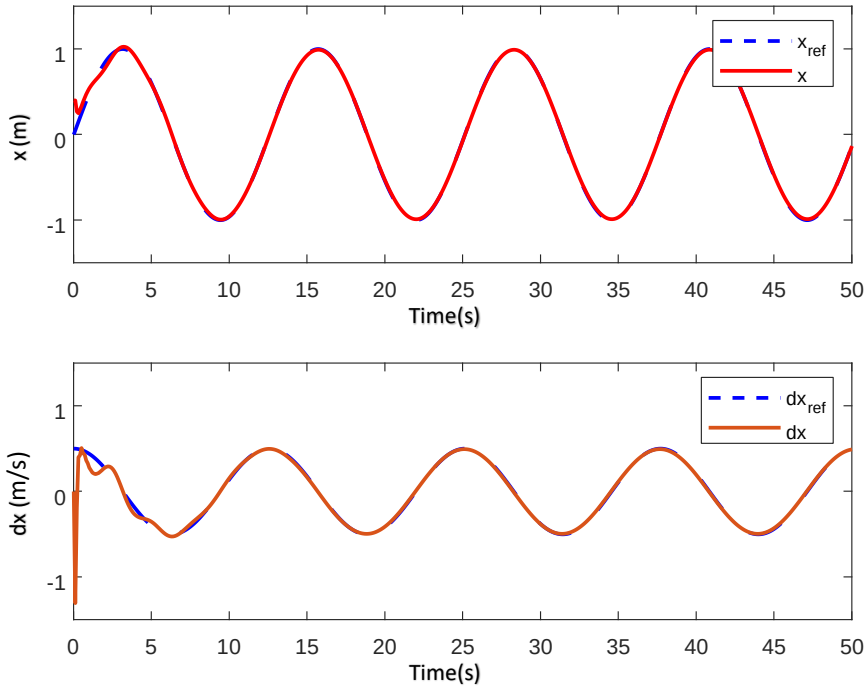

Figure 4.3: Performances of x and $\dot{x}$

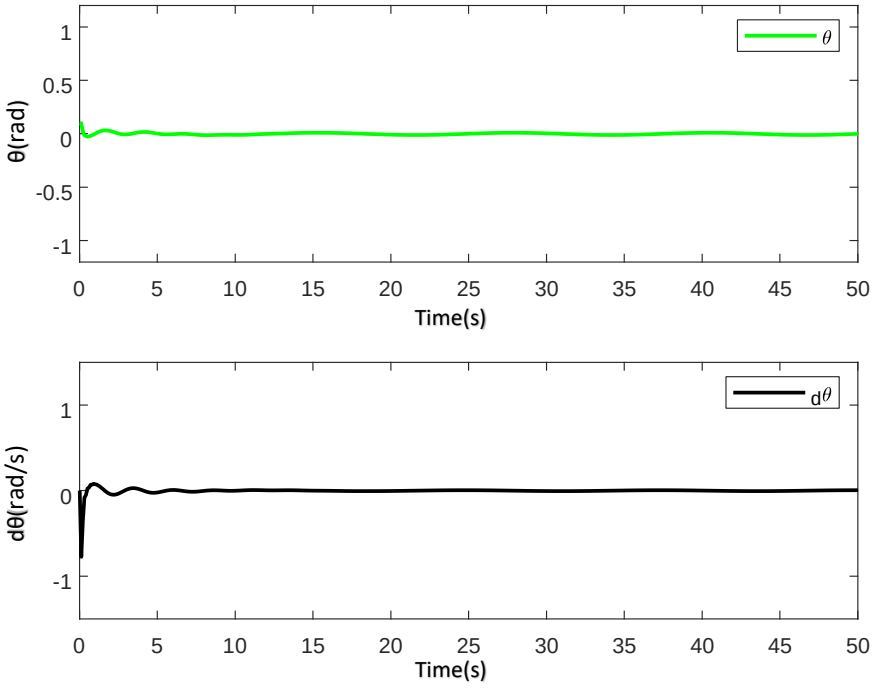

Figure 4.4: Performances of x and $\dot{x}$

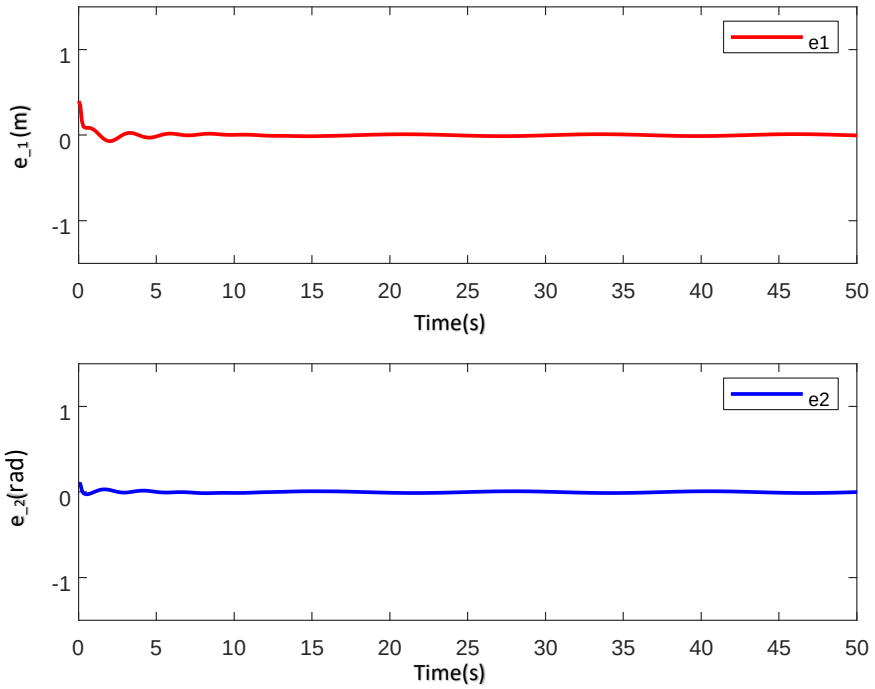

Figure 4.5: Performances of x and $\dot{x}$

the payload swing underscore the effectiveness of the proposed control strategy. The errors gradually diminish over time, ultimately converging to zero, which clearly demonstrates the system's ability to maintain closed-loop stability. Furthermore, the results indicate that precise trajectory tracking is consistently achieved, even under the influence of parametric uncertainties and external disturbances. These findings highlight the robustness and reliability of the controller, emphasizing its suitability for practical crane operations where accurate motion regulation and effective disturbance rejection are critical.

Figure 4.6 illustrates the evolution of both the control input and the sliding surface, further confirming the effectiveness of the proposed control strategy. The control signals remain well within acceptable bounds and exhibit minimal chattering, demonstrating that the method successfully mitigates excessive high-frequency switching. Simultaneously, the sliding surface progressively approaches zero, consistent with the theoretical expectations established through the Lyapunov stability analysis. Collectively, these results validate the robustness, smoothness, and practical applicability of the control law, ensuring reliable system performance under dynamic operating conditions.

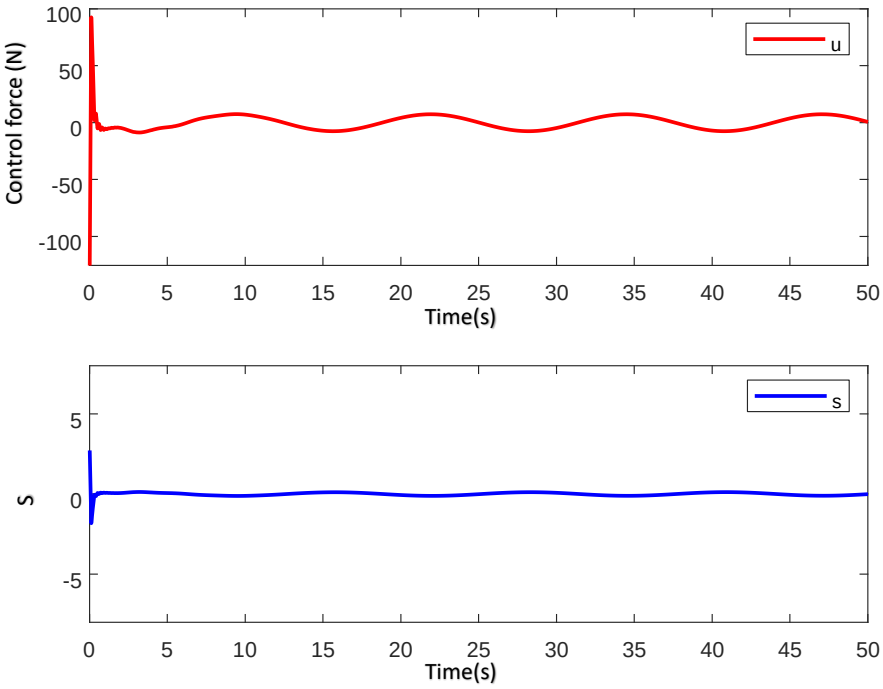

Figure 4.6: Performances of x and $\dot{x}$

4.6 Conclusion

This chapter introduced an adaptive fuzzy type-2 fast terminal sliding mode controller (AFT2-FTSMC) aimed at effectively controlling underactuated mechanical systems. The proposed design leverages the finite-time convergence property of fast terminal sliding mode control alongside the enhanced uncertainty-handling capabilities of interval type-2 fuzzy logic. In contrast to traditional type-1 fuzzy systems, which often face limitations in representing high levels of uncertainty and environmental variations, type-2 fuzzy logic incorporates an additional layer of uncertainty modeling, significantly improving both robustness and adaptability. Through an adaptive tuning mechanism, the controller efficiently estimates the required control input while simultaneously reducing the chattering phenomenon commonly observed in sliding mode approaches. Lyapunov-based analysis rigorously confirms the stability and convergence of the closed-loop system, while simulation results demonstrate that the proposed framework achieves superior tracking performance and resilience compared to conventional and type-1 fuzzy-based control methods.

In the following chapter, an adaptive Type-3 fuzzy fractional-order sliding mode control strategy without a reaching phase will be introduced. This approach unifies fractional-order

calculus, sliding mode control, and Type-3 fuzzy logic into a single framework, aiming to improve robustness, adaptability, and dynamic performance in underactuated mechanical systems.

Chapter 5

Adaptive fuzzy type-3 fractional-order free reaching phase SMC for UMS

5.1 Introduction

This chapter introduces an Adaptive Type-3 Fuzzy Fractional-Order Sliding Mode Control (AFT3FO-SMC) approach for underactuated mechanical systems (UMSs), designed to operate without a conventional reaching phase. The proposed framework integrates fractional-order calculus, sliding mode control, and Type-3 fuzzy logic into a cohesive control strategy aimed at improving robustness, adaptability, and dynamic response. By combining these methodologies, the controller effectively addresses the inherent challenges of underactuated systems, including limited actuation, nonlinear interconnections, and susceptibility to uncertainties.

As highlighted in the preceding chapter, hybrid control strategies integrating complementary aspects of multiple control methodologies provide an effective approach to address the inherent limitations of individual control schemes. By leveraging the advantages of diverse control paradigms within a unified framework, these hybrid architectures enhance adaptability, robustness, and dynamic performance, particularly in the presence of system uncertainties and external disturbances.

Recent research efforts have increasingly explored the integration of fuzzy logic mechanisms within adaptive sliding mode control (SMC) frameworks for underactuated dynamical systems. For example, the study in [111] proposed an adaptive fuzzy-based SMC scheme capable of mitigating the effects of sensor faults with time-varying characteristics, and in [112] presented an enhanced adaptive fuzzy SMC methodology tailored for fractional-order nonlinear

systems with multiple inputs and outputs. Furthermore, adaptive SMC strategies augmented with super-twisting and nonsingular terminal sliding mode techniques have been successfully implemented for quadrotor unmanned aerial vehicles (UAVs), yielding notable improvements in tracking accuracy and robustness, as reported in [113]. An adaptive fuzzy control structure addressing nonlinear underactuated systems with unknown control gain functions was introduced in [114].

Type-3 fuzzy logic systems, which extend traditional fuzzy frameworks by incorporating multi-level membership functions to capture deeper uncertainty, have also been explored. For instance, [115] presented a Type-3 FLC for vehicles with fractional-order tuning and a predictive scheme to improve lateral displacement accuracy. A fractional-order dynamic model with a non-singleton interval Type-3 fuzzy system for uncertainty estimation was proposed in [116]. Path-following for mobile robots using Type-3 FLC was studied in [117], while [118] developed a Type-3 fuzzy-based control strategy for robotic manipulator trajectory tracking. Observer-based Type-3 fuzzy SMC strategies were presented in [119] to estimate unknown nonlinear dynamics online through the design of a novel interval Type-3 FLC.

Hybrid SMC approaches and fractional-order sliding surfaces, which employ non-integer derivatives to enhance system responsiveness and control flexibility, have also been investigated.

In [120], fractional derivatives were integrated into a two-level sliding surface ensuring finite-time convergence. Event-triggered backstepping combined with fractional-order SMC was proposed in [121] to enhance attitude and position tracking while estimating unknown disturbances.

Motivated by this perspective, the control strategy presented in this chapter adopts a hybrid formulation that merges fractional-order control characteristics with intelligent fuzzy approximation and robust switching mechanisms. A key innovation of the proposed control strategy is the implementation of a time-varying switching surface, explicitly designed to coincide with the initial tracking error configuration. By satisfying the sliding condition from the very beginning of system operation, the conventional reaching phase is eliminated. This approach ensures that the system maintains its robustness throughout the entire response, including the transient period, while also markedly reducing unwanted oscillations and enhancing overall stability.

Fractional-order operators are incorporated into the switching surface formulation to enhance dynamic flexibility and tuning capability. The non-integer order term effectively serves as

an adjustable gain that allows the controller dynamics to be shaped with greater precision. This feature facilitates improved convergence characteristics and smoother system responses. The memory-dependent nature of fractional-order dynamics further supports enhanced disturbance attenuation and refined transient performance.

To further strengthen the robustness of the control scheme, an adaptive Type-3 fuzzy logic system is incorporated into the control law to estimate unknown external disturbances in real time. Owing to its multi-layered representation of uncertainty, the Type-3 fuzzy framework provides a richer and more flexible modeling capability than lower-order fuzzy systems, making it particularly effective in complex and time-varying operating conditions. The adaptive updating mechanism continuously adjusts the fuzzy parameters online, thereby removing the need for prior knowledge of uncertainty and significantly improving resilience against modeling inaccuracies and external perturbations.

5.2 Fractional calculus

Fractional calculus extends the traditional concepts of differentiation and integration by allowing operators of non-integer, and more generally real-valued order. This generalized mathematical formalism offers enhanced flexibility for representing complex system dynamics. In contrast to classical integer-order calculus, which relies solely on instantaneous system information, fractional-order operators inherently possess nonlocal characteristics. As a result, the current behavior of a system depends on its past evolution over time, allowing fractional calculus to effectively capture memory and hereditary phenomena that are commonly encountered in many physical, biological, and engineering systems.

From a theoretical perspective, fractional calculus provides a unified framework in which differentiation and integration are connected through a continuously tunable order parameter. This adjustable order enables the representation of intermediate dynamic phenomena that lie between purely integral and differential behaviors, which are often beyond the reach of conventional integer-order formulations. Consequently, fractional-order modeling offers greater expressive capability, especially for nonlinear systems.

In recent decades, the practical relevance of fractional calculus has increased significantly due to advancements in numerical methods and computational capabilities. These developments have facilitated the implementation of fractional-order operators in engineering applications, especially in control theory, signal processing, and system identification. In control engineering, fractional calculus has been shown to improve robustness, enhance tracking accuracy,

and provide additional tuning parameters for controller design. Consequently, fractional calculus has evolved from a purely theoretical concept into a powerful and versatile tool for modeling, analysis, and control of complex dynamical systems.

5.2.1 Common fractional-order operators

Fractional-order operators provide different ways to define differentiation and integration of non-integer order. Each operator has distinct mathematical properties and practical implications, making the selection of an appropriate formulation critical for modeling and control applications. The most widely used fractional operators are the Riemann–Liouville derivative, the Caputo derivative, and the Grünwald–Letnikov formulation.

5.2.1.1 Riemann–Liouville Fractional Derivative

The Riemann–Liouville (R–L) fractional derivative is one of the earliest formalizations of fractional differentiation. It generalizes the classical n^{th} order derivative through an integral operator of fractional order $\beta > 0$. For a function f(t), the R–L derivative of order β is defined as [122]:

$$I^{\beta} f(t) = \frac{1}{\Gamma(\beta)} \int_0^t (t-\tau)^{\beta-1} f(\tau)\, d\tau \tag{5.1}$$

$$D_t^{\beta} f(t) = \frac{d^n}{dt^n} \left[\frac{1}{\Gamma(n-\beta)} \int_0^t (t-\tau)^{n-\beta-1} f(\tau)\, d\tau \right] \tag{5.2}$$

Here, D and I represent the fractional derivative and fractional integral operators, respectively, and n is an integer number, $\Gamma(.)$ is Euler's Gamma function given by:

$$\Gamma(z) = \int_0^{\infty} t^{z-1} e^{-t}\, dt \tag{5.3}$$

This form combines the instantaneous rate of change e^{n-1} with the history-dependent behaviour $D^{\alpha_i} e^i$, giving the controller both fast response and long-term correction capability.

5.2.1.2 Caputo fractional derivative

The Caputo derivative modifies the Riemann–Liouville approach to facilitate the use of standard integer-order initial conditions, making it more suitable for physical systems. For $f(t)$, the Caputo derivative of order β is given by [123]:

$${}^{C}D_t^{\alpha} f(t) = \frac{1}{\Gamma(n-\alpha)} \int_0^t \frac{f^{(n)}(\tau)}{(t-\tau)^{\alpha-n+1}}\, d\tau \tag{5.4}$$

where $f^{(n)}(\tau)$ denotes the n-th ordinary derivative of f, $\Gamma(\cdot)$ is the Gamma function, and n is the smallest integer greater than α.
This formulation is particularly useful because it allows initial conditions to be expressed in terms of integer-order derivatives, which aligns naturally with physical interpretations and experimental data.

5.2.1.3 Grünwald–Letnikov formulation

The **Grünwald–Letnikov (G–L) formulation** defines fractional derivatives using a limit of finite differences, providing a natural approach for numerical computation and discrete-time implementation. For a function $f(t)$, the G–L derivative of order α is expressed as [124]:

$$D_t^{\alpha} f(t) = \lim_{h \to 0} \frac{1}{h^{\alpha}} \sum_{k=0}^{\lfloor t/h \rfloor} (-1)^k \binom{\alpha}{k} f(t - kh) \tag{5.5}$$

where h is the discretization step, $\lfloor t/h \rfloor$ denotes the greatest integer less than or equal to t/h, and the generalized binomial coefficient is given by:

$$\binom{\alpha}{k} = \frac{\Gamma(\alpha + 1)}{\Gamma(k + 1)\Gamma(\alpha - k + 1)} \tag{5.6}$$

The G–L formulation is particularly suitable for simulations and digital control implementations because it directly connects fractional calculus with finite-difference numerical methods. It also preserves the history-dependent nature of fractional derivatives, enabling accurate modeling of systems with memory effects.

5.3 Type-3 fuzzy logic system

Type-3 fuzzy logic systems represent an advanced extension of conventional fuzzy frameworks, developed to address severe uncertainty, ambiguity, and dynamic variations that cannot be effectively managed by Type-1 or Type-2 fuzzy logic systems. While Type-1 fuzzy systems rely on precise membership functions and Type-2 systems introduce uncertainty in membership grades, Type-3 fuzzy systems further generalize this concept by allowing uncertainty to exist at a higher hierarchical level. This additional degree of freedom significantly enhances the system's capability to model complex nonlinear dynamics and highly uncertain environments.
In control and decision-making applications, Type-3 fuzzy logic systems offer superior robustness and adaptability, particularly in scenarios involving unmodeled dynamics, external

disturbances, and time-varying parameters. As a result, they have gained increasing attention in advanced intelligent control designs.

5.3.1 Fundamentals of type-3 fuzzy sets

Type-3 fuzzy sets represent an advanced extension of fuzzy set theory, specifically introduced to cope with severe and highly complex uncertainty levels that cannot be adequately modeled using Type-1 or Type-2 fuzzy frameworks. In contrast to Type-1 fuzzy sets, which associate each element with a single deterministic membership value, and Type-2 fuzzy sets, which allow uncertainty within the membership grades, Type-3 fuzzy sets incorporate an additional hierarchical layer of uncertainty within the secondary membership structure. This multi-level formulation significantly enhances the system's ability to capture ambiguity, linguistic imprecision, and time-varying uncertainty, thereby providing a richer and more flexible modeling paradigm for complex dynamic systems.

The membership function of a Type-3 fuzzy logic system can be visualized as a three-dimensional surface, where the added dimension represents the tertiary uncertainty. A schematic representation of this three-dimensional membership structure is provided in Figure 5.1, illustrating how higher-order uncertainty is embedded within the fuzzy set.

Formally, a Type-3 fuzzy set introduces a tertiary variable $v \in V \subseteq [0,1]$. The membership function depends on three variables: the primary element $x \in X$, the secondary variable $u \in U \subseteq [0,1]$, and the tertiary variable $v \in V \subseteq [0,1]$. Its general definition is:

$$A^{(3)} = \{((x,u), \mu_{A^{(3)}}(x,u,v)) \mid x \in X, u \in U \subseteq [0,1], v \in V \subseteq [0,1]\}. \tag{5.7}$$

This hierarchical structure allows Type-3 fuzzy sets to capture higher-order uncertainty effectively, making them particularly suitable for complex nonlinear systems and intelligent control applications where conventional fuzzy systems may not provide robust performance.

5.3.2 Structure of adaptive type-3 fuzzy logic system

An adaptive Type-3 fuzzy logic system consists of several interconnected components designed to process uncertain inputs and generate robust control actions. The adaptive mechanism enables real-time tuning of system parameters, allowing the fuzzy system to adjust its behavior in response to changing system dynamics and external disturbances. The main components of the system include fuzzification, rule base, inference engine, type-reduction mechanism, and defuzzification.

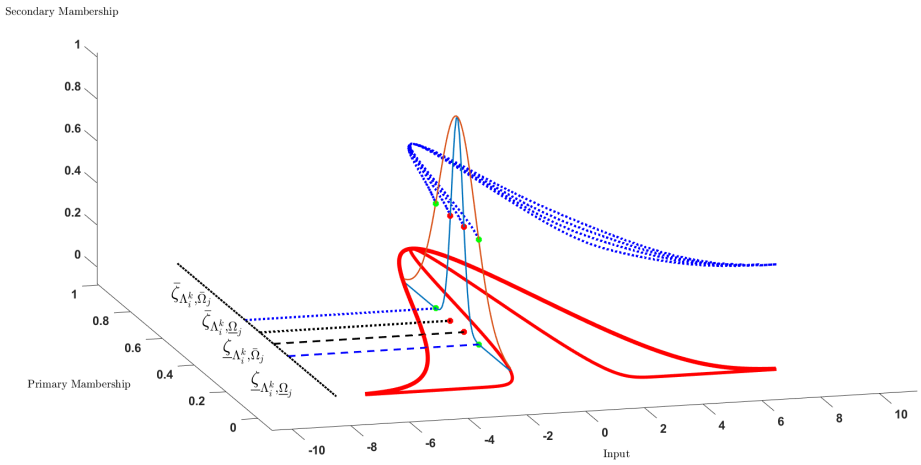

Figure 5.1: Type-3 fuzzy logic

5.3.2.1 Fuzzification

The fuzzification stage converts crisp input variables into Type-3 fuzzy sets. Unlike Type-1 and Type-2 fuzzy systems, the membership function in a Type-3 FLS is characterized by a three-dimensional structure, where the primary membership itself is associated with secondary and tertiary uncertainties. This hierarchical uncertainty modeling allows the system to represent complex, time-varying, and poorly defined input information more effectively. In adaptive Type-3 fuzzy systems, the parameters of these membership functions are updated online to reflect changes in system dynamics and external disturbances.

5.3.2.2 Rule base

The rule base contains a collection of linguistic IF–THEN rules formulated using Type-3 fuzzy sets. Each rule describes the relationship between fuzzy input variables and fuzzy output variables under higher-order uncertainty. Compared to lower-order fuzzy systems, the rules in a Type-3 FLS encapsulate uncertainty not only in the antecedents and consequents but also in the embedded membership grades. This enriched rule representation enhances the expressive power of the fuzzy model, particularly in highly nonlinear and uncertain environments.

5.3.2.3 Inference engine

The inference engine evaluates the fuzzy rules and determines their firing strengths based on Type-3 fuzzy reasoning. This process involves combining the fuzzified inputs with the rule base using appropriate fuzzy operators. Due to the presence of tertiary uncertainty,

the inference mechanism produces a Type-3 fuzzy output set rather than a crisp or Type-2 fuzzy result. The adaptive mechanism continuously adjusts inference-related parameters to maintain stability and improve tracking accuracy.

5.3.2.4 Type-reduction mechanism

The type-reduction mechanism transforms the inferred Type-3 fuzzy output into a Type-2 or Type-1 equivalent representation. This step is essential to reduce computational complexity while preserving the uncertainty information embedded in the higher-order fuzzy set. Interval-based or uncertainty-bound type-reduction strategies are commonly employed to achieve a balance between accuracy and real-time applicability. In adaptive frameworks, the type-reduction parameters are updated online to enhance robustness against modeling errors and disturbances.

5.3.2.5 Defuzzification

The final defuzzification stage converts the type-reduced fuzzy set into a crisp control output. This output is then applied to the controlled system. By operating on a type-reduced representation that retains essential uncertainty characteristics, the defuzzification process produces smoother and more reliable control signals. Consequently, the adaptive Type-3 fuzzy logic system achieves improved robustness, reduced sensitivity to noise, and enhanced performance under severe uncertainty conditions.

5.3.3 Hybrid adaptive fuzzy type-3

Hybrid adaptive Type-3 fuzzy control systems integrate Type-3 fuzzy logic with other advanced control methodologies, such as sliding mode control, fractional-order control, or neural networks. This hybridization leverages the uncertainty-handling capability of Type-3 fuzzy logic while benefiting from the fast convergence and robustness properties of conventional control techniques.

By incorporating adaptive laws, the hybrid framework enables online tuning of fuzzy parameters, ensuring improved tracking performance and reduced chattering effects in the presence of uncertainties and external disturbances. Consequently, hybrid adaptive Type-3 fuzzy control schemes offer a powerful and flexible solution for controlling complex, nonlinear, and underactuated systems.

5.4 Design of adaptive fuzzy type-3 fractional SMC

As established in the preceding chapter, the primary difficulty associated with underactuated systems arises from the inequality $m < n$, where the number of available control inputs is insufficient to independently influence all system states. Consequently, direct actuation of every state variable is not feasible, necessitating the development of control methodologies that can indirectly regulate the internal dynamics while simultaneously guiding the system outputs toward prescribed reference trajectories.

Motivated by this structural constraint, the present work aims to formulate a robust control framework that guarantees closed-loop stability of the underactuated plant and achieves high-precision tracking despite the presence of modeling inaccuracies and unknown external perturbations.

Accordingly, this study seeks to synthesize a robust adaptive Type-3 fuzzy fractional-order sliding mode control law, denoted by $U(x)$, for the nonlinear system described in (2.11), such that the output vector y asymptotically follows a desired reference signal vector y_d in the face of external disturbances.

5.4.1 Fractional-order SMC without reaching phase

The linear dynamic behavior is prescribed by the chosen sliding manifold [65] :

$$s = (\frac{d}{dt} + c)^{n-1} e = c_1 e + c_2 \dot{e} + ... + c_{n-1} e^{n-2} + e^{n-1} \tag{5.8}$$

$$s = e^{n-1} + \sum_{i=0}^{n-2} c_{i+1} e^i \tag{5.9}$$

where $e = y_d - y$ denotes the tracking error, and c_i represent positive parameters.

To suppress the reaching phase while ensuring finite-time convergence, enhanced robustness, and high-accuracy regulation of the underactuated system, a fractional-order integral sliding mode (FO-ISMC) surface is formulated based on fractional calculus principles as follows:

$$S = e^{n-1} + \sum_{i=0}^{n-2} c_{i+1} e^i + aD^{-\beta} e + \Psi(e^{n-1}(0) + \sum_{i=0}^{n-2} c_{i+1} e^i(0) + aD^{-\beta} e(0)) \tag{5.10}$$

We propose the following form of Ψ:

$$\Psi = -exp(t/T)^{\kappa} \tag{5.11}$$

where T, a, and κ are strictly positive constants, selected through simulation studies to achieve a compromise between rapid convergence and smooth control action.

The initial value of the sliding surface is defined as:

$$s_0 = e^{n-1}(0) + \sum_{i=0}^{n-2} c_{i+1} e^i(0) + aD^{-\beta} e(0) \tag{5.12}$$

where s_0 represents the initial sliding surface, and the term Ψs_0 ensures that the sliding manifold passes through the system's initial error position.

The proposed time-varying surface eliminates the reaching phase, while the inclusion of the Ψ term allows the system to respond effectively to rapid variations, thereby accelerating convergence, improving robustness, and mitigating chattering. The fractional-order components further enhance system performance and convergence, with $D^{\alpha_i} e^i$ denoting the fractional derivatives of e^i of order β. The Riemann–Liouville definitions of fractional integral and derivative of order β with respect to time t are employed for this purpose. Taking the time derivative of the sliding surfaces defined in (5.10) yields:

$$\dot{S} = e^n + \sum_{i=0}^{n-1} c_{i+1} e^i + aD^{1-\beta} e = x^n - x_r^n + \sum_{i=0}^{n-1} c_{i+1} e^i + aD^{1-\beta} e + \dot{\Psi} s_0 \tag{5.13}$$

Introducing the system dynamics into the above expression yields:

$$\dot{s} = h(x) + j(x)u + d - \ddot{x}_r + \sum_{i=0}^{n-1} c_{i+1} e^i + aD^{1-\beta} e + \dot{\Psi} s_0 \tag{5.14}$$

Consequently, the control input can be defined as:

$$u = \frac{-1}{j(x)} (h(x) + d(t) - \ddot{x}_r + \sum_{i=0}^{n-1} c_{i+1} e^i + aD^{1-\beta} e + u_{sw} + \dot{\Psi} s_0) \tag{5.15}$$

The switching control component is selected as $u_{sw} = k_1 s + k_2 tanh(s)$ where the hyperbolic tangent function is defined by $tanh(s) = \frac{e^s - e^{-s}}{e^s + e^{-s}}$.

As discussed in the preceding chapter, the global sliding manifold is defined as:

$$S = k_1 S_1 + k_2 S_2 + ... + k_n S_n = \sum_{i=1}^{n} k_i S_i \tag{5.16}$$

where $k_1, \ldots, k_n$ are positive control gains.

The corresponding sub-sliding surfaces are specified in (5.10), and the time derivatives of each sub-sliding surface are given by (5.13) and (5.14). Applying the derivative operator with respect to time on the sliding surfaces in (5.16) leads to:

$$\begin{aligned} S = {} & k_1(h_1(x) + j_1(x)u_1 + d_1 - \ddot{x}_{r1} + a_1 D^{1-\beta_1} e_1 + \dot{\Psi} s_{10}) + ... \\ & + k_n(h_n(x) + j_n(x)u_n + d_n - \ddot{x}_{rn} + a_n D^{1-\beta_n} e_n + \dot{\Psi} s_{n0}) \\ = {} & \sum_{i=1}^{n} k_i(k_i(h_i(x) + j_i(x)u_i + d_i - \ddot{x}_{ri} + a_i D^{1-\beta_i} e_i + \dot{\Psi} s_{i0})) \end{aligned} \tag{5.17}$$

For every actuated subsystem, the associated equivalent control input is formally expressed as in (5.15).

Given that the disturbance is unknown, the subsequent objective is to approximate $d_k(x)$ using a Type-3 fuzzy estimator, such that $\hat{d}_k(x) \approx d_k(x)$ for $k = 1, \ldots, n$. Type-3 fuzzy systems enhance the modeling capabilities of both Type-1 and Type-2 frameworks by incorporating an additional hierarchical layer of membership functions. This extended structure enables a more precise characterization of complex uncertainties, which is particularly important for underactuated mechanical systems, where strong nonlinearities arise from underactuation and the coupling between states.

5.4.2 Type-3 fuzzy systems

In this section, a Type-3 fuzzy logic system (T3FLS) is employed within equation (2.11), where the input variables are represented by x_i. The fuzzy sets corresponding to all inputs are denoted as Λ_i^k and $\overline{\Omega}_j$, while the i^{th} input of the T3FLS is represented by χ_i. The general scheme is given by Figure 5.2, and the membership functions are defined as in [115]:

$$\overline{\zeta}_{\Lambda_i^k,\overline{\Omega}_j}(\chi_i(t)) = \exp\left(-\frac{(\chi_i(t) - m_{\Lambda_i^k,\overline{\Omega}_j})}{\overline{\sigma}^2_{\Lambda_i^k,\overline{\Omega}_j}}\right). \tag{5.18}$$

$$\overline{\zeta}_{\Lambda_i^k,\underline{\Omega}_j}(x_i(t)) = \exp\left(-\frac{(\chi_i(t) - m_{\Lambda_i^k,\underline{\Omega}_j})}{\overline{\sigma}^2_{\Lambda_i^k,\underline{\Omega}_j}}\right). \tag{5.19}$$

$$\underline{\zeta}_{\Lambda_i^k,\overline{\Omega}_j}(\chi_i(t)) = \exp\left(-\frac{(\chi_i(t) - m_{\Lambda_i^k,\overline{\Omega}_j})}{\underline{\sigma}^2_{\Lambda_i^k,\overline{\Omega}_j}}\right). \tag{5.20}$$

$$\underline{\zeta}_{\Lambda_i^k,\underline{\Omega}_j}(\chi_i(t)) = \exp\left(-\frac{(\chi_i(t) - m_{\Lambda_i^k,\underline{\Omega}_j})}{\underline{\sigma}^2_{\Lambda_i^k,\underline{\Omega}_j}}\right). \tag{5.21}$$

where $m_{\Lambda_i^k}$ and $\overline{\sigma}_{\Lambda_i^{hi}}$, $\underline{\sigma}_{\Lambda_i^{hi}}$ are centre and upper/lower standard divisions. For rules firing, we have:

$$\overline{\vartheta}^l_{\overline{\Omega}_j} = \prod_{i=1}^{n} \overline{\zeta}_{\Lambda_i^{ki},\overline{\Omega}_j} \tag{5.22}$$

$$\overline{\vartheta}^l_{\underline{\Omega}_j} = \prod_{i=1}^{n} \overline{\zeta}_{\Lambda_i^{ki},\underline{\Omega}_j} \tag{5.23}$$

$$\underline{\vartheta}^l_{\overline{\Omega}_j} = \prod_{i=1}^{n} \underline{\zeta}_{\Lambda_i^{ki},\overline{\Omega}_j} \tag{5.24}$$

$$\underline{\vartheta}^l_{\underline{\Omega}_j} = \prod_{i=1}^{n} \underline{\zeta}_{\Lambda_i^{ki},\underline{\Omega}_j} \tag{5.25}$$

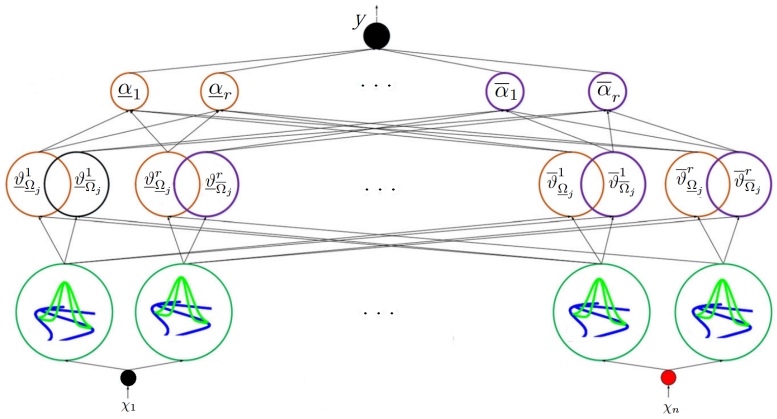

Figure 5.2: Diagram of T3-FLS

The form of l^{th} rule is given as:

If x_1 is Λ_{1,A_j}^{k1} and x_2 is Λ_{2,A_j}^{k2} ...and x_n is Λ_{n,A_j}^{kn} **Then** $y_l \in [\underline{\alpha}_{l,j}, \overline{\alpha}_{l,j}]$.

where $\underline{\alpha}_{l,j}, \overline{\alpha}_{l,j}$ represent the lower and upper bounds of the l^{th} Type-3 interval fuzzy set, respectively, and y_l denotes the fuzzy system output at the l^{th} rule.

Accordingly, the output of the T3FLS can be expressed as:

$$y = \frac{\sum_{j=1}^{k}}{\sum_{j=1}^{k} \overline{\Omega}_j} \left(\frac{\sum_{l=1}^{r} \overline{\Omega}_j (\overline{\vartheta}_{\overline{\Omega}_j}^{l} + \underline{\vartheta}_{\overline{\Omega}_j}^{l}) \overline{\alpha}_{l,j}/2}{\sum_{l=1}^{r} (\overline{\vartheta}_{\overline{\Omega}_j}^{l} + \underline{\vartheta}_{\overline{\Omega}_j}^{l})} + \underline{\Omega}_j \frac{\sum_{l=1}^{r} (\overline{\vartheta}_{\Omega_j}^{l} + \underline{\vartheta}_{\Omega_j}^{l}) \underline{\alpha}_{l,j}/2}{\sum_{l=1}^{r} (\overline{\vartheta}_{\Omega_j}^{l} + \underline{\vartheta}_{\Omega_j}^{l})} \right) \tag{5.26}$$

The resulting output can be expressed in the following form:

$$y = \alpha^T \Phi \tag{5.27}$$

where,

$$\begin{aligned} \alpha^T = [&\underline{\alpha}_{1,\underline{\Omega}_1}, ..., \underline{\alpha}_{1,\underline{\Omega}_k}, ..., \underline{\alpha}_{r,\underline{\Omega}_r}, ..., \underline{\alpha}_{r,\underline{\Omega}_r} \\ &\underline{\alpha}_{1,\overline{\Omega}_1}, ..., \underline{\alpha}_{1,\overline{\Omega}_k}, ..., \underline{\alpha}_{r,\overline{\Omega}_r}, ..., \underline{\alpha}_{r,\overline{\Omega}_r} \\ &\overline{\alpha}_{1,\underline{\Omega}_1}, ..., \overline{\alpha}_{1,\underline{\Omega}_k}, ..., \overline{\alpha}_{r,\underline{\Omega}_r}, ..., \overline{\alpha}_{r,\underline{\Omega}_r} \\ &\overline{\alpha}_{1,\overline{\Omega}_1}, ..., \overline{\alpha}_{1,\overline{\Omega}_k}, ..., \overline{\alpha}_{r,\overline{\Omega}_r}, ..., \overline{\alpha}_{r,\overline{\Omega}_r}] \end{aligned} \tag{5.28}$$

$$\Phi^T = \frac{0.5}{\sum_{j=1}^{k} \overline{\Omega}_j} \left(\frac{\underline{\Omega}_1(\overline{\vartheta}^1_{\underline{\Omega}_1} + \underline{\vartheta}^1_{\underline{\Omega}_1})}{\sum_{l=1}^{r}(\overline{\vartheta}^1_{\underline{\Omega}_j} + \underline{\vartheta}^1_{\underline{\Omega}_j})}, ..., \underline{\Omega}_k \frac{\underline{\Omega}_k(\overline{\vartheta}^1_{\underline{\Omega}_k} + \underline{\vartheta}^1_{\underline{\Omega}_k})}{\sum_{l=1}^{r}(\overline{\vartheta}^1_{\underline{\Omega}_1} + \underline{\vartheta}^1_{\underline{\Omega}_1})} \right.$$
$$, \frac{\underline{\Omega}_1(\overline{\vartheta}^r_{\underline{\Omega}_1} + \underline{\vartheta}^r_{\underline{\Omega}_1})}{\sum_{l=1}^{r}(\overline{\vartheta}^r_{\underline{\Omega}_j} + \underline{\vartheta}^r_{\underline{\Omega}_j})}, ..., \underline{\Omega}_k \frac{\underline{\Omega}_k(\overline{\vartheta}^r_{\underline{\Omega}_k} + \underline{\vartheta}^r_{\underline{\Omega}_k})}{\sum_{l=1}^{r}(\overline{\vartheta}^r_{\underline{\Omega}_1} + \underline{\vartheta}^r_{\underline{\Omega}_1})}$$
$$, \frac{\overline{\Omega}_1(\overline{\vartheta}^1_{\overline{\Omega}_1} + \underline{\vartheta}^1_{\overline{\Omega}_1})}{\sum_{l=1}^{r}(\overline{\vartheta}^1_{\overline{\Omega}_j} + \underline{\vartheta}^1_{\overline{\Omega}_j})}, ..., \overline{\Omega}_k \frac{\overline{\Omega}_k(\overline{\vartheta}^1_{\overline{\Omega}_k} + \underline{\vartheta}^1_{\overline{\Omega}_k})}{\sum_{l=1}^{r}(\overline{\vartheta}^1_{\overline{\Omega}_1} + \underline{\vartheta}^1_{\overline{\Omega}_1})}$$
$$\left. , \frac{\overline{\Omega}_1(\overline{\vartheta}^r_{\overline{\Omega}_1} + \underline{\vartheta}^r_{\overline{\Omega}_1})}{\sum_{l=1}^{r}(\overline{\vartheta}^r_{\overline{\Omega}_j} + \underline{\vartheta}^r_{\overline{\Omega}_j})}, ..., \overline{\Omega}_k \frac{\overline{\Omega}_k(\overline{\vartheta}^r_{\overline{\Omega}_k} + \underline{\vartheta}^r_{\overline{\Omega}_k})}{\sum_{l=1}^{r}(\overline{\vartheta}^r_{\overline{\Omega}_1} + \underline{\vartheta}^r_{\overline{\Omega}_1})} \right) \tag{5.29}$$

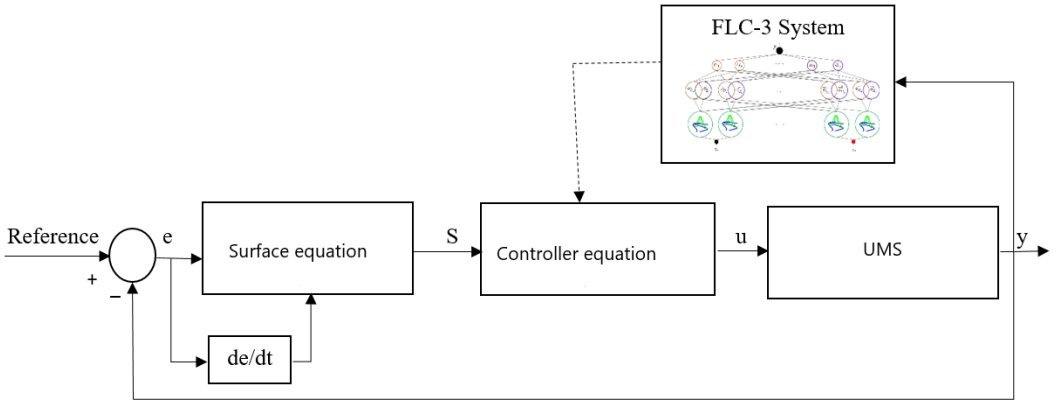

Figure 5.3: Block diagram of the proposed approach

5.5 Stability analysis

Theorem 8. *Using the sliding surface (5.10), the control law (5.15) guarantees the asymptotic convergence of the system (2.11) to the reference trajectory and the tracking error e to zero.*

Proof. Let the Lyapunov candidate function:

$$V = \frac{1}{2}s^2 + \frac{1}{2\Gamma}\tilde{\alpha}^T\tilde{\alpha} \tag{5.30}$$

Here, $\tilde{\alpha} = \alpha^* - \alpha$ is the fuzzy parameter estimation error, and Γ is a positive definite adaptation gain. Its time derivative is:

$$\dot{V} = S\dot{S} + \tilde{\alpha}^T\Gamma^{-1}\dot{\alpha} \tag{5.31}$$

$$\dot{V} = S[h(x) + j(x)u + d - \ddot{x}_r + \sum_{i=0}^{n-1} c_{i+1}e^i + aD^{1-\beta}e + \dot{\Psi}s_0] + \tilde{\alpha}^T\Gamma^{-1}\dot{\alpha} \tag{5.32}$$

Adding and subtracting the optimal fuzzy approximation $\hat{d}^*$ yields:

$$\dot{V} = S[h(x) + j(x)u + d - \ddot{x}_r + \sum_{i=0}^{n-1} c_{i+1}e^i + aD^{1-\beta}e\dot{\Psi}s_0 + \hat{d}^* - \hat{d}^*] + \tilde{\alpha}^T\Gamma^{-1}\dot{\tilde{\alpha}} \tag{5.33}$$

By definition, the fuzzy estimation error can be expressed as:

$$[\hat{d}^* - \hat{d}] = (\alpha^* - \alpha)^T\Phi = \tilde{\alpha}^T\Phi \tag{5.34}$$

The optimal error is defined as:

$$\epsilon = d - \hat{d}^* \tag{5.35}$$

Substituting (5.34) and (5.35) in (5.33) leads to:

$$\begin{aligned} \dot{V} &= S[\epsilon + \tilde{\alpha}^T\Phi - K_1S - K_2sgn(S)] + \tilde{\alpha}^T\Gamma^{-1}\dot{\tilde{\alpha}} \\ &= S\epsilon + S\tilde{\alpha}^T\Phi - K_1S^2 - K_2|S| + \tilde{\alpha}^T\Gamma^{-1}\dot{\tilde{\alpha}} \end{aligned} \tag{5.36}$$

Since $\tilde{\alpha} = \alpha^* - \alpha$, we can obtain $\dot{\tilde{\alpha}} = -\dot{\alpha}$ leading to:

$$\dot{V} = S\epsilon + S\tilde{\alpha}^T\Phi - K_1S^2 - K_2|S| - \tilde{\alpha}^T\Gamma^{-1}\dot{\alpha} \tag{5.37}$$

Rewriting this expression, we obtain:

$$\dot{V} = -K_1S^2 - K_2|S| + S\epsilon + \tilde{\alpha}^T(S\Phi - \Gamma^{-1}\dot{\alpha}) \tag{5.38}$$

Hence, the corresponding tuning laws are chosen as:

$$\dot{\alpha} = -\Gamma S\Phi \tag{5.39}$$

Substituting (5.39) into (5.38) yields:

$$\dot{V} = -K_1S^2 - K_2|S| + S\epsilon \tag{5.40}$$

Since we have $S\epsilon \leq |S||\epsilon|$, hence:

$$\dot{V} \leq |S|(|\epsilon| - K_2) - K_1S^2 \tag{5.41}$$

Equation (5.41) confirms the stability of the global sliding surface, ensuring the overall closed-loop system remains stable provided that the control gain satisfies $K_2 \leq |\epsilon|$. Under this requirement, the tracking error converges to a bounded neighborhood around zero, illustrating both the robustness and the effectiveness of the proposed control strategy. □

5.6 Simulation results

To assess the performance and robustness of the proposed controller, simulations were conducted using the MATLAB platform on the crane model, which represents an underactuated system with two degrees of freedom.

The system dynamic equations can be expressed in state-space form, using the state vector $\begin{bmatrix} x_1 & x_2 & x_3 & x_4 \end{bmatrix}^T = \begin{bmatrix} x & \dot{x} & \theta & \dot{\theta} \end{bmatrix}^T$ where the nonlinear functions h_1, j_1, h_2 and j_2 are defined as [88]:

$$\begin{aligned} h_1 &= \frac{(-m_p^2 l^2 g cos(\theta) sin(\theta + m_p l^2 (m_p l \dot{\theta}^2 sin(\theta) - D\dot{x})}{m_p l^2 (m_c + m_p (1 - cos(\theta)^2))} \\ j_1 &= \frac{m_p l^2}{m_p l^2 (m_c + m_p (1 - cos(\theta)^2))} \\ h_2 &= \frac{(m_p + m_c) m_p g l sin(\theta) - m_p l cos(\theta)(m_p l \dot{\theta}^2 sin(\theta) - D\dot{x})}{m_p l^2 (m_c + m_p (1 - cos(\theta)^2))} \\ j_2 &= \frac{m_p l cos(\theta)}{m_p l^2 (m_c + m_p (1 - cos(\theta)^2))} \end{aligned} \tag{5.42}$$

The primary control objective is to maneuver the crane to a desired target position while maintaining the pendulum angle at zero. The system is initialized with the following conditions:$x = \begin{bmatrix} 0.8 & 0 & 0.1 & 0 \end{bmatrix}^T$, with the desired trajectory $cos(0.5 * t)$. The simulation parameters of the

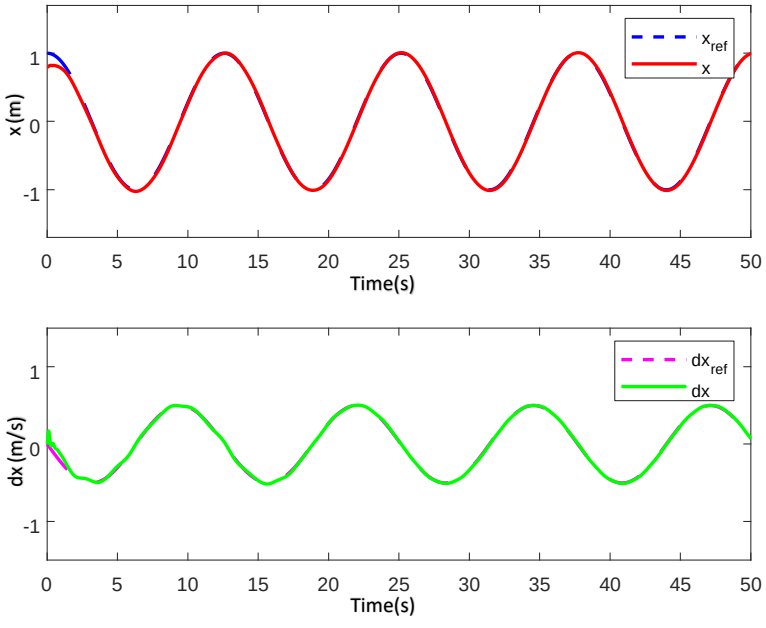

Figure 5.4: Performances of x and $\dot{x}$

crane system are set as $m_p = 6kg, m_c = 9kg, l = 2m, g = -9.81m/s, D = 0.5kg/m$, The controller parameters are chosen as $k1 = 0.1, k2 = 10, c1 = 0.5, c2 = 5, a = 0.5, \beta = 0.1$, and $[-m_{\Lambda_i^1}, -m_{\Lambda_i^2}, -m_{\Lambda_i^3}] = [-\pi/5, 0, \pi/5]$, $\overline{\sigma}_{\Lambda_i^k} = 1$ $\underline{\sigma}_{\Lambda_i^k} = 0.5$. We consider four rules and three membership functions, and we chose $D1 = D2 = 0.05 * sin(.05 * t) + .3 * exp(-((t - 1120)^2)/(2 * 50^2))$.

Figure 5.4 illustrates the system's time-domain behavior when governed by the proposed control strategy. The obtained responses show that the trolley motion closely follows the prescribed reference trajectory and converges reliably to the desired position. At the same time, oscillatory motions of the suspended load are rapidly attenuated, indicating effective swing suppression. The swift decay of payload oscillations highlights not only the precision of the controller in accomplishing the positioning task but also its strong capability to stabilize the coupled and underactuated dynamics of the crane system.

Moreover, Figure 5.5 demonstrates the controller's ability to quickly dampen payload oscil-

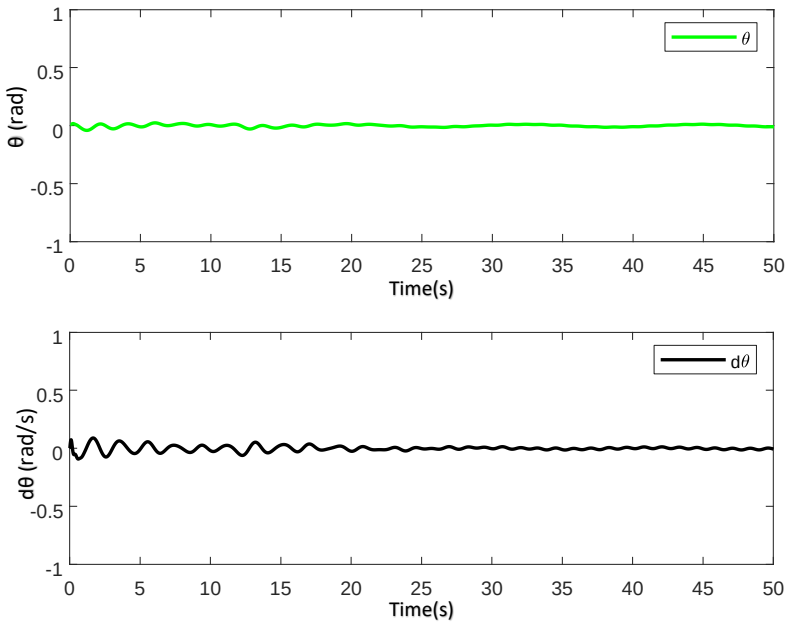

Figure 5.5: Performances of θ and $\dot{\theta}$

lations, a key challenge in overhead crane operation. The simulation results indicate that the swing is effectively mitigated throughout the motion, preventing destabilization and promoting smooth overall system performance. This successful suppression of residual vibrations underscores the robustness of the proposed control strategy in managing underactuated dynamics and improving operational safety, especially in applications where minimizing payload

swing is critical. Figure 5.6 presents a detailed analysis of the tracking error responses, which

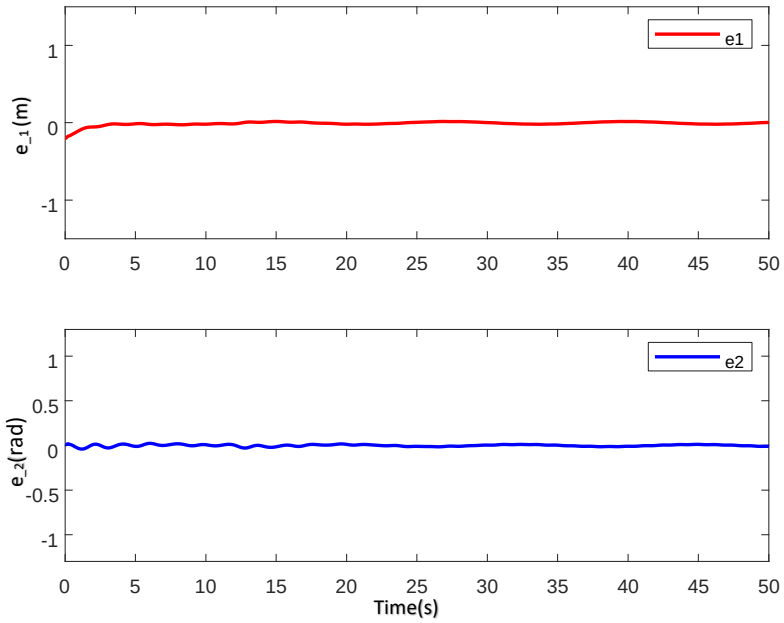

Figure 5.6: Tracking errors e_1 and e_2

clearly illustrates the efficacy of the proposed control strategy. Both the trolley position and payload swing errors decrease rapidly toward zero, reflecting a fast transient response. The short convergence time indicates that the controller effectively counteracts the system's nonlinearities while avoiding excessive overshoot or oscillatory behavior. Moreover, this precise performance is preserved even under model uncertainties and external disturbances, underscoring the robustness and practical reliability of the developed control framework. Figure 5.7 presents the response of the control signal u along with the sliding surface S. The results indicate that the control input remains within bounded limits while successfully guiding the system states toward the sliding manifold. The sliding surface S quickly converges to zero, verifying that the sliding mode condition is fulfilled and that the system operates in accordance with the intended control dynamics.

For benchmarking purposes, the performance of the proposed control strategy is compared with the approach in [125], which utilizes a sliding mode controller (SMC) augmented with a fuzzy disturbance observer, as well as an enhanced version employing a Type-2 Fuzzy Logic Controller. In this comparison, x flc1, dx flc1,θ flc1,$\dot{\theta}$ flc1,e flc1,correspond to the results obtained using the SMC with a Type-1 FLC from [125], while x flc2, dx flc2,θ flc2,$\dot{\theta}$ flc2,e flc2, represent the outcomes with the Type-2 FLC, and x_P, dxP,θP, $\dot{\theta} P$ and eP indicate the

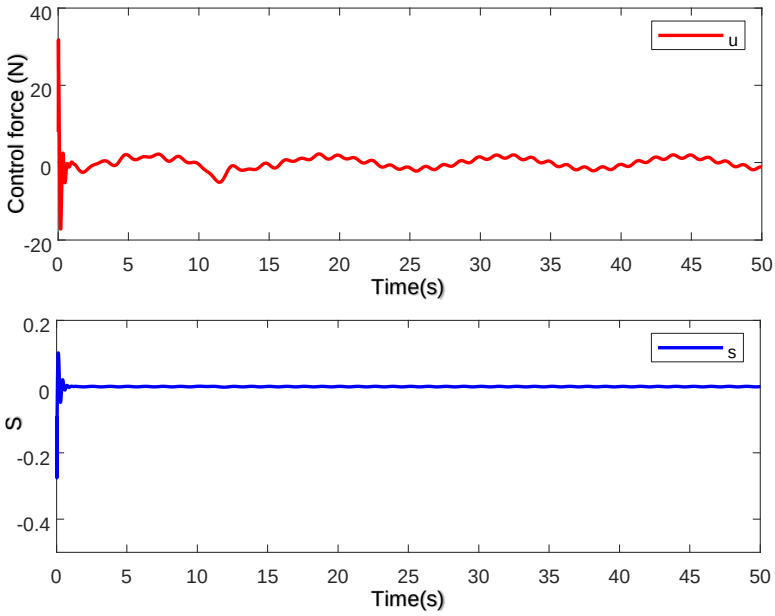

Figure 5.7: Control action u and sliding surface S

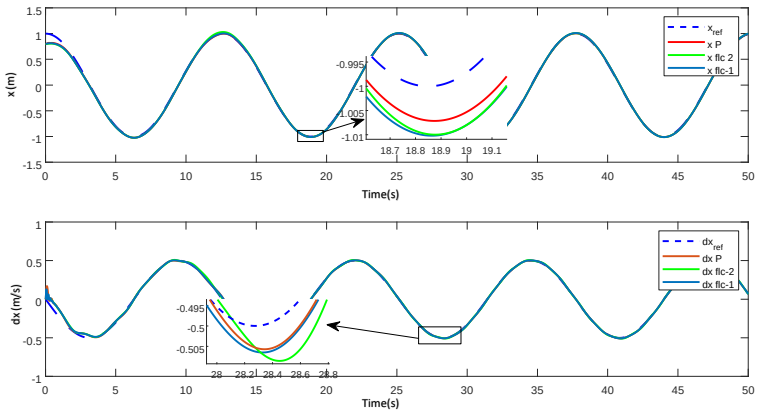

Figure 5.8: Comparison in terms of x and $\dot{x}$

performance achieved by the proposed control scheme.

Figures 5.8, 5.9, and 5.10 together provide a comprehensive evaluation of the system's state responses and tracking errors under consistent operating conditions. Figure 5.8 presents the evolution of x and $\dot{x}$, illustrating that the proposed control scheme achieves faster settling times and smaller steady-state deviations compared to the alternative methods. The responses of θ and $\dot{\theta}$ in Figure 5.9 corroborate this observation, demonstrating closer adherence to the desired reference trajectories. Figure 5.10 depicts the tracking errors e_1 and e_2, which decay more rapidly and remain at lower magnitudes under the proposed controller. The zoomed-in portions of these figures further emphasize that the proposed approach delivers superior trajectory tracking accuracy and overall improved performance relative to previously reported methods. Table 5.1 provides a comprehensive comparison of trajectory

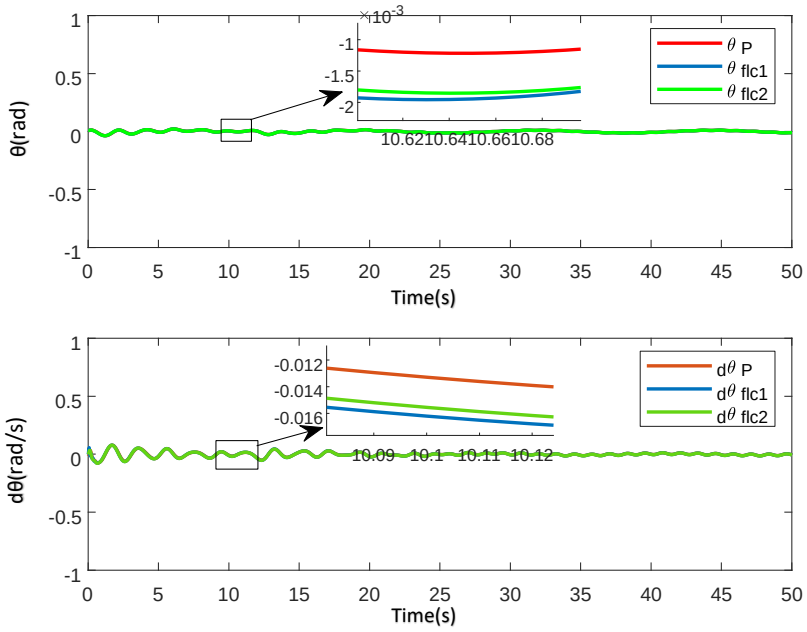

Figure 5.9: Comparison in terms of $\dot{\theta}$ and θ

tracking performance. The tracking error metrics, including RMSE, ISE, IAE, MSE, ITAE, and variance, were computed following the formulations listed in Table 5.2. These results offer a quantitative evaluation of the controllers' accuracy and highlight the superior performance of the proposed approach relative to existing SMC-FLC methods.

Evaluation across multiple performance metrics reveals that the proposed controller consistently achieves lower tracking errors compared to alternative methods. Specifically, it attains an ISE of 0.0364, outperforming the SMC–FT1 and SMC–FT2 approaches, which report

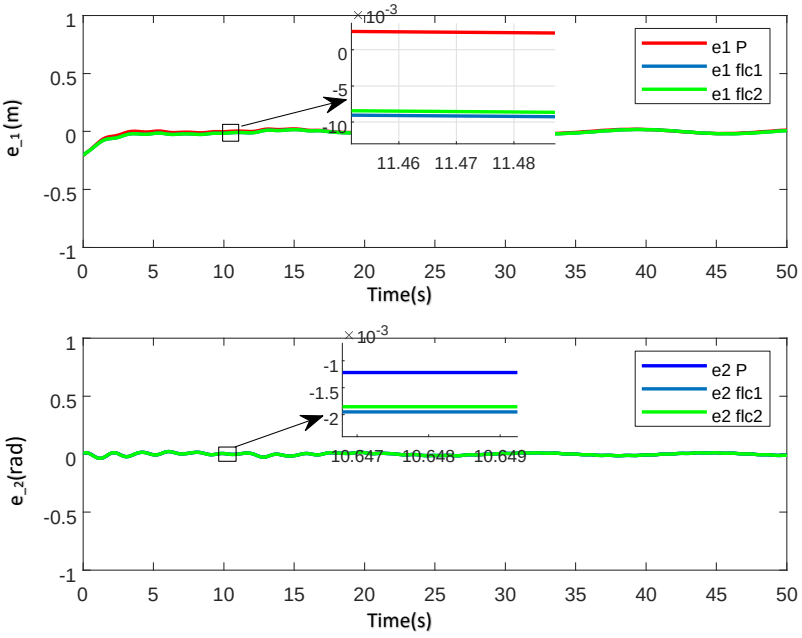

Figure 5.10: Comparison in terms of e_1 and $e2$

ISE values of 0.0424 and 0.0423, respectively [125], thereby providing more precise trajectory tracking. The convergence times for e_1 and e_2 under the proposed controller are 3.15 s and 0.55 s, whereas SMC-FLC-1 exhibits 10.45 s and 1.82 s, and SMC-FLC-2 shows 10.50 s and 1.84 s. The most notable improvement occurs for e_1, highlighting a markedly faster convergence. Overall, these findings confirm that the developed control strategy not only enhances robustness against uncertainties and external perturbations but also delivers superior tracking accuracy and rapid response performance.

Moreover, the proposed controller attains the desired performance while requiring 110.50 units of control energy, which is lower than SMC-FLC-1 (124.62) and comparable to SMC-FLC-2 (109.01). These findings indicate that the proposed approach not only improves robustness against uncertainties and external disturbances but also achieves efficient control with reduced actuator effort. Nevertheless, the energy consumption remains roughly comparable to existing methods. This limitation could be addressed by adopting an event-triggered control scheme, in which the control signal is updated only when necessary, thereby lowering computational load and communication requirements.

Table 5.1: Quantitative comparison of trajectory tracking performance under the proposed controller, SMC-FLC1 and SMC-FLC2

Controller	Error	RMSE	ISE	IAE	MSE	ITAE	TV
Proposed Controller	e_1	0.0270	0.0364	0.7213	0.00073	13.7967	0.000722
	e_2	0.0099	0.0042	0.4115	0.00009	9.3465	0.000098
SMC-FLC2	e_1	0.0291	0.0423	0.8580	0.00085	14.5388	0.000767
	e_2	0.0100	0.0049	0.4135	0.00010	9.3473	0.000099
SMC-FLC1 [125]	e_1	0.0292	0.0424	0.8601	0.00086	14.5765	0.000769
	e_2	0.0102	0.0050	0.4141	0.00011	9.3611	0.00010

5.7 Conclusion

This chapter introduced an adaptive hybrid Type-3 fuzzy fractional-order sliding mode control (T3-FO-SMC) strategy for underactuated mechanical systems (UMSs). The proposed controller incorporates a novel time-varying switching surface, which eliminates the traditional reaching phase, thereby enhancing robustness and mitigating chattering effects. The fractional-order formulation further contributes to faster convergence and smoother transient behavior. Unknown external disturbances are estimated online using an adaptive Type-3 fuzzy inference mechanism, providing improved handling of uncertainties. Simulation results indicate that the proposed approach achieves superior robustness and higher tracking accuracy relative to conventional control strategies, establishing a solid foundation for the advanced control of complex underactuated systems. Moreover, this methodology can be scaled to higher-order UMSs, where intricate dynamics can benefit from the synergistic effects of fractional-order control and adaptive fuzzy reasoning. Energy efficiency, while already improved, can be further optimized through the implementation of event-triggered control techniques.

Table 5.2: Performance indices for tracking evaluation

Index	**Equation**	**Description**
MSE	$\text{MSE} = \frac{1}{T}\int_0^T e^2(t)\,dt$	Mean Squared Error; average of squared tracking error over simulation time.
RMSE	$\text{RMSE} = \sqrt{\frac{1}{T}\int_0^T e^2(t)\,dt}$	Root Mean Squared Error; provides typical magnitude of tracking error.
ISE	$\text{ISE} = \int_0^T e^2(t)\,dt$	Integral of Squared Error; penalizes large errors heavily.
IAE	$\text{IAE} = \int_0^T \lvert e(t)\rvert\,dt$	Integral of Absolute Error; accumulates absolute error over time.
ITAE	$\text{ITAE} = \int_0^T t\,\lvert e(t)\rvert\,dt$	Integral of Time-weighted Absolute Error; emphasizes long-lasting errors and settling behavior.
TV	$\text{TV} = \frac{1}{T}\int_0^T (e(t)-\bar{e})^2\,dt$	Tracking Variance, measures variability of the tracking error around its mean; indicates smoothness and stability.
Control energy	$E_u = \int_0^T u^2(t)\,dt$	Measures the total actuator effort required by the controller over the simulation duration

Note: $e(t)$ represents the tracking error, and $\bar{e}$ denotes the mean value of $e(t)$ over the interval $[0, T]$. Δt is the sampling period. This text will automatically wrap to multiple lines inside the table cell if it exceeds the width.

General conclusion

This thesis provided a comprehensive investigation into the control of underactuated systems, which are distinguished by possessing fewer actuators than degrees of freedom. Such systems present considerable challenges related to stability, controllability, and overall performance. Conventional control techniques frequently fall short when applied to these systems, owing to their inherently nonlinear behavior and complex dynamic interactions.
The main aim of this research was the development of new and advanced control strategies tailored to the unique requirements of underactuated systems. By addressing the limitations of existing methods, this work seeks to harness the advantages of underactuated systems—including reduced complexity and cost, enhanced energy efficiency, increased flexibility and adaptability, and greater robustness—while ensuring precise and reliable operation.
In this thesis, different types of control methods have been used together with some formation control approaches in order to achieve the formation control ofunderactuated systems with a satisfactory and effective performance. The accomplished work can be summarized as follows:

- We have presented a modified method for utilizing tracking errors to formulate sliding domain equations. The primary idea was to modify the tracking errors such that the system reaction begins on the sliding surface for any initial conditions. With this feature, chattering was avoided, the tracking error's asymptotic convergence to the origin was guaranteed, and the recommended method was created without reaching phase.

- We proposed a Fuzzy Fast Terminal Sliding Mode Control (FFTSMC) technique. By combining the advantages of fuzzy logic tuning with fast terminal sliding mode control, the suggested method produced rapid convergence, stable performance, and decreased chattering. The fuzzy logic was included for tuning the FTSMC parameters. The aim was to enhance the rate of convergence and reduce the system response time. This enhanced efficiently the accuracy of the control action and quickened the system states'

convergence to the desired values.

- We introduced an adaptive fuzzy Type-2 fast terminal sliding mode control (AFT2-FTSMC) strategy. This controller integrates an adaptive fuzzy estimator to adjust the control input online, further reducing chattering, ensuring finite-time convergence, and improving robustness against system uncertainties and external disturbances.

- An adaptive hybrid control strategy combining Type-3 fuzzy logic with fractional-order sliding mode control was developed. By integrating a fractional-order operator and an adaptive Type-3 fuzzy inference system, the proposed approach achieves faster convergence, smoother transient behavior, and precise estimation of unknown nonlinearities and external disturbances. Additionally, a novel time-varying switching surface is employed, which passes through the initial error configuration, effectively removing the reaching phase and improving the overall performance and robustness of the system.

The proposed control strategies were thoroughly evaluated through simulations and representative case studies, confirming their effectiveness in enhancing the performance of underactuated systems. The results highlight their potential applicability across diverse engineering domains, including robotics, aerospace, and automotive systems. This work not only advances the theoretical understanding of underactuated system control but also provides a foundation for developing more efficient, adaptive, and resilient solutions capable of operating reliably in complex and uncertain environments.
As future work, the integration of predictive control schemes could be considered to improve decision-making over a finite horizon and enhance performance in dynamic environments. Additionally, implementing an event-triggered control strategy may further reduce computational and communication burdens by updating the control input only when necessary, thereby improving efficiency, energy consumption, and system responsiveness.

Bibliography

[1] Javier Moreno-Valenzuela and Carlos Aguilar-Avelar. *Motion control of underactuated mechanical systems*, volume 1. Springer, 2018.

[2] Jesús Sandoval, Rafael Kelly, and Víctor Santibáñez. A speed regulator for a force-driven cart-pole system. *International Journal of Systems Science*, 53(2):412–430, 2022.

[3] Jin-Xi Zhang and Tianyou Chai. Singularity-free continuous adaptive control of uncertain underactuated surface vessels with prescribed performance. *IEEE Transactions on Systems, Man, and Cybernetics: Systems*, 52(9):5646–5655, 2021.

[4] Xiaoyu Shi, Yuhua Cheng, Chun Yin, Shouming Zhong, Xuegang Huang, Kai Chen, and Gen Qiu. Adaptive fractional-order smc controller design for unmanned quadrotor helicopter under actuator fault and disturbances. *Ieee Access*, 8:103792–103802, 2020.

[5] Xiaolong Chen, Han Zhao, Hao Sun, Shengchao Zhen, and Kang Huang. A novel adaptive robust control approach for underactuated mobile robot. *Journal of the Franklin Institute*, 356(5):2474–2490, 2019.

[6] Shaobao Li, Petar Durdevic, and Zhenyu Yang. Trajectory tracking of underactuated vtol aerial vehicles with unknown system parameters via irl. *IEEE Transactions on Automatic Control*, 67(6):3043–3050, 2021.

[7] Bruce Wingo, Ching-An Cheng, Muhammad Murtaza, Munzir Zafar, and Seth Hutchinson. Extending riemmanian motion policies to a class of underactuated wheeled-inverted-pendulum robots. In *2020 IEEE International Conference on Robotics and Automation (ICRA)*, pages 3967–3973. IEEE, 2020.

[8] Yang Liu and Hongnian Yu. A survey of underactuated mechanical systems. *IET Control Theory & Applications*, 7(7):921–935, 2013.

[9] Marlen Meza-Sánchez, MC Rodríguez-Liñán, Eddie Clemente, and Leonardo Herrera. Evolutionary design of swing-up controllers for stabilization task of underactuated inverted pendulums. *Genetic Programming and Evolvable Machines*, 24(2):9, 2023.

[10] Ngo Phong Nguyen, Hyondong Oh, Yoonsoo Kim, Jun Moon, Jun Yang, and Wen-Hua Chen. Fuzzy-based super-twisting sliding mode stabilization control for under-actuated rotary inverted pendulum systems. *IEEE Access*, 8:185079–185092, 2020.

[11] Chih-Chen Yih. Sliding mode control for swing-up and stabilization of the cart-pole underactuated system. *Asian journal of control*, 15(4):1201–1214, 2013.

[12] Karl L Fetzer, Sergey Nersesov, and Hashem Ashrafiuon. Full-state nonlinear trajectory tracking control of underactuated surface vessels. *Journal of Vibration and Control*, 26(15-16):1286–1296, 2020.

[13] Jian-Xin Xu, Zhao-Qin Guo, and Tong Heng Lee. Design and implementation of integral sliding-mode control on an underactuated two-wheeled mobile robot. *IEEE Transactions on industrial electronics*, 61(7):3671–3681, 2013.

[14] Lejun Wang, Xuzhi Lai, Pan Zhang, and Min Wu. A control strategy based on trajectory planning and optimization for two-link underactuated manipulators in vertical plane. *IEEE Transactions on Systems, Man, and Cybernetics: Systems*, 52(6):3466–3475, 2021.

[15] Max Lutz and Thomas Meurer. Optimal trajectory planning and model predictive control of underactuated marine surface vessels using a flatness-based approach. In *2021 American Control Conference (ACC)*, pages 4667–4673. IEEE, 2021.

[16] Ishan Chawla and Ashish Singla. Real-time control of a rotary inverted pendulum using robust lqr-based anfis controller. *International Journal of Nonlinear Sciences and Numerical Simulation*, 19(3-4):379–389, 2018.

[17] Carlos Aguilar-Avelar and Javier Moreno-Valenzuela. A composite controller for trajectory tracking applied to the furuta pendulum. *ISA transactions*, 57:286–294, 2015.

[18] Mohammad Keshmiri, Ali Fellah Jahromi, Abolfazl Mohebbi, Mohammad Hadi Amoozgar, and Wen-Fang Xie. Modeling and control of ball and beam system using model based and non-model based control approaches. *International Journal on smart sensing and intelligent systems*, 5(1):14–35, 2012.

[19] Kakoli Majumder and BM Patre. Sliding mode control for underactuated mechanical systems via nonlinear disturbance observer: stabilization of the rotational pendulum. *International Journal of Dynamics and Control*, 6(4):1663–1672, 2018.

[20] Ibrahim Shah and Fazal Ur Rehman. Smooth second order sliding mode control of a class of underactuated mechanical systems. *IEEE Access*, 6:7759–7771, 2018.

[21] Muhammad Idrees, Saif Ullah, and Shah Muhammad. Sliding mode control design for stabilization of underactuated mechanical systems. *Advances in Mechanical Engineering*, 11(5):1687814019842712, 2019.

[22] Dianwei Qian, Jianqiang Yi, and Dongbin Zhao. Multiple layers sliding mode control for a class of under-actuated systems. In *The Proceedings of the Multiconference on" Computational Engineering in Systems Applications"*, volume 1, pages 530–535. IEEE, 2006.

[23] Djamila Zehar, Khier Benmahammed, and Khalissa Behih. Control for underactuated systems using sliding mode observer. *International Journal of Control, Automation and Systems*, 16:739–748, 2018.

[24] Luis Ovalle, Héctor Ríos, Miguel Llama, and Leonid Fridman. Continuous sliding-mode output-feedback control for stabilization of a class of underactuated systems. *IEEE Transactions on Automatic Control*, 67(2):986–992, 2021.

[25] Zhuoqing Liu, Ning Sun, Yiming Wu, Xin Xin, and Yongchun Fang. Nonlinear sliding mode tracking control of underactuated tower cranes. *International Journal of Control, Automation and Systems*, 19:1065–1077, 2021.

[26] Quang Hieu Ngo, Ngo Phong Nguyen, Quoc Bao Truong, and Gyoung-Hahn Kim. Application of fuzzy moving sliding surface approach for container cranes. *International Journal of Control, Automation and Systems*, 19:1133–1138, 2021.

[27] Pham Van Trieu, Hoang Manh Cuong, Hoang Quoc Dong, Nguyen Huu Tuan, et al. Adaptive fractional-order fast terminal sliding mode with fault-tolerant control for underactuated mechanical systems: Application to tower cranes. *Automation in Construction*, 123:103533, 2021.

[28] Ehsan Badfar and Mahdi Alinaghizadeh Ardestani. Design of adaptive fuzzy gain scheduling fast terminal sliding mode to control the radius of bubble in the blood

vessel with application in cardiology. *International Journal of Dynamics and Control*, 9(1):199–210, 2021.

[29] Moussa Labbadi and Hassan El Moussaoui. An improved adaptive fractional-order fast integral terminal sliding mode control for distributed quadrotor. *Mathematics and Computers in Simulation*, 188:120–134, 2021.

[30] Zuliana Ismail, Renuganth Varatharajoo, and Yew-Chung Chak. A fractional-order sliding mode control for nominal and underactuated satellite attitude controls. *Advances in Space Research*, 66(2):321–334, 2020.

[31] Zheping Yan, Man Wang, and Jian Xu. Robust adaptive sliding mode control of underactuated autonomous underwater vehicles with uncertain dynamics. *Ocean Engineering*, 173:802–809, 2019.

[32] Wei Liu, Si-yi Chen, and Hui-xian Huang. Double closed-loop integral terminal sliding mode for a class of underactuated systems based on sliding mode observer. *International Journal of Control, Automation and Systems*, 18:339–350, 2020.

[33] Quang Vinh Doan, Anh Tuan Vo, Tien Dung Le, Hee-Jun Kang, and Ngoc Hoai An Nguyen. A novel fast terminal sliding mode tracking control methodology for robot manipulators. *Applied Sciences*, 10(9):3010, 2020.

[34] Weilin Yang, Jiayu Chen, Dezhi Xu, and Xinggang Yan. Hierarchical global fast terminal sliding-mode control for a bridge travelling crane system. *IET Control Theory & Applications*, 15(6):814–828, 2021.

[35] Thaned Rojsiraphisal, Saleh Mobayen, Jihad H Asad, Mai The Vu, Arthur Chang, and Jirapong Puangmalai. Fast terminal sliding control of underactuated robotic systems based on disturbance observer with experimental validation. *Mathematics*, 9(16):1935, 2021.

[36] Ting Dai, Sumei Liu, Junjie Liu, Nan Jiang, Wei Liu, and Qingyan Chen. Evaluation of fast fluid dynamics with different turbulence models for predicting outdoor airflow and pollutant dispersion. *Sustainable Cities and Society*, 77:103583, 2022.

[37] E Paulo Alves and Frederico Fiuza. Data-driven discovery of reduced plasma physics models from fully kinetic simulations. *Physical Review Research*, 4(3):033192, 2022.

[38] Bang-Qing Li and Yu-Lan Ma. Optical soliton resonances and soliton molecules for the lakshmanan–porsezian–daniel system in nonlinear optics. *Nonlinear Dynamics*, 111(7):6689–6699, 2023.

[39] Matthew S Allen, Daniel Rixen, Maarten Van der Seijs, Paolo Tiso, Thomas Abrahamsson, and Randall L Mayes. *Substructuring in engineering dynamics*. Springer, 2020.

[40] Ammara Mehmood, Aneela Zameer, Muhammad Saeed Aslam, and Muhammad Asif Zahoor Raja. Design of nature-inspired heuristic paradigm for systems in nonlinear electrical circuits. *Neural Computing and Applications*, 32:7121–7137, 2020.

[41] Sourav Rana, Sabyasachi Bhattacharya, and Sudip Samanta. Spatiotemporal dynamics of leslie–gower predator–prey model with allee effect on both populations. *Mathematics and Computers in Simulation*, 200:32–49, 2022.

[42] Evelyn Tang and Danielle S Bassett. Colloquium: Control of dynamics in brain networks. *Reviews of modern physics*, 90(3):031003, 2018.

[43] Jorge Eduardo Macías-Díaz, Ali Raza, Nauman Ahmed, and Muhammad Rafiq. Analysis of a nonstandard computer method to simulate a nonlinear stochastic epidemiological model of coronavirus-like diseases. *Computer Methods and Programs in Biomedicine*, 204:106054, 2021.

[44] Nikolai A Jaeger, Nicolas A Zacharias, and Malte Brettel. Nonlinear and dynamic effects of responsive and proactive market orientation: A longitudinal investigation. *International Journal of Research in Marketing*, 33(4):767–779, 2016.

[45] Wen-Bao Lin, Ming-Kuen Wang, and Kevin P Hwang. The combined model of influencing on-line consumer behavior. *Expert Systems with Applications*, 37(4):3236–3247, 2010.

[46] Nauman Ahmed, Dumitru Baleanu, Alper Korkmaz, Muhammad Rafiq, MA Rehman, and Mubasher Ali. Positivity preserving computational techniques for nonlinear autocatalytic chemical reaction model. *Rom. Rep. Phys*, 72:121, 2020.

[47] Irina Barzykina. Chemistry and mathematics of the belousov–zhabotinsky reaction in a school laboratory. *Journal of Chemical Education*, 97(7):1895–1902, 2020.

[48] Yongming Han, Ning Ding, Zhiqiang Geng, Zun Wang, and Chong Chu. An optimized long short-term memory network based fault diagnosis model for chemical processes. *Journal of Process Control*, 92:161–168, 2020.

[49] Augusto Cheffer, Marcelo A Savi, Tiago Leite Pereira, and Aline Souza de Paula. Heart rhythm analysis using a nonlinear dynamics perspective. *Applied Mathematical Modelling*, 96:152–176, 2021.

[50] Xin Han, Xing He, Xingxing Ju, Hangjun Che, and Tingwen Huang. Distributed neurodynamic models for solving a class of system of nonlinear equations. *IEEE Transactions on Neural Networks and Learning Systems*, 2023.

[51] Christopher Avery, William Bossert, Adam Clark, Glenn Ellison, and Sara Fisher Ellison. An economist's guide to epidemiology models of infectious disease. *Journal of Economic Perspectives*, 34(4):79–104, 2020.

[52] Sunil Kumar, Amit Kumar, and Zaid M Odibat. A nonlinear fractional model to describe the population dynamics of two interacting species. *Mathematical Methods in the Applied Sciences*, 40(11):4134–4148, 2017.

[53] Aijun Xing, Enzai Du, Haihua Shen, Longchao Xu, Wim de Vries, Mengying Zhao, Xiuyuan Liu, and Jingyun Fang. Nonlinear responses of ecosystem carbon fluxes to nitrogen deposition in an old-growth boreal forest. *Ecology Letters*, 25(1):77–88, 2022.

[54] Abdelwaheb Hannachi. *Patterns identification and data mining in weather and climate*. Springer, 2021.

[55] Claudio Urrea and José Pascal. Design and validation of a dynamic parameter identification model for industrial manipulator robots. *Archive of Applied Mechanics*, 91(5):1981–2007, 2021.

[56] Jianxiong Hao, Kai Zhang, Zhiqiang Zhang, Shuxin Wang, and Chaoyang Shi. An online model-free adaptive tracking controller for cable-driven medical continuum manipulators. *IEEE Transactions on Medical Robotics and Bionics*, 2023.

[57] Birgit Graf and Jonathan Eckstein. Service robots and automation for the disabled and nursing home care. In *Springer Handbook of Automation*, pages 1331–1347. Springer, 2023.

[58] Hongliang Hua, Jie Song, Jingbo Zhao, and Zhenqiang Liao. Sensor-less grasping force control of a pneumatic underactuated robotic gripper. *Journal of Mechanisms and Robotics*, 16(3):031005, 2024.

[59] Rosa M Rodríguez, Álvaro Labella, Bapi Dutta, and Luis Martínez. Comprehensive minimum cost models for large scale group decision making with consistent fuzzy preference relations. *Knowledge-Based Systems*, 215:106780, 2021.

[60] K Khalil Hassan et al. Nonlinear systems. *Departement of Electrical and computer Engineering, Michigan State University*, 2002.

[61] TL Tai and Yu-Shen Lu. Global sliding mode control with chatter alleviation for robust eigenvalue assignment. *Journal of Systems and Control Engineering*, 220(7):573–584, 2006.

[62] Metin U Salamci, Nurdan Bilgin, S Ozcan, and Emin Yusuf Avan. Sliding mode control design for nonlinear systems without reaching phase. In *European Workshop on Advanced Control and Diagnosis*, 2011.

[63] Tai-Heng Chang and Yildirim Hurmuzlu. Sliding control without reaching phase and its application to bipedal locomotion. *Journal of Dynamic Systems, Measurement and Control*, 115(3):447–455, 1993.

[64] Seung-Bok Choi, Dong-Won Park, and Suhada Jayasuriya. A time-varying sliding surface for fast and robust tracking control of second-order uncertain systems. *Automatica*, 30(5):899–904, 1994.

[65] R Ghosh Roy and Nejat Olgac. Robust nonlinear control via moving sliding surfaces-n-th order case. In *IEEE Conference on Decision and Control*, volume 2, pages 943–948, 1997.

[66] Ayman Al-Khazraji, Najib Essounbouli, Abdelaziz Hamzaoui, Frédéric Nollet, and Janan Zaytoon. Type-2 fuzzy sliding mode control without reaching phase for nonlinear system. *Engineering applications of artificial intelligence*, 24(1):23–38, 2011.

[67] Ayman Hussain, Najib Essounbouli, and Abdelaziz Hamzaoui. Adaptive variable structure fuzzy wavelet network based controller for nonlinear systems. *IFAC Proceedings Volumes*, 40(21):157–162, 2007.

[68] A Hussain, N Essounbouli, A Hamzaoui, and Jn Zaytoon. Variable structure wavelet-neural-network based controller for second order nonlinear systems. *International Review of Automatic Control*, 1(1):28–35, 2008.

[69] Cao Van Kien, Nguyen Ngoc Son, and Ho Pham Huy Anh. A stable lyapunov approach of advanced sliding mode control for swing up and robust balancing implementation for the pendubot system. In *AETA 2015: Recent Advances in Electrical Engineering and Related Sciences*, pages 411–425. Springer, 2016.

[70] Serafin Ramos-Paz, Fernando Ornelas-Tellez, and Alexander G Loukianov. Nonlinear optimal tracking control in combination with sliding modes: Application to the pendubot. In *IEEE International Autumn Meeting on Power, Electronics and Computing (ROPEC)*, pages 1–6, 2017.

[71] Spandan Roy and Simone Baldi. Towards structure-independent stabilization for uncertain underactuated euler–lagrange systems. *Automatica*, 113:108775, 2020.

[72] Rui Qi, Yang Zhang, and Krishna D Kumar. Design and robustness analysis of a wave-based controller for tethered towing of defunct satellites. *IEEE/CAA Journal of Automatica Sinica*, 10(1):278–280, 2023.

[73] Yanhong Luo, Hang Yu, Huaguang Zhang, and Yu Zhou. A novel newton–euler method-based nonlinear anti-swing control for a quadrotor uav carrying a slung load. *IEEE Transactions on Systems, Man, and Cybernetics: Systems*, 2024.

[74] Wei He and Shuzhi Sam Ge. Cooperative control of a nonuniform gantry crane with constrained tension. *Automatica*, 66:146–154, 2016.

[75] Reza Olfati-Saber. *Nonlinear control of underactuated mechanical systems with application to robotics and aerospace vehicles*. PhD thesis, Massachusetts Institute of Technology, 2001.

[76] Mehdi Nikkhah, Hashem Ashrafiuon, and Kenneth R Muske. Optimal sliding mode control for underactuated systems. In *2006 American Control Conference*, pages 6–pp. IEEE, 2006.

[77] Alessandro De Luca, Raffaella Mattone, and Giuseppe Oriolo. Control of underactuated mechanical systems: Application to the planar 2r robot. In *Proceedings of 35th IEEE Conference on Decision and Control*, volume 2, pages 1455–1460. IEEE, 1996.

[78] Vadim I Utkin. *Sliding modes in control and optimization*. Springer Science & Business Media, 2013.

[79] Vadim Utkin. Variable structure systems with sliding modes. *IEEE Transactions on Automatic control*, 22(2):212–222, 1977.

[80] J-j E Slotine, JK Hedrick, and EA Misawa. Nonlinear state estimation using sliding observers. In *1986 25th IEEE Conference on Decision and Control*, pages 332–339. IEEE, 1986.

[81] Tianqing Wang, Bo Wang, Yong Yu, and Dianguo Xu. Fast high-order terminal sliding-mode current controller for disturbance compensation and rapid convergence in induction motor drives. *IEEE Transactions on Power Electronics*, 2023.

[82] İhsan Ömür Bucak, C Voloşencu, S Küçük, J Guerrero, and O Valero. An in-depth analysis of sliding mode control and its application to robotics. *Automation and Control*, 2020.

[83] Mohammad Javad Mahmoodabadi, S Arabani Mostaghim, Ahmad Bagheri, and Nader Nariman-Zadeh. Pareto optimal design of the decoupled sliding mode controller for an inverted pendulum system and its stability simulation via java programming. *Mathematical and Computer Modelling*, 57(5-6):1070–1082, 2013.

[84] Weibing Gao and James C Hung. Variable structure control of nonlinear systems: A new approach. *IEEE transactions on Industrial Electronics*, 40(1):45–55, 1993.

[85] Andrzej Bartoszewicz. A new reaching law for sliding mode control of continuous time systems with constraints. *Transactions of the Institute of Measurement and Control*, 37(4):515–521, 2015.

[86] Charles Aguiar, Daniel Leite, Daniel Pereira, Goran Andonovski, and Igor Škrjanc. Nonlinear modeling and robust lmi fuzzy control of overhead crane systems. *Journal of the Franklin Institute*, 358(2):1376–1402, 2021.

[87] Dianwei Qian and Jianqiang Yi. *Hierarchical sliding mode control for under-actuated cranes*. Springer, 2016.

[88] Steven L Brunton and J Nathan Kutz. *Data-driven science and engineering: Machine learning, dynamical systems, and control*. Cambridge University Press, 2019.

[89] Ansu Man Singh and Quang P. Ha. Fast terminal sliding control application for second-order underactuated systems. *Inte. Jour. Cont. Auto. Syst.*, 17(8):1884–1898, 2019.

[90] S. Aloui, O. Pages, A. El-Hajjaji, A. Chaari, and Y. Koubaa. Robust adaptive fuzzy sliding mode control design for a class of mimo underactuated system. *IFAC Proc.*, 44(1):11127–11132, 2011.

[91] Shuying Peng and Wuxi Shi. Adaptive fuzzy integral terminal sliding mode control of a nonholonomic wheeled mobile robot. *Math. Prob. Engi.*, 2017, 2017.

[92] Tiebin Wu, Weihua Guiand Dong Hu, and Chenglong Du. Adaptive fuzzy sliding mode control for translational oscillator with rotating actuator: a fuzzy model. *IEEE Access*, 6:55861–55869, 2018.

[93] Wallace M. Bessa, Svenja Otto, Edwin Kreuzer, and Robert Seifried. An adaptive fuzzy sliding mode controller for uncertain underactuated mechanical systems. *Jour. Vibr. Cont.*, 25(9):1521–1535, 2019.

[94] Lotfi Asker Zadeh. Fuzzy sets. *Information and control*, 8(3):338–353, 1965.

[95] Man Zhihong, Andrew P Paplinski, and Hong Ren Wu. A robust mimo terminal sliding mode control scheme for rigid robotic manipulators. *IEEE transactions on automatic control*, 39(12):2464–2469, 1994.

[96] Donghao Xu, Zelin Li, Ping Xin, and Xueqian Zhou. The non-singular terminal sliding mode control of underactuated unmanned surface vessels using biologically inspired neural network. *Journal of Marine Science and Engineering*, 12(1):112, 2024.

[97] Xinghuo Yu and Man Zhihong. Fast terminal sliding-mode control design for nonlinear dynamical systems. *IEEE Transactions on Circuits and Systems I: Fundamental Theory and Applications*, 49(2):261–264, 2002.

[98] Hugan Zhang, Xianku Zhang, Shihang Gao, Xu Han, and DaoCheng Ma. Global fast terminal sliding mode control for path following of ultra large underactuated ship based on predictive los guidance. *Ocean Engineering*, 285:115387, 2023.

[99] Pawel Latosinski. Sliding mode control based on the reaching law approach — a brief survey. In *Inte. Conf. Meth. Mode. Auto. Robo.*, pages 519–524. IEEE, 2017.

[100] Aissa Rebai and Kamel Guesmi. Robust adaptive fuzzy sliding mode controller for nonlinear uncertain hysteretic systems. *Transactions of the Institute of Measurement and Control*, 42(13):2519–2532, 2020.

[101] Aissa Rebai, Kamel Guesmi, Djamal Gozim, and Boualem Hemici. Design of an optimized fractional order fuzzy pid controller for a piezoelectric actuator. In *2014 15th International Conference on Sciences and Techniques of Automatic Control and Computer Engineering (STA)*, pages 456–461. IEEE, 2014.

[102] Lafi Alnufaie. Nonsingular fast terminal sliding mode controller for a robotic system: A fuzzy approach. *IEEE Access*, 11:75522–75527, 2023.

[103] Junjie Dong and Xingguang Duan. Robust control based on fast terminal sliding mode control with adaptive interval type-2 fuzzy pid. *International Journal of Fuzzy Systems*, 26(3):849–859, 2024.

[104] H Rahali, S Zeghlache, BDE Cherif, L Benyettou, and A Djerioui. Robust adaptive fuzzy type-2 fast terminal sliding mode control of robot manipulators in attendance of actuator faults and payload variation. *Electrical Engineering & Electromechanics*, 1(1):31–38, 2025.

[105] Hongzhuang Wu, Songyong Liu, Cheng Cheng, and Changlong Du. Observer based adaptive interval type-2 fuzzy sliding mode control for unknown nonlinear systems. *Journal of Intelligent & Fuzzy Systems*, 38(2):1799–1810, 2020.

[106] Han Sol Kim, Sounghwan Hwang, and Young Hoon Joo. Interval type-2 fuzzy-model-based fault-tolerant sliding mode tracking control of a quadrotor uav under actuator saturation. *IET Control Theory & Applications*, 14(20):3663–3675, 2020.

[107] Ji-hwan Hwang, Hwan-joo Kwak, and Gwi-tae Park. Adaptive interval type-2 fuzzy sliding mode control for unknown chaotic system. *Nonlinear dynamics*, 63(3):491–502, 2011.

[108] Samir Zeghlache, Mohammed Zinelaabidine Ghellab, and Abderrahmen Bouguerra. Adaptive type-2 fuzzy sliding mode control using supervisory type-2 fuzzy control for 6 dof octorotor aircraft. *International Journal of Intelligent Engineering and Systems*, 10(3):47–57, 2017.

[109] JM Medel. Uncertain rule-based fuzzy logic systems: Introduction and new direction, 2001.

[110] Nilesh N Karnik and Jerry M Mendel. Introduction to type-2 fuzzy logic systems. In *1998 IEEE international conference on fuzzy systems proceedings. IEEE world congress on computational intelligence (Cat. No. 98CH36228)*, volume 2, pages 915–920. IEEE, 1998.

[111] Dong Huixuan, Wei Sun, and Zhu Chenglong. Adaptive fuzzy sliding mode control for underactuated systems with time-varying sensor faults. *Journal of the Chinese Institute of Engineers*, 47(3):351–358, 2024.

[112] Hongbo Zou and Mengdan Wang. Enhanced sliding-mode control for tracking control of uncertain fractional-order nonlinear systems based on fuzzy logic systems. *Applied Sciences*, 15(9):4686, 2025.

[113] Omid Mofid, Saleh Mobayen, Chunwei Zhang, and Balasubramanian Esakki. Desired tracking of delayed quadrotor uav under model uncertainty and wind disturbance using adaptive super-twisting terminal sliding mode control. *ISA transactions*, 123:455–471, 2022.

[114] Alireza Mousavi and Amir HD Markazi. Adaptive fuzzy sliding-mode control of under-actuated systems with unknown input gain function. *Proceedings of the Institution of Mechanical Engineers, Part C: Journal of Mechanical Engineering Science*, 238(12):5455–5468, 2024.

[115] Ardashir Mohammadzadeh, Hamid Taghavifar, Chunwei Zhang, Khalid A Alattas, Jinping Liu, and Mai The Vu. A non-linear fractional-order type-3 fuzzy control for enhanced path-tracking performance of autonomous cars. *IET Control Theory & Applications*, 18(1):40–54, 2024.

[116] Mohammad Ahmadi Balootaki, Hossein Rahmani, Hossein Moeinkhah, and Ardashir Mohammadzadeh. Non-singleton fuzzy control for multi-synchronization of chaotic systems. *Applied Soft Computing*, 99:106924, 2021.

[117] Abdulaziz S Alkabaa, Osman Taylan, Muhammed Balubaid, Chunwei Zhang, and Ardashir Mohammadzadeh. A practical type-3 fuzzy control for mobile robots: predictive and boltzmann-based learning. *Complex & Intelligent Systems*, 9(6):6509–6522, 2023.

[118] Songhua Xu, Chunwei Zhang, and Ardashir Mohammadzadeh. Type-3 fuzzy control of robotic manipulators. *Symmetry*, 15(2):483, 2023.

[119] Amin Taghieh, Ardashir Mohammadzadeh, Chunwei Zhang, Sakthivel Rathinasamy, and Stelios Bekiros. A novel adaptive interval type-3 neuro-fuzzy robust controller for nonlinear complex dynamical systems with inherent uncertainties. *Nonlinear Dynamics*, 111(1):411–425, 2023.

[120] Hoang Manh Cuong, Nguyen Tung Lam, Hoang Quoc Dong, Pham Van Trieu, Nguyen Huu Tuan, and Le Anh Tuan. Fractional-order terminal sliding mode control for a class of underactuated nonlinear systems. In *2020 IEEE 18th International Conference on Industrial Informatics (INDIN)*, volume 1, pages 703–706. IEEE, 2020.

[121] Omid Mofid and Saleh Mobayen. Robust fractional-order sliding mode tracker for quad-rotor uavs: event-triggered adaptive backstepping approach under disturbance and uncertainty. *Aerospace Science and Technology*, 146:108916, 2024.

[122] Ahmet Dumlu. Design of a fractional-order adaptive integral sliding mode controller for the trajectory tracking control of robot manipulators. *Proceedings of the Institution of Mechanical Engineers, Part I: Journal of Systems and Control Engineering*, 232(9):1212–1229, 2018.

[123] Lei Li and Jian-Guo Liu. A generalized definition of caputo derivatives and its application to fractional odes. *SIAM Journal on Mathematical Analysis*, 50(3):2867–2900, 2018.

[124] Diego A Murio. Stable numerical evaluation of grünwald–letnikov fractional derivatives applied to a fractional ihcp. *Inverse Problems in Science and Engineering*, 17(2):229–243, 2009.

[125] Hyo-Seok Kang, Yongho Lee, Chang-Ho Hyun, Heejin Lee, and Mignon Park. Design of sliding-mode control based on fuzzy disturbance observer for minimization of switching gain and chattering. *Soft Computing*, 19(4):851–858, 2015.